ISSN 1937 - 1055

VOLUME 2, 2021

INTERNATIONAL JOURNAL OF MATHEMATICAL COMBINATORICS

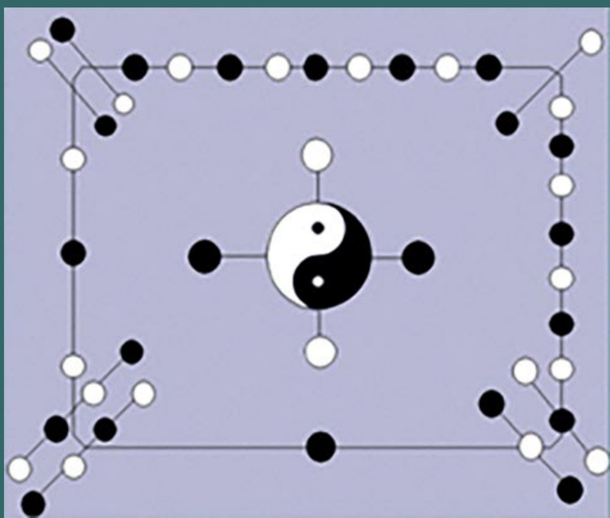

EDITED BY

THE MADIS OF CHINESE ACADEMY OF SCIENCES AND

ACADEMY OF MATHEMATICAL COMBINATORICS & APPLICATIONS, USA

June, 2021

Vol.2, 2021 **ISSN 1937-1055**

International Journal of

Mathematical Combinatorics

(www.mathcombin.com)

Edited By

The Madis of Chinese Academy of Sciences and

Academy of Mathematical Combinatorics & Applications, USA

June, 2021

Aims and Scope: The mathematical combinatorics is a subject that applying combinatorial notion to all other mathematics and all other sciences for understanding the reality of things in the universe, motivated by CC Conjecture of Dr.Linfan MAO on mathematical sciences. The **International J.Mathematical Combinatorics** is a fully refereed international journal, sponsored by the MADIS of Chinese Academy of Sciences in 2007 and published in USA quarterly, which publishes original research papers and survey articles in all aspects of mathematical combinatorics, Smarandache multi-spaces, Smarandache geometries, non-Euclidean geometry and their applications to other sciences. Topics in detail to be covered are:

Mathematical combinatorics;

Smarandache multi-spaces and Smarandache geometries with applications to other sciences;

Topological graphs; Algebraic graphs; Random graphs; Combinatorial maps; Graph and map enumeration; Combinatorial designs; Combinatorial enumeration;

Differential Geometry; Geometry on manifolds; Low Dimensional Topology; Differential Topology; Topology of Manifolds;

Geometrical aspects of Mathematical Physics and Relations with Manifold Topology;

Mathematical theory on gravitational fields and parallel universes;

Applications of Combinatorics to mathematics and theoretical physics.

Generally, papers on applications of combinatorics to other mathematics and other sciences are welcome by this journal.

It is also available from the below international databases:

Serials Group/Editorial Department of EBSCO Publishing
10 Estes St. Ipswich, MA 01938-2106, USA
Tel.: (978) 356-6500, Ext. 2262 Fax: (978) 356-9371
http://www.ebsco.com/home/printsubs/priceproj.asp

and

Gale Directory of Publications and Broadcast Media, Gale, a part of Cengage Learning
27500 Drake Rd. Farmington Hills, MI 48331-3535, USA
Tel.: (248) 699-4253, ext. 1326; 1-800-347-GALE Fax: (248) 699-8075
http://www.gale.com

Indexing and Reviews: Mathematical Reviews (USA), Zentralblatt Math (Germany), Referativnyi Zhurnal (Russia), Mathematika (Russia), Directory of Open Access (DoAJ), EBSCO (USA), International Scientific Indexing (ISI, impact factor 2.012), Institute for Scientific Information (PA, USA), Library of Congress Subject Headings (USA).

Subscription A subscription can be ordered by an email directly to

Linfan Mao

The Editor-in-Chief of *International Journal of Mathematical Combinatorics*
Chinese Academy of Mathematics and System Science Beijing, 100190, P.R.China, and also the President of Academy of Mathematical Combinatorics & Applications (AMCA), Colorado, USA

Email: maolinfan@163.com

Price: US$48.00

Famous Words:

Mathematics, rightly viewed, posses not only truth but supreme beauty – a beauty cold and austere, like that of sculpture.

By Bertrand Russell, a British philosopher and mathematician

International J.Math. Combin. Vol.2(2021), 1-16

On a Boundary Value Problem with Fuzzy Forcing Function and Fuzzy Boundary Values

Hülya GÜLTEKİN ÇİTİL

(Department of Mathematics, Faculty of Arts and Sciences, Giresun University, Giresun, Turkey)

E-mail: hulyagultekin55@hotmail.com, hulya.citil@giresun.edu.tr

Abstract: In this study, a problem with fuzzy forcing function and fuzzy boundary values is investigated. The problem is solved by two different solution methods. Theorems are proved about solutions. Comparison results are given. Example is solved on studied problem. Graphics of the solutions are drawn. Conclusions are given. It is stated which method is more useful.

Key Words: Fuzzy boundary value problems, second-order fuzzy differential equation, generalized differentiability.

AMS(2010): 03E72, 34A07.

§1. Introduction

Fuzzy logic is studied by many researchers [10, 18]. In recent years, the topic of fuzzy differential equations has been rapidly growing [1, 11, 13, 20, 23]. Because, solving the fuzzy differential equations is a very important topic. Fuzzy differential equations can be studied by different approaches. These are Hukuhara differentiability [5, 15], generalized differentiability [2, 3] and to generate the fuzzy solution from the crips solution. There are at most four solutions for fuzzy boundary value problems using the generalized differentiability [17]. Liu [19] showed that these four solutions reduce to two different solutions when the function is monotone. To generate the fuzzy solution from the crips solution can be three ways. These are extension principle [5, 6], the concept of differential inclusion [14] and fuzzy problem is to consider as a set of crips problem [8].

The aim of this study is to investigate the solutions of the fuzzy boundary value problem with fuzzy forcing function and fuzzy boundary values by two different solution methods.

§2. Preliminaries

Definition 2.1([22]) *A fuzzy number is a mapping $u : \mathbb{R} \to [0, 1]$ with the following properties:*

(1) *u is normal;*

[1]Received March 1, 2021, Accepted June 2, 2021.

(2) *u is convex fuzzy set;*
(3) *u is upper semi-continuous on* $\mathbb{R}$*;*
(4) $cl\,\{x \in \mathbb{R} \mid u(x) > 0\}$ *is compact, where cl denotes the closure of a subset.*

Let $\mathbb{R}_F$ denote the space of fuzzy numbers.

Definition 2.2([17]) *Let* $u \in \mathbb{R}_F$*. The* α*-level set of* u *is*

$$[u]^\alpha = \{x \in \mathbb{R} \mid u(x) \geq \alpha\}, \ 0 < \alpha \leq 1.$$

$[u]^\alpha = [\underline{u}_\alpha, \overline{u}_\alpha]$ *denotes the* α*-level set of* u*.*

Remark 2.1([7, 17]) The sufficient and necessary conditions for $[\underline{u}_\alpha, \overline{u}_\alpha]$ to define the parametric form of a fuzzy number as follows:

(1) $\underline{u}_\alpha$ is bounded monotonic increasing (nondecreasing) left-continuous function on $(0,1]$ and right-continuous for $\alpha = 0$,
(2) $\overline{u}_\alpha$ is bounded monotonic decreasing (nonincreasing) left-continuous function on $(0,1]$ and right-continuous for $\alpha = 0$,
(3) $\underline{u}_\alpha \leq \overline{u}_\alpha$, $0 \leq \alpha \leq 1$.

Definition 2.3([12, 17, 21]) *Let* $u, v \in \mathbb{R}_F$*. If there exists* $w \in \mathbb{R}_F$ *such that* $u = v + w$*, then* w *is called the Hukuhara difference of fuzzy numbers* u *and* v*,and it is denoted by* $w = u \ominus v$*.*

Definition 2.4([4, 12, 17]) *Let* $f : [a,b] \to \mathbb{R}_F$ *and* $t_0 \in [a,b]$*. We say that* f *is Hukuhara differentiable at* t_0*, if there exists an element* $f'(t_0) \in \mathbb{R}_F$ *such that for all* $h > 0$ *sufficiently small,* $\exists f(t_0 + h) \ominus f(t_0)$, $f(t_0) \ominus f(t_0 - h)$ *and the limits hold*

$$\lim_{h \to 0} \frac{f(t_0 + h) \ominus f(t_0)}{h} = \lim_{h \to 0} \frac{f(t_0) \ominus f(t_0 - h)}{h} = f'(t_0).$$

Definition 2.5([17]) *Let* $f : [a,b] \to \mathbb{R}_F$ *and* $t_0 \in [a,b]$*. We say that* f *is (1)-differentiable at* t_0*, if there exists an element* $f'(t_0) \in \mathbb{R}_F$ *such that for all* $h > 0$ *sufficiently small (near to 0), exist* $f(t_0 + h) \ominus f(t_0)$, $f(t_0) \ominus f(t_0 - h)$ *and the limits*

$$\lim_{h \to 0} \frac{f(t_0 + h) \ominus f(t_0)}{h} = \lim_{h \to 0} \frac{f(t_0) \ominus f(t_0 - h)}{h} = f'(t_0),$$

and f *is (2)-differentiable if for all* $h > 0$ *sufficiently small (near to 0), exist* $f(t_0) \ominus f(t_0 + h)$, $f(t_0 - h) \ominus f(t_0)$ *and the limits*

$$\lim_{h \to 0} \frac{f(t_0) \ominus f(t_0 + h)}{-h} = \lim_{h \to 0} \frac{f(t_0 - h) \ominus f(t_0)}{-h} = f'(t_0).$$

Theorem 2.6([16]) *Let* $f : [a,b] \to \mathbb{R}_F$ *be fuzzy function, where* $[f(t)]^\alpha = \left[\underline{f}_\alpha(t), \overline{f}_\alpha(t)\right]$ *for each* $\alpha \in [0,1]$*.*

(i) If f is (1)-differentiable then $\underline{f}_\alpha$ *and* $\overline{f}_\alpha$ *are differentiable functions and* $\left[f'(t)\right]^\alpha = \left[\underline{f}'_\alpha(t), \overline{f}'_\alpha(t)\right]$,

(ii) If f is (2)-differentiable then $\underline{f}_\alpha$ *and* $\overline{f}_\alpha$ *are differentiable functions and* $\left[f'(t)\right]^\alpha = \left[\overline{f}'_\alpha(t), \underline{f}'_\alpha(t)\right]$.

Theorem 2.2([16]) *Let* $f' : [a,b] \to \mathbb{R}_F$ *be fuzzy function, where* $[f(t)]^\alpha = \left[\underline{f}_\alpha(t), \overline{f}_\alpha(t)\right]$, *for each* $\alpha \in [0,1]$, *f is (1)-differentiable or (2)-differentiable.*

(i) If f and f' *are (1)-differentiable then* $\underline{f}'_\alpha$ *and* $\overline{f}'_\alpha$ *are differentiable functions and* $\left[f''(t)\right]^\alpha = \left[\underline{f}''_\alpha(t), \overline{f}''_\alpha(t)\right]$,

(ii) If f is (1)-differentiable and f' *is (2)-differentiable then* $\underline{f}'_\alpha$ *and* $\overline{f}'_\alpha$ *are differentiable functions and* $\left[f''(t)\right]^\alpha = \left[\overline{f}''_\alpha(t), \underline{f}''_\alpha(t)\right]$,

(iii) If f is (2)-differentiable and f' *is (1)-differentiable then* $\underline{f}'_\alpha$ *and* $\overline{f}'_\alpha$ *are differentiable functions and* $\left[f''(t)\right]^\alpha = \left[\overline{f}''_\alpha(t), \underline{f}''_\alpha(t)\right]$,

(iv) If f and f' *are (2)-differentiable then* $\underline{f}'_\alpha$ *and* $\overline{f}'_\alpha$ *are differentiable functions and* $\left[f''(t)\right]^\alpha = \left[\underline{f}''_\alpha(t), \overline{f}''_\alpha(t)\right]$.

§3. Main Results

Consider the two-point boundary value problem

$$y''(t) = \lambda y(t) + \widetilde{F}(t), \quad y(0) = \beta, \quad y(\ell) = \gamma, \tag{3.1}$$

where $\widetilde{F}(t) = t^2 + (-1, 0, 1)$ is fuzzy forcing function,

$$\beta = \left(\underline{c}, \frac{\underline{c} + \overline{c}}{2}, \overline{c}\right), \gamma = \left(\underline{d}, \frac{\underline{d} + \overline{d}}{2}, \overline{d}\right)$$

are symmetric triangular fuzzy numbers and $\lambda > 0$.

3.1. **Solution Method 1.**([9]) Let divide the problem (3.1) into three different problems following:

(i) The first problem is

$$y''(t) = \lambda y(t) + t^2, \ y(0) = \frac{\underline{c} + \overline{c}}{2}, \ y(\ell) = \frac{\underline{d} + \overline{d}}{2}. \tag{3.2}$$

(ii) The second problem is

$$y''(t) = \lambda y(t), \quad y(0) = \left(\frac{\underline{c} - \overline{c}}{2}, 0, \frac{\overline{c} - \underline{c}}{2}\right), \quad y(\ell) = \left(\frac{\underline{d} - \overline{d}}{2}, 0, \frac{\overline{d} - \underline{d}}{2}\right). \tag{3.3}$$

(iii) The third problem is

$$y^{''} = \lambda y + (-1, 0, 1)\,, \; y(0) = 0, \quad y(\ell) = 0. \tag{3.4}$$

The solution of the differential equation in (3.2) is

$$y\left(t\right) = c_1 e^{\sqrt{\lambda}t} + c_2 e^{-\sqrt{\lambda}t} - \frac{1}{\lambda}t^2 - \frac{2}{\lambda^2}.$$

Using the boundary conditions, the coefficients c_1 and c_2 are found as

$$c_1 = \frac{\left(\frac{\underline{d}+\overline{d}}{2} + \frac{1}{\lambda}\ell^2 + \frac{2}{\lambda^2}\right) - e^{-\sqrt{\lambda}\ell}\left(\frac{\underline{c}+\overline{c}}{2} + \frac{2}{\lambda^2}\right)}{e^{\sqrt{\lambda}\ell} - e^{-\sqrt{\lambda}\ell}},$$

$$c_2 = \frac{e^{\sqrt{\lambda}\ell}\left(\frac{\underline{c}+\overline{c}}{2} + \frac{2}{\lambda^2}\right) - \left(\frac{\underline{d}+\overline{d}}{2} + \frac{1}{\lambda}\ell^2 + \frac{2}{\lambda^2}\right)}{e^{\sqrt{\lambda}\ell} - e^{-\sqrt{\lambda}\ell}}.$$

Then, the solution of (3.2) is

$$\begin{aligned} y\left(t\right) \quad &= \quad \frac{\sinh\left(\sqrt{\lambda}\left(\ell - t\right)\right)}{\sinh\left(\sqrt{\lambda}\ell\right)}\left(\frac{\underline{c}+\overline{c}}{2} + \frac{2}{\lambda^2}\right) \\ &\quad + \frac{\sinh\left(\sqrt{\lambda}t\right)}{\sinh\left(\sqrt{\lambda}\ell\right)}\left(\frac{\underline{d}+\overline{d}}{2} + \frac{1}{\lambda}\ell^2 + \frac{2}{\lambda^2}\right) - \frac{1}{\lambda}t^2 - \frac{2}{\lambda^2}. \end{aligned} \tag{3.5}$$

Since $x_1 = e^{\sqrt{\lambda}t}$, $x_2 = e^{-\sqrt{\lambda}t}$ are the linear independent solutions of the differential equation in (3.3),

$$\begin{aligned} w_1\left(t\right) &= \frac{x_2\left(\ell\right)x_1\left(t\right) - x_1\left(\ell\right)x_2\left(t\right)}{x_1\left(0\right)x_2\left(\ell\right) - x_1\left(\ell\right)x_2\left(0\right)} \\ &= \frac{\sinh\left(\sqrt{\lambda}\left(\ell - t\right)\right)}{\sinh\left(\sqrt{\lambda}\ell\right)}, \end{aligned}$$

$$\begin{aligned} w_2\left(t\right) &= \frac{x_1\left(0\right)x_2\left(t\right) - x_2\left(0\right)x_1\left(t\right)}{x_1\left(0\right)x_2\left(\ell\right) - x_1\left(\ell\right)x_2\left(0\right)} \\ &= \frac{\sinh\left(\sqrt{\lambda}t\right)}{\sinh\left(\sqrt{\lambda}\ell\right)}. \end{aligned}$$

Then, the solution of the problem (3.3) is

$$y\left(t\right) = \frac{\sinh\left(\sqrt{\lambda}\left(\ell - t\right)\right)}{\sinh\left(\sqrt{\lambda}\ell\right)}\left(\frac{\underline{c}-\overline{c}}{2}, 0, \frac{\overline{c}-\underline{c}}{2}\right) + \frac{\sinh\left(\sqrt{\lambda}t\right)}{\sinh\left(\sqrt{\lambda}\ell\right)}\left(\frac{\underline{d}-\overline{d}}{2}, 0, \frac{\overline{d}-\underline{d}}{2}\right). \tag{3.6}$$

Since the solution of the equation $y^{''} = \lambda y - 1$ is

$$y_{-1}(t) = -\frac{1}{\lambda}\left\{\frac{\sinh\left(\sqrt{\lambda}(\ell - t)\right)}{\sinh\left(\sqrt{\lambda}\ell\right)} + \frac{\sinh\left(\sqrt{\lambda}t\right)}{\sinh\left(\sqrt{\lambda}\ell\right)} - 1\right\}$$

and the solution of the equation $y^{''} = \lambda y + 1$ is

$$y_{1}(t) = \frac{1}{\lambda}\left\{\frac{\sinh\left(\sqrt{\lambda}(\ell - t)\right)}{\sinh\left(\sqrt{\lambda}\ell\right)} + \frac{\sinh\left(\sqrt{\lambda}t\right)}{\sinh\left(\sqrt{\lambda}\ell\right)} - 1\right\},$$

the solution of fuzzy boundary value problem (3.4) is

$$y(t) = \{\min\{y_{-1}(t), 0, y_1(t)\}, 0, \max\{y_{-1}(t), 0, y_1(t)\}\}. \tag{3.7}$$

Then, from (3.6) and (3.7), the fuzzy lower solution is

$$\underline{y}(t) = \frac{\sinh\left(\sqrt{\lambda}(\ell - t)\right)}{\sinh\left(\sqrt{\lambda}\ell\right)}\left(\frac{\underline{c} - \overline{c}}{2} - \frac{1}{\lambda}\right) + \frac{\sinh\left(\sqrt{\lambda}t\right)}{\sinh\left(\sqrt{\lambda}\ell\right)}\left(\frac{\underline{d} - \overline{d}}{2} - \frac{1}{\lambda}\right) + \frac{1}{\lambda}, \tag{3.8}$$

and the fuzzy upper solution is

$$\overline{y}(t) = \frac{\sinh\left(\sqrt{\lambda}(\ell - t)\right)}{\sinh\left(\sqrt{\lambda}\ell\right)}\left(\frac{\overline{c} - \underline{c}}{2} + \frac{1}{\lambda}\right) + \frac{\sinh\left(\sqrt{\lambda}t\right)}{\sinh\left(\sqrt{\lambda}\ell\right)}\left(\frac{\overline{d} - \underline{d}}{2} + \frac{1}{\lambda}\right) - \frac{1}{\lambda}. \tag{3.9}$$

That is, the fuzzy solution is

$$\widetilde{y}(t) = \left(\underline{y}(t), 0, \overline{y}(t)\right). \tag{3.10}$$

Finally, from (3.5) and (3.10), the solution of the problem (3.1) is

$$\widetilde{Y}(t) = \left(\underline{y}(t), y(t), \overline{y}(t)\right) \tag{3.11}$$

$$\begin{aligned}
\underline{y}(t) &= \frac{\sinh\left(\sqrt{\lambda}(\ell - t)\right)}{\sinh\left(\sqrt{\lambda}\ell\right)}\left(\underline{c} + \frac{2}{\lambda^2} - \frac{1}{\lambda}\right) + \frac{\sinh\left(\sqrt{\lambda}t\right)}{\sinh\left(\sqrt{\lambda}\ell\right)}\left(\underline{d} + \frac{2}{\lambda^2} + \frac{1}{\lambda}\left(\ell^2 - 1\right)\right) \\
&\quad + \frac{1}{\lambda}\left(1 - t^2\right) - \frac{2}{\lambda^2}, \\
y(t) &= \frac{\sinh\left(\sqrt{\lambda}(\ell - t)\right)}{\sinh\left(\sqrt{\lambda}\ell\right)}\left(\frac{\underline{c} + \overline{c}}{2} + \frac{2}{\lambda^2}\right) + \frac{\sinh\left(\sqrt{\lambda}t\right)}{\sinh\left(\sqrt{\lambda}\ell\right)}\left(\frac{\underline{d} + \overline{d}}{2} + \frac{1}{\lambda}\ell^2 + \frac{2}{\lambda^2}\right) \\
&\quad - \frac{1}{\lambda}t^2 - \frac{2}{\lambda^2},
\end{aligned}$$

$$\overline{y}(t) = \frac{\sinh\left(\sqrt{\lambda}(\ell-t)\right)}{\sinh\left(\sqrt{\lambda}\ell\right)}\left(\overline{c}+\frac{2}{\lambda^2}+\frac{1}{\lambda}\right)+\frac{\sinh\left(\sqrt{\lambda}t\right)}{\sinh\left(\sqrt{\lambda}\ell\right)}\left(\overline{d}+\frac{2}{\lambda^2}+\frac{1}{\lambda}\left(\ell^2+1\right)\right)$$
$$-\frac{1}{\lambda}\left(1+t^2\right)-\frac{2}{\lambda^2}.$$

3.2. **Solution Method 2.** The solution is according to the generalized differentiability. Consider $\alpha-$level sets of the boundary value problem (3.1), that is

$$y''(t)=\lambda y(t)+\left[t^2\right]^{\alpha}, y(0)=[\beta]^{\alpha}, y(\ell)=[\gamma]^{\alpha}, \tag{3.12}$$

where

$$\left[t^2\right]^{\alpha}=\left[t^2-1+\alpha, t^2+1-\alpha\right],$$
$$[\beta]^{\alpha}=\left[\underline{c}+\left(\frac{\overline{c}-\underline{c}}{2}\right)\alpha, \overline{c}-\left(\frac{\overline{c}-\underline{c}}{2}\right)\alpha\right],$$
$$[\gamma]^{\alpha}=\left[\underline{d}+\left(\frac{\overline{d}-\underline{d}}{2}\right)\alpha, \overline{d}-\left(\frac{\overline{d}-\underline{d}}{2}\right)\alpha\right].$$

Also, (i,j) solution means that y is i-differentiable and y' is j-differentiable (i,j=1,2).

Using the generalized differentiability and fuzzy arithmetic, for the solutions $(1,1)$ and $(2,2)$,

$$\begin{cases} \underline{y}_{\alpha}''=\lambda\underline{y}_{\alpha}+t^2-1+\alpha \\ \underline{y}_{\alpha}(0)=\underline{c}+\left(\frac{\overline{c}-\underline{c}}{2}\right)\alpha \\ \underline{y}_{\alpha}(\ell)=\underline{d}+\left(\frac{\overline{d}-\underline{d}}{2}\right)\alpha \end{cases} \tag{3.13}$$

$$\begin{cases} \overline{y}_{\alpha}''=\lambda\overline{y}_{\alpha}+t^2+1-\alpha \\ \overline{y}_{\alpha}(0)=\overline{c}-\left(\frac{\overline{c}-\underline{c}}{2}\right)\alpha \\ \overline{y}_{\alpha}(\ell)=\overline{d}-\left(\frac{\overline{d}-\underline{d}}{2}\right)\alpha \end{cases} \tag{3.14}$$

must be solved and for the solutions (1,2) and (2,1)

$$\begin{cases} \overline{y}_{\alpha}''=\lambda\underline{y}_{\alpha}+t^2-1+\alpha \\ \underline{y}_{\alpha}''=\lambda\overline{y}_{\alpha}+t^2+1-\alpha \\ \underline{y}_{\alpha}(0)=\underline{c}+\left(\frac{\overline{c}-\underline{c}}{2}\right)\alpha,\ \overline{y}_{\alpha}(0)=\overline{c}-\left(\frac{\overline{c}-\underline{c}}{2}\right)\alpha \\ \underline{y}_{\alpha}(\ell)=\underline{d}+\left(\frac{\overline{d}-\underline{d}}{2}\right)\alpha,\ \overline{y}_{\alpha}(\ell)=\overline{d}-\left(\frac{\overline{d}-\underline{d}}{2}\right)\alpha \end{cases} \tag{3.15}$$

must be solved.

(1) The solutions (1,1) and (2,2)

From the solutions of the differential equations in (3.13) and (3.14), the lower and the upper solutions of the boundary value problem (3.12) are obtained as

$$\underline{y}_{\alpha}(t)=\underline{c}_1e^{\sqrt{\lambda}t}+\underline{c}_2e^{-\sqrt{\lambda}t}-\frac{1}{\lambda}t^2-\frac{2}{\lambda^2}+\frac{1}{\lambda}(1-\alpha),$$

$$\overline{y}_{\alpha}(t)=\overline{c}_1e^{\sqrt{\lambda}t}+\overline{c}_2e^{-\sqrt{\lambda}t}-\frac{1}{\lambda}t^2-\frac{2}{\lambda^2}+\frac{1}{\lambda}(\alpha-1).$$

Using the boundary conditions, $\underline{c}_1,\underline{c}_2,\overline{c}_1,\overline{c}_2$ are solved as

$$\underline{c}_1=\frac{\left(\underline{d}+\left(\frac{\overline{d}-\underline{d}}{2}\right)\alpha+\frac{2}{\lambda^2}+\frac{1}{\lambda}\left(\ell^2+\alpha-1\right)\right)-e^{-\sqrt{\lambda}\ell}\left(\underline{c}+\left(\frac{\overline{c}-\underline{c}}{2}\right)\alpha+\frac{2}{\lambda^2}-\frac{1}{\lambda}(1-\alpha)\right)}{e^{\sqrt{\lambda}\ell}-e^{-\sqrt{\lambda}\ell}},$$

$$\underline{c}_2=\frac{e^{\sqrt{\lambda}\ell}\left(\underline{c}+\left(\frac{\overline{c}-\underline{c}}{2}\right)\alpha+\frac{2}{\lambda^2}-\frac{1}{\lambda}(1-\alpha)\right)-\left(\underline{d}+\left(\frac{\overline{d}-\underline{d}}{2}\right)\alpha+\frac{2}{\lambda^2}+\frac{1}{\lambda}\left(\ell^2+\alpha-1\right)\right)}{e^{\sqrt{\lambda}\ell}-e^{-\sqrt{\lambda}\ell}},$$

$$\overline{c}_1=\frac{\left(\overline{d}-\left(\frac{\overline{d}-\underline{d}}{2}\right)\alpha+\frac{2}{\lambda^2}+\frac{1}{\lambda}\left(\ell^2+1-\alpha\right)\right)-e^{-\sqrt{\lambda}\ell}\left(\overline{c}-\left(\frac{\overline{c}-\underline{c}}{2}\right)\alpha+\frac{2}{\lambda^2}-\frac{1}{\lambda}(\alpha-1)\right)}{e^{\sqrt{\lambda}\ell}-e^{-\sqrt{\lambda}\ell}},$$

$$\overline{c}_2=\frac{e^{\sqrt{\lambda}\ell}\left(\overline{c}-\left(\frac{\overline{c}-\underline{c}}{2}\right)\alpha+\frac{2}{\lambda^2}-\frac{1}{\lambda}(\alpha-1)\right)-\left(\overline{d}-\left(\frac{\overline{d}-\underline{d}}{2}\right)\alpha+\frac{2}{\lambda^2}+\frac{1}{\lambda}\left(\ell^2+1-\alpha\right)\right)}{e^{\sqrt{\lambda}\ell}-e^{-\sqrt{\lambda}\ell}}.$$

From this, for the solutions (1,1) and (2,2) the solution of (3.12) is

$$[y(t)]^{\alpha}=\left[\underline{y}_{\alpha}(t),\overline{y}_{\alpha}(t)\right], \tag{3.16}$$

$$\begin{aligned}\underline{y}_{\alpha}(t) &= \frac{\sinh\left(\sqrt{\lambda}(\ell-t)\right)}{\sinh\left(\sqrt{\lambda}\ell\right)}\left(\underline{c}+\left(\frac{\overline{c}-\underline{c}}{2}\right)\alpha+\frac{2}{\lambda^2}-\frac{1}{\lambda}(1-\alpha)\right) \\ &\quad+\frac{\sinh\left(\sqrt{\lambda}t\right)}{\sinh\left(\sqrt{\lambda}\ell\right)}\left(\underline{d}+\left(\frac{\overline{d}-\underline{d}}{2}\right)\alpha+\frac{2}{\lambda^2}+\frac{1}{\lambda}\left(\ell^2+\alpha-1\right)\right) \\ &\quad-\frac{1}{\lambda}t^2-\frac{2}{\lambda^2}+\frac{1}{\lambda}(1-\alpha),\end{aligned} \tag{3.17}$$

$$\begin{aligned}\overline{y}_{\alpha}(t) &= \frac{\sinh\left(\sqrt{\lambda}(\ell-t)\right)}{\sinh\left(\sqrt{\lambda}\ell\right)}\left(\overline{c}-\left(\frac{\overline{c}-\underline{c}}{2}\right)\alpha+\frac{2}{\lambda^2}-\frac{1}{\lambda}(\alpha-1)\right) \\ &\quad+\frac{\sinh\left(\sqrt{\lambda}t\right)}{\sinh\left(\sqrt{\lambda}\ell\right)}\left(\overline{d}-\left(\frac{\overline{d}-\underline{d}}{2}\right)\alpha+\frac{2}{\lambda^2}+\frac{1}{\lambda}\left(\ell^2+1-\alpha\right)\right) \\ &\quad-\frac{1}{\lambda}t^2-\frac{2}{\lambda^2}+\frac{1}{\lambda}(\alpha-1).\end{aligned} \tag{3.18}$$

Proposition 3.1 *The solution* (3.11) *according to the solution method 1 is the same as the solution* (3.16) *according to the solution method 2.*

Proof If $\alpha-cut$ of the solution (3.11) is taken, we have

$$\underline{y}_{\alpha}(t)=\underline{y}(t)+\left(\frac{\overline{y}(t)-\underline{y}(t)}{2}\right)\alpha,\quad \overline{y}_{\alpha}(t)=\overline{y}(t)-\left(\frac{\overline{y}(t)-\underline{y}(t)}{2}\right)\alpha,$$

$$\left[\widetilde{Y}(t)\right] = \left[\underline{y}_\alpha(t), \overline{y}_\alpha(t)\right].$$

That is, the proof is complete. □

Theorem 3.1 *The* $(1,1)$ *solution of the problem* (3.12) *is a valid* $\alpha-$ *level set for* $t\in[0,\ell]$ *satisfying the inequality*

$$\tanh\left(\sqrt{\lambda}t\right) - \left(\frac{\cosh\left(\sqrt{\lambda}\ell\right) - \left(\frac{\overline{d}-\underline{d}+\frac{2}{\lambda}}{\overline{c}-\underline{c}+\frac{2}{\lambda}}\right)}{\sinh\left(\sqrt{\lambda}\ell\right)}\right) \geq 0, \tag{3.19}$$

The $(2,2)$ *solution of the problem* (3.12) *is a valid* $\alpha-$ *level set for* $t\in[0,\ell]$ *satisfying the inequality*

$$\tanh\left(\sqrt{\lambda}t\right) - \left(\frac{\cosh\left(\sqrt{\lambda}\ell\right) - \left(\frac{\overline{d}-\underline{d}+\frac{2}{\lambda}}{\overline{c}-\underline{c}+\frac{2}{\lambda}}\right)}{\sinh\left(\sqrt{\lambda}\ell\right)}\right) \leq 0. \tag{3.20}$$

Proof If

$$\frac{\partial \underline{y}_\alpha(t)}{\partial\alpha} > 0,\ \frac{\partial \overline{y}_\alpha(t)}{\partial\alpha} < 0,\ \underline{y}_\alpha(t) \leq \overline{y}_\alpha(t),\ \underline{y}'_\alpha(t) \leq \overline{y}'_\alpha(t) \text{ and } \underline{y}''_\alpha(t) \leq \overline{y}''_\alpha(t),$$

the $(1,1)$ solution of the problem (3.12) is a valid $\alpha-$ level set.

If

$$\frac{\partial \underline{y}_\alpha(t)}{\partial\alpha} > 0,\ \frac{\partial \overline{y}_\alpha(t)}{\partial\alpha} < 0,\ \underline{y}_\alpha(t) \leq \overline{y}_\alpha(t),\ \overline{y}'_\alpha(t) \leq \underline{y}'_\alpha(t) \text{ and } \underline{y}''_\alpha(t) \leq \overline{y}''_\alpha(t),$$

the $(2,2)$ solution of the problem (3.12) is a valid $\alpha-$ level set.

For the $(1,1)$ solution,

$$\frac{\partial \underline{y}_\alpha(t)}{\partial\alpha} = \frac{\sinh\left(\sqrt{\lambda}(\ell-t)\right)}{\sinh\left(\sqrt{\lambda}\ell\right)}\left(\frac{\overline{c}-\underline{c}}{2}+\frac{1}{\lambda}\right) + \frac{\sinh\left(\sqrt{\lambda}t\right)}{\sinh\left(\sqrt{\lambda}\ell\right)}\left(\frac{\overline{d}-\underline{d}}{2}+\frac{1}{\lambda}\right) - \frac{1}{\lambda} > 0,$$

$$\frac{\partial \overline{y}_\alpha(t)}{\partial\alpha} = -\frac{\sinh\left(\sqrt{\lambda}(\ell-t)\right)}{\sinh\left(\sqrt{\lambda}\ell\right)}\left(\frac{\overline{c}-\underline{c}}{2}+\frac{1}{\lambda}\right) - \frac{\sinh\left(\sqrt{\lambda}t\right)}{\sinh\left(\sqrt{\lambda}\ell\right)}\left(\frac{\overline{d}-\underline{d}}{2}+\frac{1}{\lambda}\right) + \frac{1}{\lambda} < 0,$$

$$\begin{aligned}\overline{y}_\alpha(t) - \underline{y}_\alpha(t) &= (1-\alpha)\left(\frac{\sinh\left(\sqrt{\lambda}(\ell-t)\right)}{\sinh\left(\sqrt{\lambda}\ell\right)}\left(\overline{c}-\underline{c}+\frac{2}{\lambda}\right)\right.\\ &\left.+\frac{\sinh\left(\sqrt{\lambda}t\right)}{\sinh\left(\sqrt{\lambda}\ell\right)}\left(\overline{d}-\underline{d}+\frac{2}{\lambda}\right) - \frac{2}{\lambda}\right) \geq 0\end{aligned}$$

Also, derivating of (3.17) and (3.18), we have

$$\begin{aligned}\overline{y}_{\alpha}^{'}(t)-\underline{y}_{\alpha}^{'}(t) &= (1-\alpha)\left(-\frac{\sqrt{\lambda}\cosh\left(\sqrt{\lambda}\,(\ell-t)\right)}{\sinh\left(\sqrt{\lambda}\ell\right)}\left(\overline{c}-\underline{c}+\frac{2}{\lambda}\right)\right.\\ &\left.+\frac{\sqrt{\lambda}\cosh\left(\sqrt{\lambda}t\right)}{\sinh\left(\sqrt{\lambda}\ell\right)}\left(\overline{d}-\underline{d}+\frac{2}{\lambda}\right)\right).\end{aligned}$$

Then, if

$$\cosh\left(\sqrt{\lambda}t\right)\left(\overline{d}-\underline{d}+\frac{2}{\lambda}\right)\geq\cosh\left(\sqrt{\lambda}\,(\ell-t)\right)\left(\overline{c}-\underline{c}+\frac{2}{\lambda}\right),$$

we have

$$\underline{y}_{\alpha}^{'}(t)\leq\overline{y}_{\alpha}^{'}(t).$$

From this, making the necessary operations, it must be

$$\tanh\left(\sqrt{\lambda}t\right)\geq\frac{\cosh\left(\sqrt{\lambda}\ell\right)-\left(\frac{\overline{d}-\underline{d}+\frac{2}{\lambda}}{\overline{c}-\underline{c}+\frac{2}{\lambda}}\right)}{\sinh\sqrt{\lambda}\ell)}.$$

Also, again derivating of (3.17) and (3.18), we have

$$\begin{aligned}\overline{y}_{\alpha}^{''}(t)-\underline{y}_{\alpha}^{''}(t) &= (1-\alpha)\left(\frac{\lambda\sinh\left(\sqrt{\lambda}\,(\ell-t)\right)}{\sinh\left(\sqrt{\lambda}\ell\right)}\left(\overline{c}-\underline{c}+\frac{2}{\lambda}\right)\right.\\ &\left.+\frac{\lambda\sinh\left(\sqrt{\lambda}t\right)}{\sinh\left(\sqrt{\lambda}\ell\right)}\left(\overline{d}-\underline{d}+\frac{2}{\lambda}\right)\right)\geq 0.\end{aligned}$$

Consequently, the $(1,1)$ solution of the problem (3.12) is a valid $\alpha-$ level set for t$\in[0,\ell]$ satisfying the inequality (3.19). For the $(2,2)$ solution, the proof is similar. □

Theorem 3.2 *For any $t\in[0,\ell]$, the solutions (1,1) and (2,2) of the problem* (3.12) *are symmetric triangle fuzzy numbers.*

Proof Since

$$\begin{aligned}\underline{y}_{1}(t) &= \frac{\sinh\left(\sqrt{\lambda}\,(\ell-t)\right)}{\sinh\left(\sqrt{\lambda}\ell\right)}\left(\frac{\overline{c}+\underline{c}}{2}+\frac{2}{\lambda^{2}}\right)\\ &+\frac{\sinh\left(\sqrt{\lambda}t\right)}{\sinh\left(\sqrt{\lambda}\ell\right)}\left(\frac{\overline{d}+\underline{d}}{2}+\frac{2}{\lambda^{2}}+\frac{\ell^{2}}{\lambda}\right)-\frac{1}{\lambda}t^{2}-\frac{2}{\lambda^{2}}\\ &= \overline{y}_{1}(t),\end{aligned}$$

$$\begin{aligned}\underline{y}_1(t)-\underline{y}_\alpha(t) &= (1-\alpha)\left(\frac{\sinh\left(\sqrt{\lambda}(\ell-t)\right)}{\sinh\left(\sqrt{\lambda}\ell\right)}\left(\frac{\overline{c}-\underline{c}}{2}+\frac{1}{\lambda}\right)\right.\\ &\left.+\frac{\sinh\left(\sqrt{\lambda}t\right)}{\sinh\left(\sqrt{\lambda}\ell\right)}\left(\frac{\overline{d}-\underline{d}}{2}+\frac{1}{\lambda}\right)-\frac{1}{\lambda}\right)\\ &= \overline{y}_\alpha(t)-\overline{y}_1(t),\end{aligned}$$

the solutions $(1,1)$ and $(2,2)$ of the problem (3.12) are symmetric triangle fuzzy numbers for any $t\in[0,\ell]$. □

(2) The solutions (1,2) and (2,1)

Using the generalized differentiability and fuzzy arithmetic, the solution of (3.15) is

$$[y(t)]^\alpha=\left[\underline{y}_\alpha(t),\overline{y}_\alpha(t)\right], \tag{3.21}$$

$$\underline{y}_\alpha(t)=c_1e^{\sqrt{\lambda}t}+c_2e^{-\sqrt{\lambda}t}-c_3\sin\left(\sqrt{\lambda}t\right)-c_4\cos\left(\sqrt{\lambda}t\right)-\frac{1}{\lambda}t^2-\frac{2}{\lambda^2}+\frac{1}{\lambda}(1-\alpha),$$
$$\overline{y}_\alpha(t)=c_1e^{\sqrt{\lambda}t}+c_2e^{-\sqrt{\lambda}t}+c_3\sin\left(\sqrt{\lambda}t\right)+c_4\cos\left(\sqrt{\lambda}t\right)-\frac{1}{\lambda}t^2-\frac{2}{\lambda^2}-\frac{1}{\lambda}(1-\alpha).$$

From the boundary conditions, the coefficients c_1, c_2, c_3 and c_4 are obtained as

$$c_1=\frac{\left(\frac{1}{\lambda}\ell^2+\frac{2}{\lambda^2}+\frac{\overline{d}+\underline{d}}{2}\right)-e^{-\sqrt{\lambda}\ell}\left(\frac{2}{\lambda^2}+\frac{\overline{c}+\underline{c}}{2}\right)}{e^{\sqrt{\lambda}\ell}-e^{-\sqrt{\lambda}\ell}},$$

$$c_2=\frac{e^{\sqrt{\lambda}\ell}\left(\frac{2}{\lambda^2}+\frac{\overline{c}+\underline{c}}{2}\right)-\left(\frac{1}{\lambda}\ell^2+\frac{2}{\lambda^2}+\frac{\overline{d}+\underline{d}}{2}\right)}{e^{\sqrt{\lambda}\ell}-e^{-\sqrt{\lambda}\ell}},$$

$$c_3=\frac{(1-\alpha)\left(\frac{2}{\lambda}+\frac{\overline{c}-\underline{c}}{2}+\frac{\overline{d}-\underline{d}}{2}\right)}{\sin\left(\sqrt{\lambda}\ell\right)},\ \ \ell\neq\frac{n\pi}{\sqrt{\lambda}},$$

$$c_4=(1-\alpha)\left(\frac{1}{\lambda}+\frac{\overline{c}-\underline{c}}{2}\right).$$

Theorem 3.3 *The $(1,2)$ solution of the problem (3.12) is a valid $\alpha-$ level set for $t\in[0,\ell]$ satisfying the inequalities*

$$\left(\frac{\frac{2}{\lambda}+\frac{\overline{c}-\underline{c}}{2}+\frac{\overline{d}-\underline{d}}{2}}{\sin\left(\sqrt{\lambda}\ell\right)}\right)\sin\left(\sqrt{\lambda}t\right)+\left(\frac{1}{\lambda}+\frac{\overline{c}-\underline{c}}{2}\right)\cos\left(\sqrt{\lambda}t\right)-\frac{1}{\lambda}\geq 0, \tag{3.22}$$

$$\left(\frac{\frac{2}{\lambda}+\frac{\overline{c}-\underline{c}}{2}+\frac{\overline{d}-\underline{d}}{2}}{\sin\left(\sqrt{\lambda}\ell\right)}\right)\cos\left(\sqrt{\lambda}t\right)-\left(\frac{1}{\lambda}+\frac{\overline{c}-\underline{c}}{2}\right)\sin\left(\sqrt{\lambda}t\right)\geq 0. \tag{3.23}$$

The $(2,1)$ solution of the problem (3.12) is a valid $\alpha-$ level set for $t\in[0,\ell]$ satisfying the *inequalities*

$$\left(\frac{\frac{2}{\lambda}+\frac{\overline{c}-\underline{c}}{2}+\frac{\overline{d}-\underline{d}}{2}}{\sin\left(\sqrt{\lambda}\ell\right)}\right)\sin\left(\sqrt{\lambda}t\right)+\left(\frac{1}{\lambda}+\frac{\overline{c}-\underline{c}}{2}\right)\cos\left(\sqrt{\lambda}t\right)-\frac{1}{\lambda}\geq 0, \tag{3.24}$$

$$\left(\frac{\frac{2}{\lambda}+\frac{\overline{c}-\underline{c}}{2}+\frac{\overline{d}-\underline{d}}{2}}{\sin\left(\sqrt{\lambda}\ell\right)}\right)\cos\left(\sqrt{\lambda}t\right)-\left(\frac{1}{\lambda}+\frac{\overline{c}-\underline{c}}{2}\right)\sin\left(\sqrt{\lambda}t\right)\leq 0. \tag{3.25}$$

Proof If

$$\frac{\partial \underline{y}_{\alpha}(t)}{\partial\alpha}>0,\ \frac{\partial \overline{y}_{\alpha}(t)}{\partial\alpha}<0,\ \underline{y}_{\alpha}(t)\leq\overline{y}_{\alpha}(t),\ \underline{y}_{\alpha}^{'}(t)\leq\overline{y}_{\alpha}^{'}(t)\ \text{ and } \overline{y}_{\alpha}^{''}(t)\leq\underline{y}_{\alpha}^{''}(t),$$

the $(1,2)$ solution of the problem (3.12) is a valid $\alpha-$ level set.

If

$$\frac{\partial \underline{y}_{\alpha}(t)}{\partial\alpha}>0,\ \frac{\partial \overline{y}_{\alpha}(t)}{\partial\alpha}<0,\ \underline{y}_{\alpha}(t)\leq\overline{y}_{\alpha}(t),\ \overline{y}_{\alpha}^{'}(t)\leq\underline{y}_{\alpha}^{'}(t)\ \text{ and } \overline{y}_{\alpha}^{''}(t)\leq\underline{y}_{\alpha}^{''}(t),$$

the $(2,1)$ solution of the problem (3.12) is a valid $\alpha-$ level set.

For the $(1,2)$ solution, from

$$\frac{\partial \underline{y}_{\alpha}(t)}{\partial\alpha}>0,\ \frac{\partial \overline{y}_{\alpha}(t)}{\partial\alpha}<0 \text{ and } \overline{y}_{\alpha}(t)-\underline{y}_{\alpha}(t)\geq 0,$$

it must satisfies the inequality (3.22), from $\overline{y}_{\alpha}^{'}(t)-\underline{y}_{\alpha}^{'}(t)\geq 0$, it must satisfies the inequality (3.23). Also, from $\underline{y}_{\alpha}^{''}(t)-\overline{y}_{\alpha}^{''}(t)\geq 0$, it must be

$$\left(\frac{\frac{2}{\lambda}+\frac{\overline{c}-\underline{c}}{2}+\frac{\overline{d}-\underline{d}}{2}}{\sin\left(\sqrt{\lambda}\ell\right)}\right)\sin\left(\sqrt{\lambda}t\right)+\left(\frac{1}{\lambda}+\frac{\overline{c}-\underline{c}}{2}\right)\cos\left(\sqrt{\lambda}t\right)\geq 0.$$

Then, the $(1,2)$ solution of the problem (3.12) is a valid $\alpha-$ level set for t$\in[0,\ell]$ satisfying the inequalities (3.22) and (3.23). For the $(2,1)$ solution, the proof is similar. □

Theorem 3.4 *For any $t\in[0,\ell]$, the solutions (1,2) and (2,1) of the problem* (3.12) *are symmetric triangle fuzzy numbers.*

Proof Since

$$\underline{y}_{1}(t)=c_1e^{\sqrt{\lambda}t}+c_2e^{-\sqrt{\lambda}t}-\frac{1}{\lambda}t^2-\frac{2}{\lambda^2}=\overline{y}_1(t),$$

$$\underline{y}_{1}(t)-\underline{y}_{\alpha}(t)=c_3\sin\left(\sqrt{\lambda}t\right)+c_4\cos\left(\sqrt{\lambda}t\right)-\frac{1}{\lambda}(1-\alpha)=\overline{y}_{\alpha}(t)-\overline{y}_1(t),$$

the solutions (1,2) and (2,1) of the problem (3.12) are symmetric triangle fuzzy numbers for any $t\in[0,\ell]$. □

Example 3.1 Consider the fuzzy boundary value problem

$$y^{''}(t) = y(t) + \left[t^2\right]^\alpha, y(0) = [0]^\alpha, y(1) = [1]^\alpha, \tag{3.26}$$

and $[0]^\alpha = [-1+\alpha, 1-\alpha]$, $[1]^\alpha = [\alpha, 2-\alpha]$. Then, the $(1,1)$ and $(2,2)$ solutions of the problem (3.26) are

$$\underline{y}_\alpha(t) = \frac{2\alpha\sinh(1-t)}{\sinh(1)} + \frac{(2\alpha+2)\sinh(t)}{\sinh(1)} - t^2 - 1 - \alpha, \tag{3.27}$$

$$\overline{y}_\alpha(t) = \frac{(4-2\alpha)\sinh(1-t)}{\sinh(1)} + \frac{(6-2\alpha)\sinh(t)}{\sinh(1)} - t^2 - 3 + \alpha. \tag{3.28}$$

$$[y(t)]^\alpha = \left[\underline{y}_\alpha(t), \overline{y}_\alpha(t)\right]. \tag{3.29}$$

The $(1,2)$ and $(2,1)$ solutions of the problem (3.26) are

$$\begin{aligned} \underline{y}_\alpha(t) &= \left(\frac{4-2e^{-1}}{e-e^{-1}}\right)e^t + \left(\frac{2e-4}{e-e^{-1}}\right)e^{-t} - \left(\frac{4(1-\alpha)}{\sin(1)}\right)\sin(t) \\ &\quad -2(1-\alpha)\cos(t) - t^2 - \alpha - 1, \end{aligned} \tag{3.30}$$

$$\begin{aligned} \overline{y}_\alpha(t) &= \left(\frac{4-2e^{-1}}{e-e^{-1}}\right)e^t + \left(\frac{2e-4}{e-e^{-1}}\right)e^{-t} + \left(\frac{4(1-\alpha)}{\sin(1)}\right)\sin(t) \\ &\quad +2(1-\alpha)\cos(t) - t^2 + \alpha - 3. \end{aligned} \tag{3.31}$$

$$[y(t)]^\alpha = \left[\underline{y}_\alpha(t), \overline{y}_\alpha(t)\right]. \tag{3.32}$$

The $(1,1)$ solution is a valid $\alpha-$ level set for t$\in[0,1]$ satisfying the inequality $\tanh(t) - \left(\frac{\cosh(1)-1}{\sinh(1)}\right) \geq 0$, the $(2,2)$ solution is a valid $\alpha-$ level set for t$\in[0,1]$ satisfying the inequality $\tanh(t) - \left(\frac{\cosh(1)-1}{\sinh(1)}\right) \leq 0$.

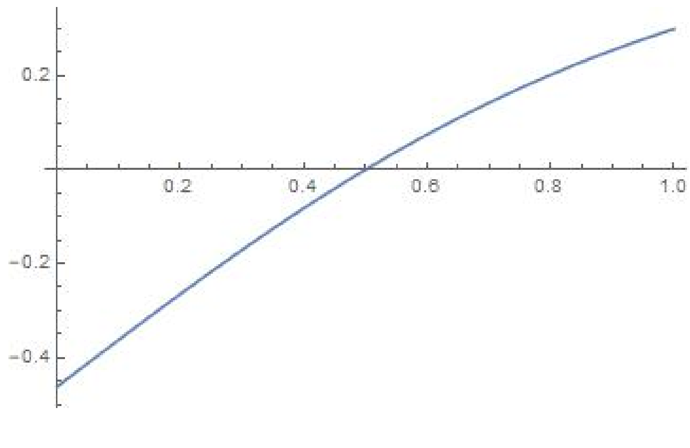

Figure 1. Graphic of the function $\tanh(t) - \left(\frac{\cosh(1)-1}{\sinh(1)}\right)$

According to Figure 1, the $(1,1)$ solution is a valid $\alpha-$ level set for $t \geq 0.5$ and the $(2,2)$ solution is a valid $\alpha-$ level set for $t \leq 0.5$

The $(1,2)$ solution is a valid $\alpha-$ level set for t$\in[0,1]$ satisfying the inequalities $\frac{4\sin(t)}{\sin(1)}+2\cos(t)-1\geq 0$ and $\frac{4\cos(t)}{\sin(1)}-2\sin(t)\geq 0$. The $(1,2)$ solution is a valid $\alpha-$ level set for t$\in[0,1]$ satisfying the inequalities $\frac{4}{\sin(1)}\sin(t)+2\cos(t)-1\geq 0$ and $\frac{4}{\sin(1)}\cos(t)-2\sin(t)\leq 0$.

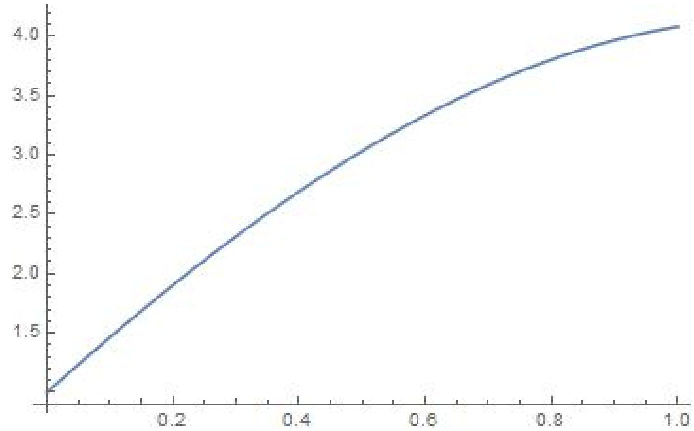

Figure 2. Graphic of the function $\frac{4\sin(t)}{\sin(1)}+2\cos(t)-1$

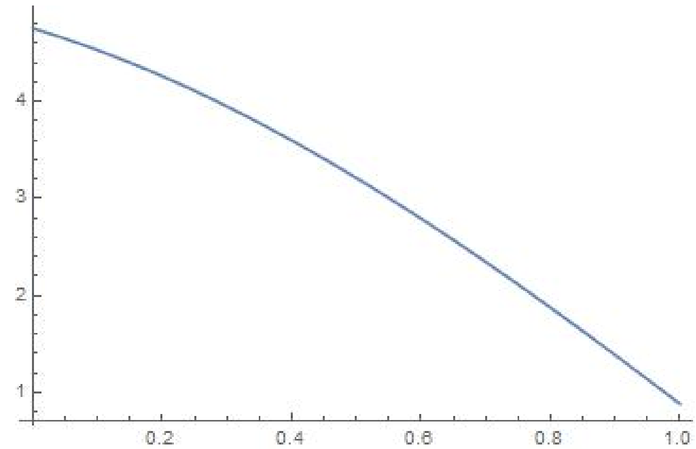

Figure 3. Graphic of the function $\frac{4\cos(t)}{\sin(1)}-2\sin(t)$

According to Figure 2 and Figure 3, the $(1,2)$ solution is a valid $\alpha-$ level set and the $(2,1)$ solution is not a valid $\alpha-$ level set.

Also, the solutions (3.27)-(3.29) and (3.30)-(3.32) are symmetric triangular fuzzy numbers for any $t\in[0,1]$.

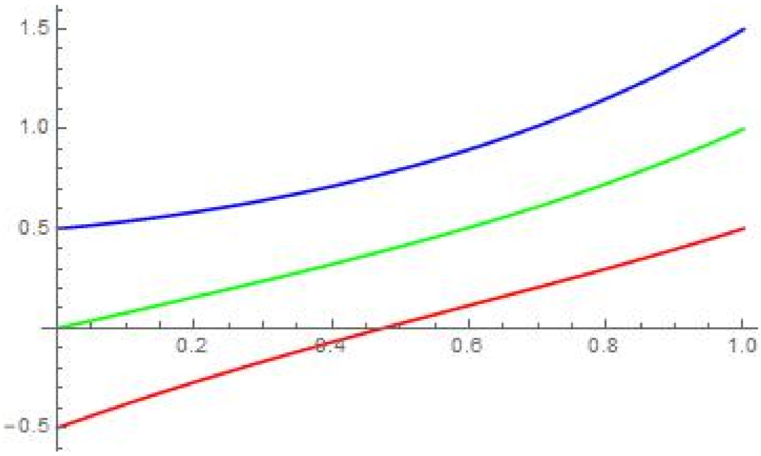

Figure 4. Graphic of (3.27)-(3.29) for $\alpha = 0.5$
Blue $\rightarrow \overline{y}_\alpha(t)$, Red $\rightarrow \underline{y}_\alpha(t)$, Green $\rightarrow \overline{y}_1(t) = \underline{y}_1(t)$

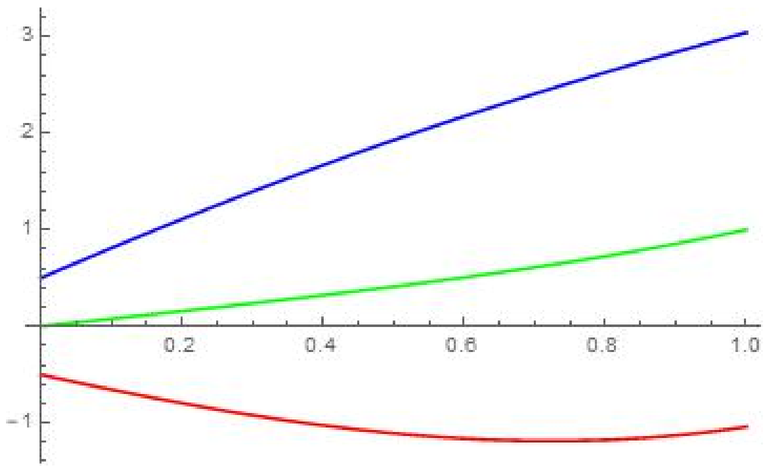

Figure 5. Graphic of (3.30)-(3.32) for $\alpha = 0.5$
Blue $\rightarrow \overline{y}_\alpha(t)$, Red $\rightarrow \underline{y}_\alpha(t)$, Green $\rightarrow \overline{y}_1(t) = \underline{y}_1(t)$

§4. **Conclusion**

In this paper, a problem with fuzzy forcing function and fuzzy boundary values is investigated. The problem is solved by two different solution methods. It is found that the solution of the problem according to the solution method 1 is the same as the solution according to the solution method 2 for the solutions (1,1) and (2,2). It is shown whether the solutions (1,1), (2,2), (1,2) and (2,1) are valid $\alpha-$level sets or not. Also, all the solutions are symmetric triangle fuzzy numbers for any $t \in [0, \ell]$. Example is solved. It is shown whether the solutions are valid fuzzy functions or not. Graphics of solutions are drawn. The solution method 2, that is, solution method according to the generalized differentiability is more useful than the solution method 1. Because, it is found the wider solutions of the problem with the solution method 2.

References

[1] Allahviranloo T., Abbasbandy S. and Behzadi S. S., Solving nonlinear fuzzy differential equations by using fuzzy variational iteration method, *Soft Computing*, 18(11)(2014), 2191-2200.

[2] Allahviranloo T., Abbasbandy S., Sedaghgatfar O. and Darabi P., A new method for solving fuzzy integro-differential equation under generalized differentiability, *Neural Computing and Applications*, 21(1) (2012), 191-196.

[3] Altınışık N. and Ceylan T., Second order fuzzy boundary value problem with fuzzy parameter, *Journal of the Institute of Science and Tecnology*, 10(1) (2020), 584-594.

[4] Bede B., Note on "Numerical solutions of fuzzy differential equations by predictor-corrector method", *Information Sciences*, 178(7) (2008), 1917-1922.

[5] Buckley J.J. and Feuring T., Fuzzy differential equations, *Fuzzy Sets and Systems*, 110(1) (2000), 43-54.

[6] Buckley J.J. and Feuring T., Fuzzy initial value problem for Nth-order linear differential equations, *Fuzzy Sets and Systems*,121(2) (2001), 247-255.

[7] Dubois D. and Prade H., Operations on fuzzy numbers, *International Journal of Systems Sciences* 9(6) (1978), 613-626.

[8] Gasilov N., Amrahov Ş.E. and Fatullayev A.G., A geometric approach to solve fuzzy linear systems of differential equations, *Applied Mathematics and Information Sciences,* 5(3) (2011), 484-499.

[9] Gasilov N., Amrahov Ş.E., Fatullayev A.G. and Hashimoğlu I.F., Solution method for a boundary value problem with fuzzy forcing function, *Information Sciences*, 317 (2015), 349-368.

[10] Ghavami B., Raji M., Rasaizadi R. and Mashinchi M., Process variation-aware gate sizing with fuzzy geometric programming, *Computers and Electrical Engineering,* 78 (2019), 259-270.

[11] Gouyandeh Z., Allahviranloo T., Abbasbandy S. and Armand A., A fuzzy solution of heat equation under generalized Hukuhara differentiability by fuzzy Fourier transform, *Fuzzy Sets and Systems*, 309 (2017), 81-97.

[12] Guo X., Shang D. and Lu X., Fuzzy approximate solutions of second-order fuzzy linear boundary value problems, *Boundary Value Problems*, 2013:212, doi:10.1186/1687-2770-2013-212, (2013), 1-17.

[13] Gültekin Çitil H., Comparisons of the exact and the approximate solutions of second-order fuzzy linear boundary value problems, *Miskolc Mathematical Notes,* 20(2) (2019), 823-837.

[14] Hüllermeier E., An approach to modelling and simulation of uncertain dynamical systems, *International Journal of Uncertainty, Fuzziness and Knowledge-Based Systems,* 5(2) (1997), 117-137.

[15] Kaleva O., Fuzzy differential equations, *Fuzzy Sets and Systems*, 24(3) (1987), 301-317.

[16] Khastan A., Bahrami F. and Ivaz K., New results on multiple solutions for Nth-order fuzzy differential equations under generalized differentiability, *Boundary Value Problems,* doi:10.1155/2009/395714, (2009), 1-13.

[17] Khastan A. and Nieto J.J, A boundary value problem for second order fuzzy differential equations, *Nonlinear Analysis:Theory, Methods and Applications*, 72(9-10) (2010), 3583-3593.

[18] Kouchakinejad F., Mashinchi M. and Meisar R., Solution-set invariant matrices and vektors in fuzzy relation inequalities based on max-aggregation function composition, *Iranian Journal of Fuzzy Systems,* 13(7) (2016), 91-100.

[19] Liu H.-K., Comparison results of two-point fuzzy boundary value problems*, International Journal of Computational and Mathematical Sciences*, 5(1) (2011), 1-7.

[20] Mosleh M. and Otadi M., Approximate solution of fuzzy differential equations under generalized differentiability*, Applied Mathematical Modelling*, 39(10-11) (2015), 3003-3015.

[21] Puri M.L. and Ralescu D.A., Differentials of fuzzy functions, *Journal of Mathematical Analysis and Applications*, 91(2) (1983), 552-558.

[22] Salahshour S. and Allahviranloo T., Applications of fuzzy Laplace transforms, *Soft Computing*, 17(1) (2013), 145-158.

[23] Thangamuthu M. and Thippan J., Numerical solution for Hybrid fuzzy differential equation by fifth order Runge-Kutta Nystrom method, *Journal of Mathematical Sciences and Modelling*, 2(1) (2019), 39-50.

International J.Math. Combin. Vol.2(2021), 17-32

The Variation of Electric Field With Respect to Darboux Triad in Euclidean 3-Space

Nevin Ertuğ Gürbüz

(Eskişehir Osmangazi University, Mathematics-Computer Department, Turkey)

E-mail: ngurbuz@ogu.edu.tr

Abstract: In this paper three electric fields are described via Darboux triad components in Euclidean 3-space. Later variations of three cases of electric field with respect to Darboux triad are studied. Finally Lorentz force equations are presented via electromagnetic magnetic curves with respect to Darboux triad in Euclidean 3-space.

Key Words: Geometric phase, Darboux frame, electric field.

AMS(2010): 53A35, 53B30, 78A05.

§1. Introduction

The geometric phase is described as the angle of rotation a light wave travelling in optic. The phenomenon of a geometric phase have many applications in condensed-matter physics, optics, particle physics, gravity, cosmology, chemical physics and mathematics [1-6]. The geometric phase is connected with parallel transport of the polarization along curved light [7-9].

Berry studied adiabatic phase and Pancharatnam's phase for polarized light [10]. Recently numerous authors presented the the electric field variation of along an optical fiber [11-14].

Balakrishnan *et al.* presented anholonomy density via Frenet triad in Euclidean 3-space $\mathcal{E}^3$ [15]. Three geometric phases and parallel transports for numerous frames have been investigated by Gürbüz in [16-20]. Balakrishnan introduced geometric phase for first class associated with some solitons for Darboux triad in $\mathcal{E}^3$ [21]. New classes associated with the nonlinear Schrödinger NLS equation for Darboux triad in $\mathcal{E}^3$ have been given in [22].

The electric polarization theory contains the geometric phase phenomenon [23]. Mukunda and Simon showed that the unit electric vector field $\mathbf{E}$ is written via the principal normal vector field $\mathbf{N}$ and the binormal vector field $\mathbf{B}$ of the Frenet triad $\{\mathbf{T}, \mathbf{N}, \mathbf{B}\}$ in Euclidean 3-space [24]. In this paper we express three electric fields via Darboux triad apparatus. Later evolutions of three electric fields are studied via Darboux triad in $\mathcal{E}^3$. Eventually Lorentz force equations are obtained via electromagnetic curves with respect to Darboux triad in $\mathcal{E}^3$.

[1]Supported by the Scientific Research Agency of Eskişehir Osmangazi University (ESOGU BAP Project No.202019016).

[2]Received January 3, 2021, Accepted June 5, 2021.

§2. Preliminaries

Let Γ_1 be a curve on a connected surface S with the arc length σ in $\mathcal{E}^3$. Apart from Frenet triad, at every point of curve, there is a Darboux triad $\{\mathbf{t},\mathbf{g},\mathbf{n}\}$. $\mathbf{t}$ is the tangent vector, $\mathbf{n}$ is the normal of surface and $\mathbf{g}=\mathbf{t}\times\mathbf{n}$. The spatial evolution of the Darboux triad $\{\mathbf{t},\mathbf{g},\mathbf{n}\}$ is given by [25]

$$\begin{bmatrix} \mathbf{t}_\sigma \\ \mathbf{g}_\sigma \\ \mathbf{n}_\sigma \end{bmatrix} = \begin{bmatrix} 0 & \kappa_g^{(\varsigma)} & \kappa_n^{(\varsigma)} \\ -\kappa_g^{(\varsigma)} & 0 & \tau_g^{(\varsigma)} \\ -\kappa_n^{(\varsigma)} & -\tau_g^{(\varsigma)} & 0 \end{bmatrix} \begin{bmatrix} \mathbf{t} \\ \mathbf{g} \\ \mathbf{n} \end{bmatrix} \tag{1}$$

$\kappa_g^{(\varsigma)}$ is the geodesic curvature, the normal curvature is $\kappa_n^{(\varsigma)}$ and $\tau_g^{(\varsigma)}$ is the geodesic torsion of the curve Γ_1. The time evolution of the Darboux triad $\{\mathbf{t},\mathbf{g},\mathbf{n}\}$ is given by

$$\begin{bmatrix} \mathbf{t}_u \\ \mathbf{g}_u \\ \mathbf{n}_u \end{bmatrix} = \begin{bmatrix} 0 & \kappa_g^{(o)} & \kappa_n^{(o)} \\ -\kappa_g^{(o)} & 0 & \tau_g^{(o)} \\ -\kappa_n^{(o)} & -\tau_g^{(o)} & 0 \end{bmatrix} \begin{bmatrix} \mathbf{t} \\ \mathbf{g} \\ \mathbf{n} \end{bmatrix} \tag{2}$$

where u denotes time and $\mathbf{t}_u = \frac{\partial \mathbf{t}}{\partial u}$.

A magnetic field is a closed 2-form $\mathcal{F}$ in $\mathcal{E}^3$. The Lorentz force Φ of a magnetic background $(\mathcal{E}^3, \langle,\rangle)$ is a (1,1) type skew-symmetric tensor and it is described as

$$\mathcal{F}(x,y) = \langle \Phi x, y\rangle$$

$x, y \in \chi(\mathcal{E}^3)$. A smooth curve Γ in $(\mathcal{E}^3, \langle,\rangle)$ is described as a magnetic curve of the dynamical system connected with the magnetic field $\mathcal{F}$ if its velocity vector field satisfies the following differential equation $\Gamma_{\sigma\sigma} = \Phi(\Gamma_\sigma)$. Divergence free vector fields and magnetic fields are one to one correspondence, the Lorentz force Φ concerned with the magnetic field $\mathbf{M}$ [26], [27]

$$\Phi(x) = \mathbf{M} \wedge x.$$

§3. Geometric Phase for First Case of Electric Field with Darboux Triad in $\mathcal{E}^3$

Balakrishan introduced first frame $\{\mathbf{P}_1,\mathbf{P}_2,\mathbf{P}_2^*\}$ and first transformation ξ of curve evolution concerned with the NLS equation with respect to Darboux triad in $\mathcal{E}^3$ as following [21] :

$$\begin{aligned} \mathbf{P}_1 &= \mathbf{t},\ \mathbf{P}_2 = \frac{\mathbf{g}+i\mathbf{n}}{\sqrt{2}} e^{i\int^\sigma \tau_g^{(\varsigma)} d\sigma'},\ \ \mathbf{P}_2^* = \frac{\mathbf{g}-i\mathbf{n}}{\sqrt{2}} e^{-i\int^\sigma \tau_g^{(\varsigma)} d\sigma'} && (3) \\ \xi &= \frac{\kappa_g + i\kappa_n}{\sqrt{2}} e^{i\int^\sigma \tau_g^{(\varsigma)} d\sigma'}. && (4) \end{aligned}$$

The spatial evolution of the first frame $\{\mathbf{P}_1,\mathbf{P}_2,\mathbf{P}_2^*\}$ is given by

$$\mathbf{P}_{1\sigma} = \xi^*\mathbf{P}_2 + \xi\mathbf{P}_2^*,\ \ \mathbf{P}_{2\sigma} = -\xi\mathbf{P}_1,\ \ \mathbf{P}_{2\sigma}^* = -\xi^*\mathbf{P}_1 \tag{5}$$

where ξ^* is the conjugate of ξ. Also temporal evolution of $\{\mathbf{P}_1, \mathbf{P}_2, \mathbf{P}_2^*\}$ is

$$\mathbf{P}_{1u} = \mathbf{t}_u = -\lambda^* \mathbf{P}_2 - \lambda \mathbf{P}_2^* \tag{6}$$

$$\mathbf{P}_{2u} = \lambda \mathbf{P}_1 + i\mathcal{I}\mathbf{P}_2 \tag{7}$$

where $\mathcal{I}(\sigma, u)$ is a real function. From $\mathbf{P}_{2u\sigma} = \mathbf{P}_{2\sigma u}$, it can be obtained:

$$\mathcal{I}_\sigma = i\lambda\xi^* - i\lambda^*\xi. \tag{8}$$

where

$$\mathcal{AD}_1 d\sigma du = (\tau_{gu}^{(o)} - \tau_{gs}^{(\varsigma)}) d\sigma du$$

is first anholonomy density measure for polarization plane of linearized light wave travelling along optic fiber in $\mathcal{E}^3$ [21].

$$\lambda = -\frac{(r + iw)}{\sqrt{2}} e^{i\int \tau_g^{(\varsigma)} d\sigma'} \tag{9}$$

satisfies Eqs.(6), (7) and (8). The time evolution of the Darboux triad is given by

$$\mathbf{t}_u = \varsigma_1^{(o)} \times \mathbf{t} = r\mathbf{g} + w\mathbf{n} \tag{10}$$

$$\mathbf{g}_u = \varsigma_1^{(o)} \times \mathbf{g} = -r\mathbf{t} + \tau_g^{(o)}\mathbf{n} \tag{11}$$

$$\mathbf{n}_u = \varsigma_1^{(o)} \times \mathbf{n} = -w\mathbf{t} - \tau_g^{(o)}\mathbf{g} \tag{12}$$

where $\varsigma_1^{(o)} = (\tau_g^{(o)}\mathbf{t} + B_1\mathbf{g} + C_1\mathbf{n})$, $r = C_1$, $w = -B_1$. Using Eq.(4) and Eq.(9), $\mathcal{I}_\sigma = \kappa_n^{(\varsigma)} r - \kappa_g^{(\varsigma)} w$. The time evolution of Darboux triad for first class can be written by

$$\mathbf{t}_u = r\mathbf{g} + w\mathbf{n} \tag{13}$$

$$\mathbf{g}_u = -r\mathbf{t} + \left(\int^{\sigma_1} \tau_{gu}^{(\varsigma)} d\sigma' - \mathcal{I}\right)\mathbf{n} \tag{14}$$

$$\mathbf{n}_u = -w\mathbf{t} - \left(\int^{\sigma_1} \tau_{gu}^{(\varsigma)} d\sigma' - \mathcal{I}\right)\mathbf{g} \tag{15}$$

and anholonomy density

$$\mathcal{AD}_1(\sigma, u) = -\mathcal{I}_\sigma = -r\kappa_n^{(\varsigma)} + w\kappa_g^{(\varsigma)}$$

for first class. Total phase $\mathcal{P}$ for first class with respect to Darboux triad in Euclidean 3-space is given by

$$\begin{aligned} \mathcal{P} &= -\int_{u_1}^{u_2}\int_{\sigma_0}^{\sigma_1} \mathcal{I}_\sigma d\sigma du = \int_{u_1}^{u_2}\int_{\sigma_0}^{\sigma_1} \langle \mathbf{t}, \mathbf{t}_\sigma \times \mathbf{t}_u \rangle \, d\sigma du \\ &= \int_{u_1}^{u_2}\int_{\sigma_0}^{\sigma_1} (-r\kappa_n^{(\varsigma)} + w\kappa_g^{(\varsigma)}) d\sigma du \end{aligned}$$

Also [22]

$$\begin{aligned}
\mathbf{P}_{1u} &= -i\xi_\sigma^*\mathbf{P}_2 + i\xi_\sigma\mathbf{P}_2^* \\
\mathbf{P}_{2u} &= -i\xi_\sigma\mathbf{P}_1 + \mathcal{I}\mathbf{P}_2, \\
\mathbf{P}_{2u}^* &= i\xi_\sigma^* - \mathcal{I}\mathbf{P}_2^*,\ \mathcal{I} = i\xi\xi^*.
\end{aligned}$$

From $\mathbf{P}_{1u\sigma} = \mathbf{P}_{1\sigma u}$ and $\mathbf{P}_{2u\sigma} = \mathbf{P}_{2\sigma u}$, the NLS equation system

$$\begin{aligned}
\xi_u &= i\xi_{\sigma\sigma} + i\left|\xi\right|^2\xi \\
\xi_u^* &= -i\xi_{\sigma\sigma} - i\left|\xi\right|^2\xi.
\end{aligned}$$

is obtained.

A optical fiber can be described by the curve $\Gamma_1(\sigma)$ on any surface with respect to Darboux triad in $\mathcal{E}^3$. The change of the electric field $\mathbf{E}_1$ can be written by

$$\mathbf{E}_{1\sigma} = \varphi_1\mathbf{t} + \varphi_2\mathbf{g} + \varphi_3\mathbf{n}. \tag{16}$$

Case 1. Assume that

$$\langle\mathbf{E}_1, \mathbf{t}\rangle = 0. \tag{17}$$

Using Eq.(16) and Eq.(17), it can be obtained

$$\varphi_1 = -\kappa_g\langle\mathbf{E}_1, \mathbf{g}\rangle - \kappa_n\langle\mathbf{E}_1, \mathbf{n}\rangle\ . \tag{18}$$

When no various loss mechanism along the optic fiber,

$$\langle\mathbf{E}_1, \mathbf{E}_1\rangle = const. \tag{19}$$

Using Eq.(16) and taking derivative with respect to σ of Eq.(19), it can be derived

$$\varphi_2\langle\mathbf{E}_1, \mathbf{g}\rangle = -\varphi_3\langle\mathbf{E}_1, \mathbf{n}\rangle\,. \tag{20}$$

Via Eq.(20), it can be obtained

$$\varphi_2 = \varpi\langle\mathbf{E}_1, \mathbf{n}\rangle\,, \quad \varphi_3 = -\langle\mathbf{E}_1, \mathbf{g}\rangle \tag{21}$$

The evolution for the polarization of light wave travelling from the point $\Gamma_1(\sigma_0)$ to the point $\Gamma_1(\sigma_1)$ along the $\Gamma_1 = \Gamma_1(\sigma)$ curve with respect to Darboux triad is given by the evolution of the electric field $\mathbf{E}_1$.

Consider $\langle\mathbf{E}_1, \mathbf{g}\rangle \neq 0$, $\langle\mathbf{E}_1, \mathbf{n}\rangle \neq 0$. Substituting Eqs.(18) and (21) in Eq.(16), the change of the electric field $\mathbf{E}_1$ is written by

$$\mathbf{E}_{1\sigma} = (-\kappa_g\langle\mathbf{E}_1, \mathbf{g}\rangle - \kappa_n\langle\mathbf{E}_1, \mathbf{n}\rangle)\mathbf{t} + \varpi\langle\mathbf{E}_1, \mathbf{n}\rangle\mathbf{g} - \varpi\langle\mathbf{E}_1, \mathbf{g}\rangle\mathbf{n} \tag{22}$$

where ϖ is a parameter. Using Eq.(20) for $\varpi = 0$, Eq.(22) is rewritten by

$$\mathbf{E}_{1\sigma} = (-\kappa_g \langle \mathbf{E}_1, \mathbf{g} \rangle - \kappa_n \langle \mathbf{E}_1, \mathbf{n} \rangle)\mathbf{t} \tag{23}$$

The Fermi-Walker derivative of the electric field $\mathbf{E}_1$ with respect to Darboux triad in $\mathcal{E}^3$ is given by

$$^{DFW}\mathbf{E}_{1\sigma} = \mathbf{E}_{1\sigma} - \langle \mathbf{t}, \mathbf{E}_1 \rangle \mathbf{t}_\sigma + \langle \mathbf{t}_\sigma, \mathbf{E}_1 \rangle \mathbf{t}. \tag{24}$$

The electric field $\mathbf{E}_1$ is the Fermi-Walker parallel transport if and only if

$$^{DFW}\mathbf{E}_{1\sigma} = 0. \tag{25}$$

Using Eqs.(17), (24) and (25) it can be obtained

$$\mathbf{E}_{1\sigma} = \langle \mathbf{t}_\sigma, \mathbf{E}_1 \rangle \mathbf{n}. \tag{26}$$

The electric field vector $\mathbf{E}_1$ with aid of the Darboux triad apparatus $\mathbf{g}$ and $\mathbf{n}$ is expressed by

$$\mathbf{E}_{1\sigma}(\sigma) = \Omega(\sigma)\frac{(\mathbf{g} + i\mathbf{n})}{\sqrt{2}} + \Omega^*(\sigma)\frac{\mathbf{g} - i\mathbf{n}}{\sqrt{2}}. \tag{27}$$

where $\mathbf{E}_1\mathbf{E}_1^* = 1$ and $|\Omega(\sigma)|^2 + |\Omega^*(\sigma)|^2 = 1, \mathbf{E}_1^*$ is complex conjugate of $\mathbf{E}_1$.

$$\mathcal{P} = \int^{\sigma_1} \tau_g^{(\varsigma)} d\sigma'$$

is the change phase of the polarization light injected into this fiber with respect to Darboux triad in $\mathcal{E}^3$.

$$\Omega(\sigma) = e^{i \int^{\sigma_1} \tau_g^{(\varsigma)} d\sigma'} \Omega(\sigma_0)$$

$$\Omega^*(\sigma) = e^{-i \int^{\sigma_1} \tau_g^{(\varsigma)} d\sigma'} \Omega^*(\sigma_0)$$

with the polarization coefficients are

$$\Omega(\sigma_0) = \left(\frac{\mathbf{g} + i\mathbf{n}}{\sqrt{2}}\right)^* \mathbf{E}_1(\sigma_0)$$

$$\Omega^*(\sigma_0) = \left(\frac{\mathbf{g} - i\mathbf{n}}{\sqrt{2}}\right)^* \mathbf{E}_1(\sigma_0).$$

Also via $\mathbf{P}_2$, $\mathbf{P}_2^*$, $\Omega(\sigma_0)$ and $\Omega^*(\sigma_0)$, the electric field $\mathbf{E}_1(\sigma)$ is expressed as

$$\mathbf{E}_1(\sigma) = \mathbf{P}_2\Omega(\sigma_0) + \mathbf{P}_2^*\Omega^*(\sigma_0) \tag{28}$$

Respectively, taking derivative with respect to σ and the time u of Eq.(28), the spatial and temporal evolutions of the electric field $\mathbf{E}_1$ for Darboux triad are derived as following:

$$\begin{aligned} \mathbf{E}_{1\sigma} &= \mathbf{P}_{2\sigma}\Omega(\sigma_0) + \mathbf{P}^*_{2\sigma}\Omega^*(\sigma_0) \\ \mathbf{E}_{1u} &= \mathbf{P}_{2u}\Omega(\sigma_0) + \mathbf{P}^*_{2u}\Omega^*(\sigma_0). \end{aligned}$$

From compatibility condition $\mathbf{E}_{1\sigma u} = \mathbf{E}_{1u\sigma}$, the nonlinear Schrödinger NLS equation system.

The Lorentz force equation $\Phi^{(t)}$ of the electric field vector $\mathbf{E}_1$ is given by

$$\Phi^{(t)}\mathbf{E}_1 = \mathbf{E}_{1\sigma} = \mathbf{M}^{(t)} \times \mathbf{E}_1 \tag{29}$$

and

$$\left\langle \Phi^{(t)}\mathbf{E}_1, \mathbf{t} \right\rangle = -\left\langle \mathbf{E}_1, \Phi^{(t)}\mathbf{t} \right\rangle, \ \left\langle \Phi^{(t)}\mathbf{E}_1, \mathbf{g} \right\rangle = -\left\langle \mathbf{E}_1, \Phi^{(t)}\mathbf{g} \right\rangle \tag{30}$$

$$\left\langle \Phi^{(t)}\mathbf{E}_1, \mathbf{n} \right\rangle = -\left\langle \mathbf{E}_1, \Phi^{(t)}\mathbf{n} \right\rangle. \tag{31}$$

The trajectory of travelling particle along the magnetic field $\mathbf{M}^{(t)}$ with respect to Darboux triad in $\mathcal{E}^3$ is described as electromagnetic trajectory. If $\mathbf{DEM}^{(t)}$ curve follows the magnetic trajectory, it is described as the Darboux electromagnetic curve in $\mathcal{E}^3$. With the help of Eqs. (30), (31) the Lorentz force Φ^t equations in the Darboux force equations of the $\mathbf{DEM}^{(t)}$ curve of the Γ_1 are given by

$$\begin{bmatrix} \Phi^{(t)}(\mathbf{t}) \\ \Phi^{(t)}(\mathbf{g}) \\ \Phi^{(t)}(\mathbf{n}) \end{bmatrix} = \begin{bmatrix} 0 & -\kappa_g^{(\varsigma)} & -\kappa_n^{(\varsigma)} \\ \kappa_g^{(\varsigma)} & 0 & -\varpi \\ \kappa_n^{(\varsigma)} & \varpi & 0 \end{bmatrix} \begin{bmatrix} \mathbf{t} \\ \mathbf{g} \\ \mathbf{n} \end{bmatrix} \tag{32}$$

$\mathbf{DEM}^{(t)}$ curve of the Γ_1 is a magnetic trajectory of the magnetic field $\mathbf{M}^{(t)}$ divergence free field iff $\mathbf{M}^{(t)}$ is given by in the following

$$\mathbf{M}^{(t)} = -\varpi\mathbf{t} + \kappa_n\mathbf{g} - \kappa_g\mathbf{n}$$

§4. Geometric Phase for Second Case of Electric Field with Darboux Triad in $\mathcal{E}^3$

Respectively, the second frame $\{\mathbf{Q}_1, \mathbf{Q}_2, \mathbf{Q}_2^*\}$ and second transformation ϕ associated with the NLS equation via Darboux triad is given by [22]

$$\mathbf{Q}_1 = \mathbf{g}, \tag{33}$$

$$\mathbf{Q}_2 = \frac{\mathbf{t} + i\mathbf{n}}{\sqrt{2}} e^{i\int^{\sigma_1} \kappa_n^{(\varsigma)} d\sigma'}, \ \mathbf{Q}_2^* = \frac{\mathbf{t} - i\mathbf{n}}{\sqrt{2}} e^{-i\int^{\sigma_1} \kappa_n^{(\varsigma)} d\sigma'} \tag{34}$$

$$\phi = \frac{(-\kappa_g^{(\varsigma)} + i\tau_g^{(\varsigma)})}{\sqrt{2}} e^{i\int^{\sigma} \kappa_n^{(\varsigma)} d\sigma'} \tag{35}$$

Using Eqs.(33) and (34) the spatial evolution of the frame $\{\mathbf{Q}_1, \mathbf{Q}_2, \mathbf{Q}_2^*\}$ is given by

$$\begin{aligned}
\mathbf{Q}_{1\sigma} &= \phi^* \mathbf{Q}_2 + \phi \mathbf{Q}_2^* \\
\mathbf{Q}_{2\sigma} &= -\phi \mathbf{Q}_1 \\
\mathbf{Q}_{2\sigma}^* &= -\phi^* \mathbf{Q}_1
\end{aligned}$$

where $\phi^* = \frac{(-\kappa_g^{(\varsigma)} - i\tau_g^{(\varsigma)})}{\sqrt{2}} e^{-i\int^\sigma \kappa_n^{(\varsigma)} d\sigma}$.

Consider

$$\mathbf{Q}_{1u} = \mathbf{g}_u = a_2 \mathbf{Q}_2 + b_2 \mathbf{Q}_2^* + c_2 \mathbf{Q}_1 \tag{36}$$

$$\mathbf{Q}_{2u} = h_2 \mathbf{Q}_2 + f_2 \mathbf{Q}_2^* + \vartheta \mathbf{Q}_1. \tag{37}$$

From $\langle \mathbf{Q}_{1u}, \mathbf{Q}_1 \rangle = 0 \Rightarrow c_2 = 0$, $\langle \mathbf{Q}_{1u}, \mathbf{Q}_2 \rangle = b_2$, $\langle \mathbf{Q}_{2u}, \mathbf{Q}_1 \rangle = \vartheta \Rightarrow b_2 = -\vartheta$, $\langle \mathbf{Q}_{2u}, \mathbf{Q}_2 \rangle = f_2 = 0$, $\langle \mathbf{Q}_{2u}^*, \mathbf{Q}_2 \rangle = -h_2 \Rightarrow h_2 = -f_2^*$ and $a_2 = -\vartheta^*$.
Eqs.(36) and (37) are rewritten by

$$\mathbf{Q}_{1u} = \mathbf{g}_u = -\vartheta^* \mathbf{Q}_2 - \vartheta \mathbf{Q}_2^* \tag{38}$$

$$\mathbf{Q}_{2u} = \vartheta \mathbf{Q}_1 + i\mathcal{J} \mathbf{Q}_2 \tag{39}$$

with $\mathcal{J}(\sigma, u)$ a real function. From $\mathbf{Q}_{2u\sigma} = \mathbf{Q}_{2\sigma u}$ the followings are obtained

$$\begin{aligned}
\phi_u &= -\vartheta_\sigma + i\mathcal{J}\phi \\
\mathcal{J}_\sigma &= i\vartheta\phi^* - i\vartheta^*\phi.
\end{aligned} \tag{40}$$

When $\mathbf{t}$ and $\mathbf{n}$ rotates around $\mathbf{g}$ with $\kappa_n^{(\varsigma)}(\sigma)$, a geometric phase $\mathcal{P} = \int\limits_{\sigma_0}^{\sigma_1} \kappa_n^{(\varsigma)}(\sigma) d\sigma'$ arises between $\mathbf{t}$, $\mathbf{n}$ and corresponding nonrotating Darboux triad in $\mathcal{E}^3$.
When the linearized light wave travelling moves from u_1 to u_2 along the curve in optic fiber, a geometric phase $\mathcal{P} = \int\limits_{u_1}^{u_2} \kappa_n^{(o)}(u) du$ arises between natural Darboux triad and nonrotating Darboux triad in Euclidean 3-space. The rotation angles of polarization plane can be given by

$$\begin{aligned}
\mathcal{P}_1 &= \kappa_n^{(\varsigma)}(\sigma, u)\Delta\sigma + \kappa_n^{(o)}(\sigma + \Delta\sigma, u)\Delta u \\
\mathcal{P}_2 &= \kappa_n^{(o)}(\sigma, u)\Delta u + \kappa_n^{(\varsigma)}(\sigma, u + \Delta u)\Delta\sigma
\end{aligned}$$

The phase difference are given by $\delta\mathcal{P} = \mathcal{P}_1 - \mathcal{P}_2 = \mathcal{AD}_2(\sigma, u)\Delta\sigma\Delta u$.
$\mathcal{AD}_2 = (\kappa_{n\sigma}^{(\varsigma)} - \kappa_{nu}^{(o)})$ is second anholonomy density measure for polarization plane of linearized light wave travelling along optic fiber for second case in $\mathcal{E}^3$. Also

$$\vartheta = -\frac{(l + iw)}{\sqrt{2}} e^{i\int^{\sigma_1} \kappa_n^{(\varsigma)} d\sigma'} \tag{41}$$

satisfies Eqs.(39) and (40). The time evolution of Darboux triad for second class is given by

[22]

$$\mathbf{t}_u = \varsigma_2^{(o)} \times \mathbf{t} = -\,l\mathbf{g} + \kappa_n^{(o)}\mathbf{n} \tag{42}$$

$$\mathbf{g}_u = \varsigma_2^{(o)} \times \mathbf{g} = l\mathbf{t} + w\mathbf{n} \tag{43}$$

$$\mathbf{n}_u = \varsigma_2^{(o)} \times \mathbf{n} = -\kappa_n^{(o)}\mathbf{t} - w\mathbf{g} \tag{44}$$

where $\varsigma_2^{(o)} = A_2\mathbf{t} - \kappa_n^{(\varsigma)}\mathbf{g} + C_2\mathbf{n}$, $l = -C_2$, $w = -A_2$.

Using Eqs.(35), (40) and (41) it can be obtained

$$\mathcal{J}_\sigma = -(\tau_g^{(\varsigma)} l + \kappa_g^{(\varsigma)} w). \tag{45}$$

From Eqs.(34), (39), (42), (43) and (44), the time evolution of Darboux triad for second class with Eq.(43) is given by

$$\mathbf{t}_u = l\mathbf{g} + (\int^{\sigma_1} \kappa_{nu}^{(\varsigma)} d\sigma' - \mathcal{J})\mathbf{n}$$

$$\mathbf{n}_u = -(\int^{\sigma_1} \kappa_{nu}^{(\varsigma)} d\sigma' - \mathcal{J})\mathbf{t} - w\mathbf{g}$$

and the anholonomy density $\mathcal{AD}_2(\sigma, u) = -\mathcal{J}_\sigma = (\tau_g^{(\varsigma)} l + \kappa_g^{(\varsigma)} w)$ for second class. Total phase $\mathcal{P}$ for second class with respect to Darboux triad in $\mathcal{E}^3$ is given by

$$\begin{aligned}
\mathcal{P} &= -\int_{u_1}^{u_2}\int_{\sigma_0}^{\sigma_1} \mathcal{J}_\sigma d\sigma du = \int_{u_1}^{u_2}\int_{\sigma_0}^{\sigma_1} (\tau_g^{(\varsigma)} l + \kappa_g^{(\varsigma)} w) d\sigma du \\
&= \int_{u_1}^{u_2}\int_{\sigma_0}^{\sigma_1} \langle \mathbf{g}, \mathbf{g}_\sigma \times \mathbf{g}_u \rangle \, d\sigma du.
\end{aligned}$$

The quantum geometric phase for second class of curve evolution with respect to Darboux triad in $\mathcal{E}^3$ is obtained

$$\mathcal{P} = i\int_{\sigma_0}^{\sigma_1} d\sigma \frac{\partial}{\partial\sigma} \int_{u_1}^{u_2} \langle \mathbf{Q}_{2u}, \mathbf{Q}_2^* \rangle \; du.$$

Also [22]

$$\begin{aligned}
\mathbf{Q}_{1u} &= -i\phi_\sigma^* \mathbf{Q}_2 + i\phi_\sigma \mathbf{Q}_2^*, \quad \mathbf{Q}_{2u} = -i\phi_\sigma \mathbf{Q}_1 + \mathcal{J}\mathbf{Q}_2, \\
\mathbf{Q}_{2u}^* &= i\phi_\sigma^* \mathbf{Q}_1 - \mathcal{J}\mathbf{Q}_2^*, \; \mathcal{J} = i\phi\phi^*
\end{aligned}$$

From $\phi_{1u\sigma} = \phi_{1\sigma u}$ and $\phi_{2u\sigma} = \phi_{2\sigma u}$, the NLS equation

$$\phi_u = i\phi_{\sigma\sigma} + i \mid \phi \mid^2 \phi$$

is obtained.

A optical fiber can be described by a curve $\Gamma_2(\sigma)$ with respect to Darboux triad in $\mathcal{E}^3$. The direction of electric field $\mathbf{E}_2$ is given by the direction of the state of the linearly polarized light wave injected to the fiber with respect to Darboux triad in $\mathcal{E}^3$. The change of the electric field

$\mathbf{E}_2$ with respect to Darboux frame in $\mathcal{E}^3$ can be given by

$$\mathbf{E}_{2\sigma} = \zeta_1 \mathbf{t} + \zeta_2 \mathbf{g} + \zeta_3 \mathbf{n}. \tag{46}$$

Case 2. Assume that

$$\langle \mathbf{E}_2, \mathbf{g} \rangle = 0. \tag{47}$$

Using Eqs. (46) and (47), it can be written by

$$\zeta_2 = -\kappa_g \langle \mathbf{E}_2, \mathbf{t} \rangle - \tau_g \langle \mathbf{E}_2, \mathbf{n} \rangle \tag{48}$$

Consider

$$\langle \mathbf{E}_2, \mathbf{E}_2 \rangle = const. \tag{49}$$

Taking derivative with respect to σ of Eq.(49), the followings are obtained

$$\zeta_1 \langle \mathbf{E}_2, \mathbf{t} \rangle = -\zeta_3 \langle \mathbf{E}_2, \mathbf{n} \rangle \tag{50}$$

$$\zeta_1 = \chi \langle \mathbf{E}_2, \mathbf{n} \rangle, \quad \zeta_3 = -\chi \langle \mathbf{E}_2, \mathbf{t} \rangle \tag{51}$$

where χ is a parameter.

Using Eq.(20) and $\langle \mathbf{E}_2, \mathbf{t} \rangle \neq 0$, $\langle \mathbf{E}_2, \mathbf{n} \rangle \neq 0$. Substituting Eqs. (48) and (51) in (46), the evolution of the electric field vector $\mathbf{E}_2$ with respect to Darboux triad is given by

$$\mathbf{E}_{2\sigma} = \chi \langle \mathbf{E}_2, \mathbf{n} \rangle \mathbf{t} + (-\kappa_g \langle \mathbf{E}_2, \mathbf{t} \rangle - \tau_g \langle \mathbf{E}_2, \mathbf{n} \rangle)\mathbf{g} - \chi \langle \mathbf{E}_2, \mathbf{t} \rangle \mathbf{n} \tag{52}$$

Via Eq.(52) for $\chi = 0$,

$$\mathbf{E}_{2\sigma} = (-\kappa_g \langle \mathbf{E}_2, \mathbf{t} \rangle - \tau_g \langle \mathbf{E}_2, \mathbf{n} \rangle)\mathbf{g} \tag{53}$$

The modified Fermi-Walker derivative for the electric field vector $\mathbf{E}_2$ with respect to Darboux triad for second class is described by

$$^{DmFW}\mathbf{E}_{2\sigma} = \mathbf{E}_{2\sigma} - \langle \mathbf{g}, \mathbf{E}_2 \rangle \mathbf{g}_\sigma + \langle \mathbf{g}_\sigma, \mathbf{E}_2 \rangle \mathbf{g} \tag{54}$$

The electric field $\mathbf{E}_2$ is the modified Fermi-Walker parallel if and only if

$$^{DmFW}\mathbf{E}_{2\sigma} = 0. \tag{55}$$

Via Eqs.(47), (54) and (55), one obtains $\mathbf{E}_{2\sigma} = \langle \mathbf{g}_\sigma, \mathbf{E}_2 \rangle \mathbf{n}$.

The electric field vector $\mathbf{E}_2$ with aid of the Darboux triad apparatus $\mathbf{t}$ and $\mathbf{n}$ can be expressed by

$$\mathbf{E}_2(\sigma) = \Upsilon(\sigma)\frac{(\mathbf{t} + i\mathbf{n})}{\sqrt{2}} + \Upsilon^*(\sigma)\frac{\mathbf{t} - i\mathbf{n}}{\sqrt{2}}. \tag{56}$$

where $\mathbf{E}_2\mathbf{E}_2^* = 1$ and $|\Upsilon(\sigma)|^2 + |\Upsilon^*(\sigma)|^2 = 1$.

Here $\Upsilon(\sigma)$ and $\Upsilon^*(\sigma)$ are

$$\Upsilon(\sigma)=e^{i\int^{\sigma_1}\kappa_n^{(\varsigma)}d\sigma'}\Upsilon(\sigma_0),\ \Upsilon^*(\sigma)=e^{-i\int^{\sigma_1}\kappa_n^{(\varsigma)}d\sigma'}\Upsilon^*(\sigma_0) \tag{57}$$

and the polarization coefficients are

$$\Upsilon(\sigma_0)=\left(\frac{\mathbf{t}+i\mathbf{n}}{\sqrt{2}}\right)^*\mathbf{E}_2(\sigma_0),\ \Upsilon^*(\sigma_0)=\left(\frac{\mathbf{t}-i\mathbf{n}}{\sqrt{2}}\right)^*\mathbf{E}_2(\sigma_0) \tag{58}$$

Via Eqs.(34) and (57), Eq.(56) is re-expressed by

$$\mathbf{E}_2(\sigma)=\mathbf{Q}_2\Upsilon(\sigma_0)+\mathbf{Q}_2^*\Upsilon^*(\sigma_0). \tag{59}$$

Respectively, the spatial and temporal evolutions of the electric field $\mathbf{E}_2$ for Darboux triad are derived as following:

$$\begin{aligned}\mathbf{E}_{2\sigma} &= \mathbf{Q}_{2\sigma}\Upsilon(\sigma_0)+\mathbf{Q}_{2\sigma}^*\Upsilon^*(\sigma_0)\\ \mathbf{E}_{2u} &= \mathbf{Q}_{2u}\Upsilon(\sigma_0)+\mathbf{Q}_{2u}^*\Upsilon^*(\sigma_0).\end{aligned}$$

From compatibility condition $\mathbf{E}_{2\sigma u}=\mathbf{E}_{2u\sigma}$, the NLS equation system connected with the electric field $\mathbf{E}_2$ is derived.

Geometric phase for polarized light injected into a fiber with respect to Darboux triad for second case in $\mathcal{E}^3$ is given by

$$\mathcal{P}=\int^{\sigma_1}\kappa_n^{(\varsigma)}d\sigma'.$$

Consider the Lorentz force equation $\Phi^{(g)}$ for second case of the electric field vector

$$\Phi^{(g)}\mathbf{E}_2=\mathbf{E}_{2\sigma}=\mathbf{M}^{(g)}\times\mathbf{E}_2 \tag{60}$$

and

$$\left\langle\Phi^{(g)}\mathbf{E}_2,\mathbf{t}\right\rangle = -\left\langle\mathbf{E}_2,\Phi^{(g)}\mathbf{t}\right\rangle,\left\langle\Phi^{(g)}\mathbf{E}_2,\mathbf{g}\right\rangle=-\left\langle\mathbf{E}_2,\Phi^{(g)}\mathbf{g}\right\rangle, \tag{61}$$

$$\left\langle\Phi^{(g)}\mathbf{E}_2,\mathbf{n}\right\rangle = -\left\langle\mathbf{E}_2,\Phi^{(g)}\mathbf{n}\right\rangle. \tag{62}$$

The trajectory of travelling particle along the magnetic field $\mathbf{M}^{(g)}$ with respect to Darboux triad is described as the electromagnetic trajectory. If $\mathbf{DEM}^{(g)}$ curve follows the magnetic trajectory, it is described as the Darboux electromagnetic curve. With the help of Eqs. (61) and(62), the Lorentz force Φ^g in the Darboux triad of the $\mathbf{DEM}^{(g)}$ curve of Γ_2 are given by

$$\begin{bmatrix}\Phi^{(g)}(\mathbf{t})\\ \Phi^{(g)}(\mathbf{g})\\ \Phi^{(g)}(\mathbf{n})\end{bmatrix}=\begin{bmatrix}0 & -\kappa_g^{(\varsigma)} & -\chi\\ \kappa_g^{(\varsigma)} & 0 & \tau_g\\ \chi & -\tau_g^{(\varsigma)} & 0\end{bmatrix}\begin{bmatrix}\mathbf{t}\\ \mathbf{g}\\ \mathbf{n}\end{bmatrix} \tag{63}$$

Via Eq. (63), the vector field divergence free $\mathbf{M}^{(g)}$ is given by

$$\mathbf{M}^{(g)} = \chi \mathbf{g} + \tau_g t - \kappa_g \mathbf{n}.$$

§5. Geometric Phase for Third Case of Electric Field with Darboux Triad

The third frame $\{\mathbf{R}_1, \mathbf{R}_2, \mathbf{R}_2^*\}$ and the third transformation ψ for third class of curve evolution concerned with the NLS equation with respect to Darboux triad in $\mathcal{E}^3$ are given by [22]

$$\mathbf{R}_1 = \mathbf{n}, \tag{64}$$

$$\mathbf{R}_2 = \frac{\mathbf{t}+i\mathbf{g}}{\sqrt{2}} e^{i\int^{\sigma_1} \kappa_g^{(\varsigma)} d\sigma'}, \ \mathbf{R}_2^* = \frac{\mathbf{t}-i\mathbf{g}}{\sqrt{2}} e^{-i\int^{\sigma_1} \kappa_g^{(\varsigma)} d\sigma'} \tag{65}$$

$$\psi = \frac{(\kappa_n^{(\varsigma)} + i\tau_g^{(\varsigma)})}{\sqrt{2}} e^{i\int^{\sigma} \kappa_g^{(\varsigma)} d\sigma'} \tag{66}$$

Using Eqs. (65) and (66), the spatial evolution of $\{\mathbf{R}_1, \mathbf{R}_2, \mathbf{R}_2^*\}$ is given by [22]

$$\mathbf{R}_{1\sigma} = -\psi^* \mathbf{R}_2 - \psi \mathbf{R}_2^*, \ \mathbf{R}_{2\sigma} = \psi \mathbf{R}_1, \ \mathbf{R}_{2\sigma}^* = \psi^* \mathbf{R}_1 \tag{67}$$

where $\psi^* = \frac{(\kappa_n^{(\varsigma)} - i\tau_g^{(\varsigma)})}{\sqrt{2}} e^{-i\int^{\sigma} \kappa_g^{(\varsigma)} d\sigma'}$.

Consider

$$\mathbf{R}_{1u} = \mathbf{n}_u = a_3 \mathbf{R}_2 + b_3 \mathbf{R}_2^* + c_3 \mathbf{R}_1, \tag{68}$$

$$\mathbf{R}_{2u} = h_3 \mathbf{R}_2 + f_3 \mathbf{R}_2^* + \eta \mathbf{R}_1. \tag{69}$$

From $\langle \mathbf{R}_{1u}, \mathbf{R}_1 \rangle = 0 \Rightarrow c_3 = 0$, $\langle \mathbf{R}_{1u}, \mathbf{R}_2 \rangle = b_3$, $\langle \mathbf{R}_{2u}, \mathbf{R}_1 \rangle = \eta \Rightarrow b_3 = -\eta$, $\langle \mathbf{R}_{2u}, \mathbf{R}_2 \rangle = f_3 = 0, \langle \mathbf{R}_{1u}, \mathbf{R}_2^* \rangle = a_3 \Rightarrow \eta^* = a_3$, $\langle \mathbf{R}_{2u}^*, \mathbf{R}_2 \rangle = -h_3 \Rightarrow h_3 = -f_3^*$.
Eqs. (68) and (69) can be rewritten by

$$\mathbf{R}_{1u} = \mathbf{n}_u = -\eta^* \mathbf{R}_2 - \eta \mathbf{V}_2^*, \tag{70}$$

$$\mathbf{R}_{2u} = \eta \mathbf{R}_1 + i\mathcal{L} \mathbf{R}_2 \tag{71}$$

with $\mathcal{L}(\sigma, u)$ is a real function. From $\mathbf{R}_{2u\sigma} = \mathbf{R}_{2\sigma u}$ the followings can be derived by

$$\psi_u = \eta_\sigma + i\mathcal{L}_\sigma \psi, \tag{72}$$

$$\mathcal{L}_\sigma = i\eta^* \psi - i\eta \psi^*. \tag{73}$$

When $\mathbf{t}$ and $\mathbf{g}$ rotates around $\mathbf{n}$ with $\kappa_g^{(\varsigma)}(\sigma)$, a geometric phase $\mathcal{P} = \int\limits_{\sigma_0}^{\sigma_1} \kappa_g^{(\varsigma)} d\sigma$ arises between $\mathbf{t}$, $\mathbf{g}$ and corresponding nonrotating Darboux triad in $\mathcal{E}^3$. When the linearized light wave travelling moves from u_1 to u_2 along the curve in optic fiber, a geometric phase $\mathcal{P} = \int\limits_{u_1}^{u_2} \kappa_g^{(o)} du$ develops between natural Darboux triad and nonrotating Darboux triad in $\mathcal{E}^3$. The rotation angles of polarization plane can be given by

$$\mathcal{P}_1 = \kappa_g^{(\varsigma)}(\sigma,u)\Delta\sigma + \kappa_g^{(o)}(\sigma+\Delta\sigma,u)\Delta u$$

$$\mathcal{P}_2 = \kappa_g^{(o)}(\sigma,u)\Delta u + \kappa_g^{(\varsigma)}(\sigma,u+\Delta u)\Delta\sigma.$$

Phase difference are given as $\delta\mathcal{P} = \mathcal{P}_1 - \mathcal{P}_2 = \mathcal{AD}_3(\sigma,u)\Delta\sigma\Delta u$, where $\mathcal{AD}_3 = (\kappa_{g\sigma}^{(\varsigma)} - \kappa_{gu}^{(o)})$ is third anholonomy density measure for polarization plane of linearized light wave travelling along optic fiber for third class in $\mathcal{E}^3$. Also

$$\eta = -\frac{(j+iz)}{\sqrt{2}}e^{i\int^{\sigma_1}\kappa_g^{(\varsigma)}d\sigma'} \tag{74}$$

satisfies Eqs.(70), (71) and (73). The time evolution of Darboux triad is given by [22]

$$\mathbf{t}_u = \varsigma_3^{(o)} \times \mathbf{t} = \kappa_g^{(o)}\mathbf{g} - jn, \tag{75}$$

$$\mathbf{g}_u = \varsigma_3^{(o)} \times \mathbf{g} = -\kappa_g^{(o)}\mathbf{t} - z\mathbf{n}, \tag{76}$$

$$\mathbf{n}_u = \varsigma_3^{(o)} \times \mathbf{n} = j\mathbf{t} + z\mathbf{g} \tag{77}$$

where $\varsigma_3^{(o)} = A_3\mathbf{t} + B_3\mathbf{g} + \kappa_g^{(o)}\mathbf{n}$, $z = -A_3$, $j = B_3$. Using Eqs. (66), (74) it can be obtained

$$\mathcal{L}_\sigma = j\tau_g^{(\varsigma)} - \kappa_n^{(\varsigma)}z. \tag{78}$$

The time evolution of Darboux triad for third class connected with the NLS equation is given by

$$\mathbf{n}_u = j\mathbf{t} + z\mathbf{g} \tag{79}$$

$$\mathbf{t}_u = -j\mathbf{n} - (\int^{\sigma_1}\kappa_{gu}^{(\varsigma)}d\sigma' - \mathcal{L})\mathbf{g} \tag{80}$$

$$\mathbf{g}_u = (\mathcal{L} - \int^{\sigma_1}\kappa_{gu}^{(\varsigma)}d\sigma')\mathbf{t} - z\mathbf{n}. \tag{81}$$

The anholonomy density $\mathcal{AD}_3$ for third class with respect to Darboux frame in Euclidean 3-space:

$$\mathcal{AD}_3(\sigma,u) = -\mathcal{L}_\sigma = \kappa_n^{(\varsigma)}z - j\tau_g^{(\varsigma)}. \tag{82}$$

and the total phase $\mathcal{P}$ for third class with respect to Darboux triad in $\mathcal{E}^3$ is given by

$$\begin{aligned}\mathcal{P} &= -\int_{u_1}^{u_2}\int_{\sigma_0}^{\sigma_1}\mathcal{L}_\sigma d\sigma du \\ &= \int_{u_1}^{u_2}\int_{\sigma_0}^{\sigma_1}(\kappa_n^{(\varsigma)}z - j\tau_g^{(\varsigma)})d\sigma du = \int_{u_1}^{u_2}\int_{\sigma_0}^{\sigma_1}\langle\mathbf{n},\mathbf{n}_\sigma\times\mathbf{n}_u\rangle\, d\sigma du.\end{aligned}$$

The quantum geometric phase is given

$$\mathcal{P} = i\int_{\sigma_0}^{\sigma_1}d\sigma\frac{\partial}{\partial\sigma}\int_{u_1}^{u_2}\langle\mathbf{R}_{2u},\mathbf{R}_2^*\rangle\ du.$$

A optical fiber can be described by a curve $\Gamma_3(\sigma)$ with respect to Darboux frame in $\mathcal{E}^3$. The direction of electric field $\mathbf{E}_3$ denotes the direction of the state of the linearly polarized light wave injected to fiber with respect to Darboux frame in $\mathcal{E}^3$. The change of the electric field $\mathbf{E}_3$ with respect to Darboux triad can be written by

$$\mathbf{E}_{3\sigma} = \pi_1 \mathbf{t} + \pi_2 \mathbf{g} + \pi_3 \mathbf{n}. \tag{83}$$

Case 3. Assume that

$$\langle \mathbf{E}_3, \mathbf{n} \rangle = 0. \tag{84}$$

From Eq.(84)

$$\langle \mathbf{E}_{3\sigma}, \mathbf{n} \rangle = \langle \mathbf{E}_3, \kappa_n \mathbf{t} + \tau_g \mathbf{g} \rangle$$

$$\pi_3 = \kappa_n \langle \mathbf{E}_3, \mathbf{t} \rangle + \tau_g \langle \mathbf{E}_3, \mathbf{g} \rangle \tag{85}$$

Also

$$\langle \mathbf{E}_3, \mathbf{E}_3 \rangle = const. \tag{86}$$

Using Eq.(83) and taking derivative with respect to σ of Eq.(86), it can be obtained

$$\pi_1 \langle \mathbf{E}_3, \mathbf{t} \rangle = -\pi_2 \langle \mathbf{E}_3, \mathbf{g} \rangle \tag{87}$$

$$\pi_1 = \epsilon \langle \mathbf{E}_3, \mathbf{g} \rangle, \quad \pi_2 = -\epsilon \langle \mathbf{E}_3, \mathbf{t} \rangle \tag{88}$$

where ϵ is a parameter. The evolution in the polarization of light wave travelling from the point $\Gamma_3(\sigma_0)$ to $\Gamma_3(\sigma_1)$ along curve with respect to Darboux triad is given by the evolution of the electric field $\mathbf{E}_3$. $\langle \mathbf{E}_3, \mathbf{t} \rangle \neq 0$, $\langle \mathbf{E}_3, \mathbf{n} \rangle \neq 0$. Substituting Eqs. (85) and (88) in (83), the Eq.(83) is rewritten by

$$\mathbf{E}_{3\sigma} = \epsilon \langle \mathbf{E}_3, \mathbf{g} \rangle \mathbf{t} - \epsilon \langle \mathbf{E_2}, \mathbf{t} \rangle \mathbf{g} + (\kappa_n \langle \mathbf{E}_3, \mathbf{t} \rangle + \tau_g \langle \mathbf{E}_3, \mathbf{g} \rangle) n \tag{89}$$

Via Eq.(89) for $\epsilon = 0$,

$$\mathbf{E}_{3\sigma} = (\kappa_n \langle \mathbf{E}_3, \mathbf{t} \rangle + \tau_g \langle \mathbf{E}_3, \mathbf{g} \rangle) n \tag{90}$$

The modified Fermi-Walker derivative for the electric field $\mathbf{E}_3$ with respect to Darboux triad for third class is described by

$$^{DmFW}\mathbf{E}_{3\sigma} = \mathbf{E}_{3\sigma} - \langle \mathbf{n}, \mathbf{E}_2 \rangle \mathbf{n}_\sigma + \langle \mathbf{n}_\sigma, \mathbf{E}_2 \rangle \mathbf{n} \tag{91}$$

The electric field $\mathbf{E}_3$ is the Fermi-Walker parallel if and only if

$$^{DmFW}\mathbf{E}_{3\sigma} = 0. \tag{92}$$

Via (84), (91), (92), one obtains $\mathbf{E}_{3\sigma} = \langle \mathbf{n}_\sigma, \mathbf{E}_2 \rangle \mathbf{n}$.

The electric field vector $\mathbf{E}_3$ with respect to the Darboux triad apparatus $\mathbf{t}$ and $\mathbf{g}$ can be written by

$$\mathbf{E}_3(\sigma) = \Sigma(\sigma) \frac{(\mathbf{t} + i\mathbf{g})}{\sqrt{2}} + \Sigma^*(\sigma) \frac{\mathbf{t} - i\mathbf{g}}{\sqrt{2}}. \tag{93}$$

where $\mathbf{E}_3\mathbf{E}_3^* = 1$ and $|\Sigma(\sigma)|^2 + |\Sigma^*(\sigma)|^2 = 1$. Here

$$\Sigma(\sigma) = e^{i\int^{\sigma_1}\kappa_g^{(\varsigma)}d\sigma'}\Sigma(\sigma_0),\ \Sigma^*(\sigma) = e^{-i\int^{\sigma_1}\kappa_g^{(\varsigma)}d\sigma'}\Sigma^*(\sigma_0). \tag{94}$$

The polarization coefficients are

$$\Sigma(\sigma_0) = \left(\frac{\mathbf{t}+i\mathbf{g}}{\sqrt{2}}\right)^*\mathbf{E}_3(\sigma_0)$$

$$\Sigma^*(\sigma_0) = \left(\frac{\mathbf{t}-i\mathbf{g}}{\sqrt{2}}\right)^*\mathbf{E}_3(\sigma_0).$$

Eq.(93) is re-expressed as the following

$$\mathbf{E}_3(\sigma) = \mathbf{R}_2\Sigma(\sigma_0) + \mathbf{R}_2^*\Sigma^*(\sigma_0) \tag{95}$$

When taking derivative with respect to σ and the time u of Eq. (95), the spatial and temporal evolutions of the electric field $\mathbf{E}_3$ for Darboux triad are derived as follows

$$\begin{aligned}
\mathbf{E}_{3\sigma} &= \mathbf{R}_{2\sigma}\Sigma(\sigma_0) + \mathbf{R}_{2\sigma}^*\Sigma^*(\sigma_0)\\
\mathbf{E}_{3u} &= \mathbf{R}_{2u}\Sigma(\sigma_0) + \mathbf{R}_{2u}^*\Sigma^*(\sigma_0)
\end{aligned}$$

From compatibility condition $\mathbf{E}_{3\sigma u} = \mathbf{E}_{3u\sigma}$, the nonlinear Schrödinger equation NLS system connected with the electric field $\mathbf{E}_3$ is obtained.

$$\mathcal{P} = \int^{\sigma_1}\kappa_g^{(\varsigma)}d\sigma'$$

is the change phase of the polarization light injected into a fiber for third case of the electric field with respect to Darboux frame in $\mathcal{E}^3$. Consider the Lorentz force equation $\Phi^{(n)}$ for third case of the electric field vector

$$\begin{aligned}
\Phi^{(n)}\mathbf{E}_3 &= \mathbf{E}_{3\sigma} = \mathbf{M}^{(n)}\times\mathbf{E}_3,\\
\left\langle\Phi^{(n)}\mathbf{E}_3,\mathbf{t}\right\rangle &= -\left\langle\mathbf{E}_3,\Phi^{(n)}\mathbf{t}\right\rangle, \left\langle\Phi^{(n)}\mathbf{E}_3,\mathbf{g}\right\rangle = -\left\langle\mathbf{E}_3,\Phi^{(n)}\mathbf{g}\right\rangle\\
\left\langle\Phi^{(n)}\mathbf{E}_3,\mathbf{n}\right\rangle &= -\left\langle\mathbf{E}_3,\Phi^{(n)}\mathbf{n}\right\rangle.
\end{aligned}$$

The trajectory of travelling particle along the magnetic field $\mathbf{M}^{(n)}$ with respect to Darboux frame is described as the electromagnetic trajectory. If the curve $\mathbf{DEM}^{(n)}$ follows the magnetic trajectory, it is described as the Darboux electromagnetic curve. With the help of Eq. (61) the Darboux Lorentz force equations along the optic fiber for third case the electric field are obtained

$$\begin{bmatrix}\Phi^{(n)}(\mathbf{t})\\ \Phi^{(n)}(\mathbf{g})\\ \Phi^{(n)}(\mathbf{n})\end{bmatrix} = \begin{bmatrix}0 & -\epsilon & \kappa_n^{(\varsigma)}\\ \epsilon & \tau_g^{(\varsigma)} & 0\\ -\kappa_n^{(\varsigma)} & -\tau_g^{(\varsigma)} & 0\end{bmatrix}\begin{bmatrix}\mathbf{t}\\ \mathbf{g}\\ \mathbf{n}\end{bmatrix} \tag{96}$$

$\mathbf{DEM}^{(n)}$ curve of the Γ_3 is the magnetic trajectory of the magnetic field $\mathbf{M}^{(n)}$ iff the vector field divergence free $\mathbf{M}^{(n)}$ is given by

$$\mathbf{M}^{(n)} = -\kappa_n^{(\varsigma)}\mathbf{g} - \epsilon\mathbf{n} + \tau_g^{(\varsigma)}\mathbf{t}.$$

References

[1] M.V. Berry, Quantal phase factors accompanying adiabatic changes, *Proc. Roy. Soc. London A*, 392 (1984), 45-57.

[2] K.Y. Bliokh, Geometrodynamics of polarized light: Berry phase and spin Hall effect in a gradient-index medium, *J. Opt. A* 11(2009), 094009 .

[3] J.N. Ross, The rotation of the polarization in low birefringence monomode optical fibres due to geometric effects, *Opt. Quantum Electron* 16 (1984), 455–461.

[4] N.E. Gürbüz, The variation of the electric field along optic fiber for null Cartan and pseudo-null frames, *International Journal of Geometric Methods in Modern Physics*, Vol.18, No.8 (2021), 2150122 (10 pages)

[5] D.P. Datta, Geometric phase in vacuum instability: applications in quantum cosmology, *Phys. Rev. D,* 48 (1993), 5746 .

[6] A. Kuppermann and Y. S. M. Wu, The geometric phase effect shows up in chemical reactions, *Chem. Phys. Lett.*, 205 (1993), 577–586 .

[7] V. V. Vladimirskii, The rotation of a polarization plane for curved light ray, *Dokl. Akad. Nauk. SSSR,* 31(1941), 222–224 .

[8] R. Ulrich and A. Simon, Polarization optics of twisted single-mode fibers, *Appl. Opt.*, 18 (1979) 2241–2251.

[9] N. Gürbüz, Parallel transports and related phases according to Frenet and Darboux frame in R_1^3, *International Journal of Geometric Methods in Modern Physics* 151 (2018), 850208.

[10] M. V. Berry, The adiabatic phase and Pancharatnam's phase for polarized light, *J. Mod. Opt.* 34 (1987) 1401–1407 .

[11] E.M. Frins and W. Dultz, Rotation of the Polarization Plane in Optical Fibers, *Journal of light wave technologhy* 15 (1997) 144-147.

[12] T. Körpinar, R.C. Demirkol, Electromagnetic curves of the linearly polarized light wave along an optical fiber in a 3D Riemannian manifold with Bishop equations,*Optik*, 200 (2020), 163334.

[13] T. Körpinar, R.C. Demirkol, Electromagnetic curves of the polarized light wave along the optical fiber in De-Sitter 2-space S_1^2, *Indian Journal of Phys*, 95 (2021),147–156.

[14] Z. Özdemir, A new calculus for the treatment of Rytov's law in the optical fiber, Optic İnternational Journal of Light and electron optics 216 (2020), 164892.

[15] R. Balakrishnan, R. Bishop and R. Dandoloff, Geometric Phase in the Classical Continuous Antiferromagnetic Heisenberg Spin Chain, *Phys Rev Lett.* 64 (1990), 2107-2110.

[16] N.Gürbüz, Anholonomy according to three formulations of non-null curve evolution, *International Journal of Geometric Methods in Modern Physics* 14 (2017), 1750175 (16 pages).

[17] N. Gürbüz, Three anholonomy densities according to Bishop frame in Euclidean 3-space, *Journal of Mathematical Physics, Analysis, Geometry* 15 (2019), 510–525.

[18] N. Gürbüz, Total Anholonomies with Bishop 2-Type Frame in R_1^3, *Nonlinear Analysis and Differential Equations* 7 (2019), 115-124.

[19] N.Gürbüz,Three classes of non-lightlike curve evolution according to Darboux frame and geometric phase, *Int. J. Geom. Methods Mod. Phys.*15 (2018), 1850023.

[20] N.Gürbüz and Dae Won Yoon, Fermi-Walker parallel transport according to quasi frame in three dimensional Minkowski space, *JGSP* 54 (2019) 1–12.

[21] R. Balakrishan, Space curve evolution, geometric phase and solitons, *Theoretical and Mathematical Physics,* 99 (1994) 501–504.

[22] N. Gürbüz, Öklidyen uzayda Darboux çatısına göre eğri evolüsyonunun üç sınıfına göre Hasimoto yüzeyleri, Fen bilimleri ve matematik alanında akademik çalışmalar, Gece Publishing, Chapter 4 (2018) 49-62.

[23] R. Resta, Theory of the electric polarization in crystals, *Ferroelectrics* 136 (1992), 51–55 .

[24] N. Mukunda and R. Simon, Quantum kinematic approach to the geometric phases, *Ann. Phys.* 228 (1993) 205-268.

[25] I. Vaisman, *A First Course in Differential Geometry*, Marcel Dekker, 1984.

[26] M. Barros, J. L. Cabrerizo, M. Fernandez, and A. Romero, Magnetic vortex filament flows, *J. Math. Phys.,* 48 (2007), 082904.

[27] M. Barros, A. Romero, J. L. Cabrerizo, and M. Fernandez, The Gauss-Landau-Hall problem on Riemannian surfaces, *J. Math. Phys.* 46 (2005), 112905.

International J.Math. Combin. Vol.2(2021), 33-40

Computation of Inverse Nirmala Indices of Certain Nanostructures

V.R.Kulli

(Department of Mathematics, Gulbarga University, Gulbarga 585106, Karnataka, India)

V.Lokesha and Nirupadi K

(Department of Mathematics, Vijayanagara Sri Krishnadevaraya University, Ballari, Karnataka, India)

E-mail: vrkulli@gmail.com, v.lokesha@gmail.com, nirupadik80@gmail.com

Abstract: Recently, a novel invariant is considered, which is the Nirmala index defined as the sum of the square root of the degrees of the pairs of adjacent vertices. In this paper, we introduce the first and second inverse Nirmala indices of a graph and compute exact formulas for certain nanostructures.

Key Words: Topological index, inverse Nirmala indices, dendrimer.

AMS(2010): 05C05, 05C12, 05C35.

§1. Introduction

Let G be a simple, finite, connected graph with the vertex set $V(G)$ and edge set $E(G)$. The degree $d_G(u)$ of a vertex u is the number of vertices adjacent to u. The additional definitions and notations, the reader may refer to [1].

A molocular graph is a graph in which the vertices correspond to the atoms and the edges to the bonds of a molecule. A topological index is a numeric quantity from structural graph of a molecule. Several topological indices have been considered in Theoretical Chemistry, and have found some applications, especially in $QSPR/QSAR$ study, see [2, 3, 4].

In chemical science, numerous vertex degree based topological indices or graph indices have been introduced and extensively studied in [4, 5].

The Sombor index was defined by Gutman in [6] as

$$SO(G) = \sum_{uv \in E(G)} \sqrt{d_G(u)^2 + d_G(v)^2}.$$

Recently, some Sombor indices were studied in [7, 8,9, 10, 11, 12, 13, 14].

In [15], Kulli introduced the Nirmala index of a graph G and it is defined as

$$N(G) = \sum_{uv \in E(G)} \sqrt{d_G(u) + d_G(v)}.$$

[1]Received April 19, 2021, Accepted June 6, 2021.

We now define the first and second inverse Nirmala indices of a graph G as

$$IN_1(G) = \sum_{uv\in E(G)} \left[\frac{1}{d_G(u)} + \frac{1}{d_G(v)}\right]^{\frac{1}{2}},$$
$$IN_2(G) = \sum_{uv\in E(G)} \left[\frac{1}{d_G(u)} + \frac{1}{d_G(v)}\right]^{-\frac{1}{2}}.$$

In this study, we compute the first and second inverse Nirmala indices for four families of dendrimers. For dendrimers, see [16].

§2. Results for Porphyrin Dendrimer D_nP_n

We consider the family of porphyrin dendrimers. This family of dendrimers is denoted by D_nP_n. The molecular graph of D_nP_n is shown in Figure 1.

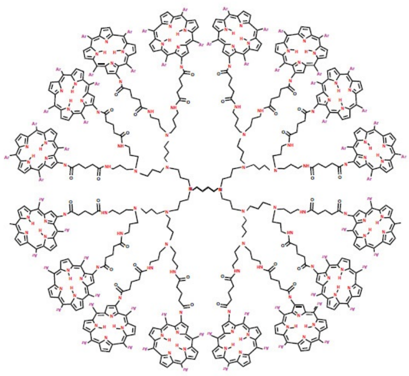

Figure 1. The molecular graph of D_nP_n

Let G be the molecular graph of D_nP_n. By calculation, we find that G has $96n-10$ vertices and $105n-11$ edges. In D_nP_n, there are six types of edges based on degrees of end vertices of each edge as given in Table 1.

$d_G(u), d_G(v) \setminus uv \in E(G)$	$(1,3)$	$(1,4)$	$(2,2)$	$(2,3)$	$(3,3)$	$(3,4)$
Number of edges	$2n$	$24n$	$10n-5$	$48n-6$	$13n$	$8n$

Table 1: Edge partition of D_nP_n

In the following theorem, we compute the first and second inverse Nirmala indices of D_nP_n.

Theorem 2.1 *Let D_nP_n be the family of porphyrin dendrimers. Then*

$$IN_1(D_nP_n) = \left(\frac{4}{\sqrt{3}} + 12\sqrt{5} + 10 + 48\frac{\sqrt{5}}{\sqrt{6}} + 13\frac{\sqrt{2}}{\sqrt{3}} + \frac{4\sqrt{7}}{\sqrt{3}}\right)n - 5 - 6\frac{\sqrt{5}}{\sqrt{6}},$$
$$IN_2(D_nP_n) = \left(\sqrt{3} + \frac{48}{\sqrt{5}} + 10 + 48\frac{\sqrt{6}}{\sqrt{5}} + 13\frac{\sqrt{3}}{\sqrt{2}} + \frac{16\sqrt{3}}{\sqrt{7}}\right)n - 5 - 6\frac{\sqrt{6}}{\sqrt{5}}.$$

Proof From the definitions and by using Table 1, we deduce

$$\begin{aligned}
IN_1(D_nP_n) &= 2n\left[\frac{1}{1}+\frac{1}{3}\right]^{\frac{1}{2}} + 24n\left[\frac{1}{1}+\frac{1}{4}\right]^{\frac{1}{2}} + (10n-5)\left[\frac{1}{2}+\frac{1}{2}\right]^{\frac{1}{2}} \\
&+ (48n-6)\left[\frac{1}{2}+\frac{1}{3}\right]^{\frac{1}{2}} + 13n\left[\frac{1}{3}+\frac{1}{3}\right]^{\frac{1}{2}} + 8n\left[\frac{1}{3}+\frac{1}{4}\right]^{\frac{1}{2}} \\
&= \left(\frac{4}{\sqrt{3}} + 12\sqrt{5} + 10 + 48\frac{\sqrt{5}}{\sqrt{6}} + 13\frac{\sqrt{2}}{\sqrt{3}} + \frac{4\sqrt{7}}{\sqrt{3}}\right)n - 5 - 6\frac{\sqrt{5}}{\sqrt{6}}.
\end{aligned}$$

and

$$\begin{aligned}
IN_2(D_nP_n) &= 2n\left[\frac{1}{1}+\frac{1}{3}\right]^{-\frac{1}{2}} + 24n\left[\frac{1}{1}+\frac{1}{4}\right]^{-\frac{1}{2}} + (10n-5)\left[\frac{1}{2}+\frac{1}{2}\right]^{-\frac{1}{2}} \\
&+ (48n-6)\left[\frac{1}{2}+\frac{1}{3}\right]^{-\frac{1}{2}} + 13n\left[\frac{1}{3}+\frac{1}{3}\right]^{-\frac{1}{2}} + 8n\left[\frac{1}{3}+\frac{1}{4}\right]^{-\frac{1}{2}} \\
&= \left(\sqrt{3} + \frac{48}{\sqrt{5}} + 10 + 48\frac{\sqrt{6}}{\sqrt{5}} + 13\frac{\sqrt{3}}{\sqrt{2}} + \frac{16\sqrt{3}}{\sqrt{7}}\right)n - 5 - 6\frac{\sqrt{6}}{\sqrt{5}}. \qquad \square
\end{aligned}$$

§3. Results for Propyl Ether Imine Dendrimer PETIM

We consider the family of propyl ether imine dendrimers. This family of dendrimers is denoted by PETIM. The molecular graph of PETIM is depicted in Figure 2.

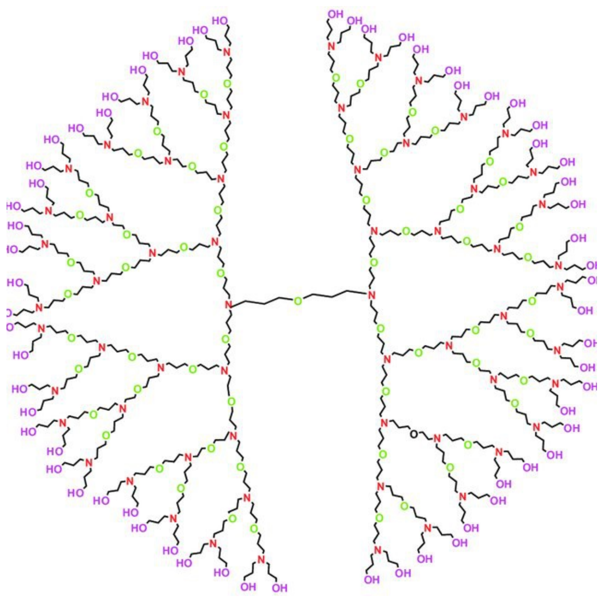

Figure 2. The molecular graph of $PETIM$

Let G be the molecular graph of $PETIM$. By calculation, we find that G has $24 \times 2^n - 23$

vertices and $24 \times 2^n - 24$ edges. In $PETIM$, there are three types of edges based on degrees of end vertices of each edge as given in Table 2.

$d_G(u), d_G(v) \setminus uv \in E(G)$	$(1,2)$	$(2,2)$	$(2,3)$
Number of edges	2×2^n	$16 \times 2^n - 18$	$6 \times 2^n - 6$

Table 2: Edge partition of $PETIM$

In the following theorem, we compute the first and second inverse Nirmala indices of $PETIM$.

Theorem 3.1 *Let $PETIM$ be the family of propyl ether imine dendrimers. Then*

$$\begin{aligned} IN_1(PETIM) &= (\sqrt{6} + 16 + \sqrt{30})2^n - (18 + \sqrt{30}), \\ IN_2(PETIM) &= \left(\frac{2\sqrt{2}}{\sqrt{3}} + 16 + \frac{6\sqrt{6}}{\sqrt{5}}\right)2^n - \left(18 + \frac{6\sqrt{6}}{\sqrt{5}}\right). \end{aligned}$$

Proof From definitions and by using Table 2, we derive

$$\begin{aligned} IN_1(PETIM) =& (2 \times 2^n)\left[\frac{1}{1} + \frac{1}{2}\right]^{\frac{1}{2}} + (16 \times 2^n - 18)\left[\frac{1}{2} + \frac{1}{2}\right]^{\frac{1}{2}} + (6 \times 2^n - 6)\left[\frac{1}{2} + \frac{1}{3}\right]^{\frac{1}{2}} \\ =& (\sqrt{6} + 16 + \sqrt{30})2^n - (18 + \sqrt{30}), \\ IN_2(PETIM) =& (2 \times 2^n)\left[\frac{1}{1} + \frac{1}{2}\right]^{-\frac{1}{2}} + (16 \times 2^n - 18)\left[\frac{1}{2} + \frac{1}{2}\right]^{-\frac{1}{2}} + (6 \times 2^n - 6)\left[\frac{1}{2} + \frac{1}{3}\right]^{-\frac{1}{2}} \\ =& \left(\frac{2\sqrt{2}}{\sqrt{3}} + 16 + \frac{6\sqrt{6}}{\sqrt{5}}\right)2^n - \left(18 + \frac{6\sqrt{6}}{\sqrt{5}}\right). \end{aligned}$$

□

§4. Results for Poly Ethylene Amide Dendrimer $PETAA$

We consider the family of poly ethylene amide amine dendrimers. This family of dendrimers is denoted by $PETAA$. The molecular graph of $PETAA$ is presented in Figure 3.

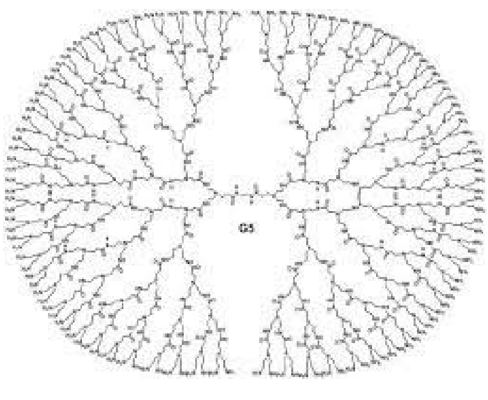

Figure 3. The molecular graph of $PETAA$

Let G be the molecular graph of $PETAA$. By calculation, we find that G has $44 \times 2^n - 18$ vertices and $44 \times 2^n - 19$ edges. In $PETAA$, there are four types of edges based on degrees of end vertices of each edge as given in Table 3.

$d_G(u), d_G(v) \setminus uv \in E(G)$	$(1,2)$	$(1,3)$	$(2,2)$	(2,3)
Number of edges	4×2^n	$4 \times 2^n - 2$	$16 \times 2^n - 8$	$20 \times 2^n - 9$

Table 3: Edge partition of $PETAA$

In the following theorem, we compute the first and second inverse Nirmala indices of $PETAA$.

Theorem 4.1 *Let $PETAA$ be the family of poly ethylene amide amine dendrimers. Then*

$$\begin{aligned} IN_1(PETAA) &= \left(\frac{4\sqrt{3}}{\sqrt{2}} + \frac{8}{\sqrt{3}} + 16 + \frac{20\sqrt{5}}{\sqrt{6}}\right)2^n - \left(\frac{4}{\sqrt{3}} + 8 + \frac{9\sqrt{5}}{\sqrt{6}}\right), \\ IN_2(PETAA) &= \left(\frac{4\sqrt{2}}{\sqrt{3}} + 2\sqrt{3} + 16 + \frac{20\sqrt{6}}{\sqrt{5}}\right)2^n - \left(\sqrt{3} + 8 + \frac{9\sqrt{6}}{\sqrt{5}}\right). \end{aligned}$$

Proof By using definitions and Table 3, we obtain

$$\begin{aligned} IN_1(PETAA) &= (4 \times 2^n)\left[\frac{1}{1} + \frac{1}{2}\right]^{\frac{1}{2}} + (4 \times 2^n - 2)\left[\frac{1}{1} + \frac{1}{3}\right]^{\frac{1}{2}} + (16 \times 2^n - 8)\left[\frac{1}{2} + \frac{1}{2}\right]^{\frac{1}{2}} \\ &+ (20 \times 2^n - 9)\left[\frac{1}{2} + \frac{1}{3}\right]^{\frac{1}{2}} \\ &= \left(\frac{4\sqrt{3}}{\sqrt{2}} + \frac{8}{\sqrt{3}} + 16 + \frac{20\sqrt{5}}{\sqrt{6}}\right)2^n - \left(\frac{4}{\sqrt{3}} + 8 + \frac{9\sqrt{5}}{\sqrt{6}}\right). \end{aligned}$$

and

$$\begin{aligned} IN_2(PETAA) &= (4 \times 2^n)\left[\frac{1}{1} + \frac{1}{2}\right]^{-\frac{1}{2}} + (4 \times 2^n - 2)\left[\frac{1}{1} + \frac{1}{3}\right]^{-\frac{1}{2}} + (16 \times 2^n - 8)\left[\frac{1}{2} + \frac{1}{2}\right]^{-\frac{1}{2}} \\ &+ (20 \times 2^n - 9)\left[\frac{1}{2} + \frac{1}{3}\right]^{-\frac{1}{2}} \\ &= \left(\frac{4\sqrt{2}}{\sqrt{3}} + 2\sqrt{3} + 16 + \frac{20\sqrt{6}}{\sqrt{5}}\right)2^n - \left(\sqrt{3} + 8 + \frac{9\sqrt{6}}{\sqrt{5}}\right). \qquad \square \end{aligned}$$

§5. Results for Zinc Prophyrin Dendrimer DPZ_n

We consider the family of zinc prophyrin dendrimers. This family of dendrimers is denoted by DPZ_n, where n is the steps of growth in this type of dendrimers. The molecular graph of DPZ_n is shown in Figure 4.

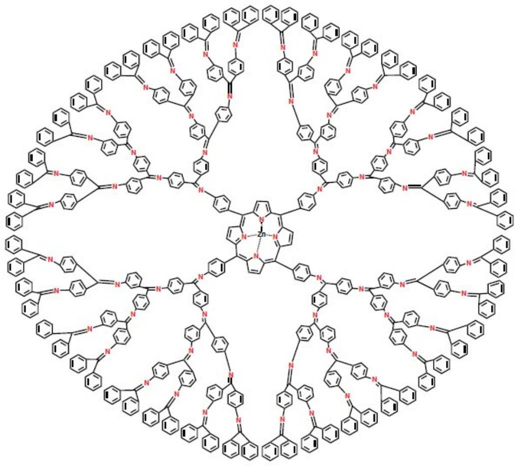

Figure 4. The molecular graph of DPZ_n

Let G be the molecular graph of DPZ_n. By calculation, we obtain that G has $56 \times 2^n - 7$ vertices and $64 \times 2^n - 4$ edges. In DPZ_n, there are four types of edges based on degrees of end vertices of each edge as given in Table 4.

$d_G(u), d_G(v) \setminus uv \in E(G)$	$(2,2)$	$(2,3)$	$(3,3)$	(3,4)
Number of edges	$16 \times 2^n - 4$	$40 \times 2^n - 16$	$8 \times 2^n + 12$	4

Table 4: Edge partition of DPZ_n

In the following theorem, we determine the Nirmala index and its exponential of DPZ_n.

Theorem 5.1 *Let DPZ_n be the family of zinc prophyrin dendrimers. Then*

$$IN_1(DPZ_n) = \left(16 + \frac{40\sqrt{5}}{\sqrt{6}} + \frac{8\sqrt{2}}{\sqrt{3}}\right)2^n - \left(4 + \frac{16\sqrt{5}}{\sqrt{6}} + \frac{12\sqrt{2}}{\sqrt{3}} - \frac{2\sqrt{7}}{\sqrt{3}}\right),$$

$$IN_2(DPZ_n) = \left(16 + \frac{40\sqrt{6}}{\sqrt{5}} + \frac{8\sqrt{3}}{\sqrt{2}}\right)2^n - \left(4 + \frac{16\sqrt{6}}{\sqrt{5}} - \frac{12\sqrt{3}}{\sqrt{2}} - \frac{8\sqrt{3}}{\sqrt{7}}\right).$$

Proof From definitions and by using Table 4, we deduce

$$\begin{aligned} IN_1(DPZ_n) &= (16 \times 2^n - 4)\left[\frac{1}{2} + \frac{1}{2}\right]^{\frac{1}{2}} + (40 \times 2^n - 16)\left[\frac{1}{2} + \frac{1}{3}\right]^{\frac{1}{3}} \\ &+ (8 \times 2^n + 12)\left[\frac{1}{3} + \frac{1}{3}\right]^{\frac{1}{2}} + 4\left[\frac{1}{3} + \frac{1}{4}\right]^{\frac{1}{2}} \\ &= \left(16 + \frac{40\sqrt{5}}{\sqrt{6}} + \frac{8\sqrt{2}}{\sqrt{3}}\right)2^n - \left(4 + \frac{16\sqrt{5}}{\sqrt{6}} + \frac{12\sqrt{2}}{\sqrt{3}} - \frac{2\sqrt{7}}{\sqrt{3}}\right). \end{aligned}$$

and

$$\begin{aligned} IN_2(DPZ_n) &= (16\times 2^n - 4)\left[\frac{1}{2}+\frac{1}{2}\right]^{-\frac{1}{2}} + (40\times 2^n - 16)\left[\frac{1}{2}+\frac{1}{3}\right]^{-\frac{1}{3}} \\ &+ (8\times 2^n + 12)\left[\frac{1}{3}+\frac{1}{3}\right]^{-\frac{1}{2}} + 4\left[\frac{1}{3}+\frac{1}{4}\right]^{-\frac{1}{2}} \\ &= \left(16+\frac{40\sqrt{6}}{\sqrt{5}}+\frac{8\sqrt{3}}{\sqrt{2}}\right)2^n - \left(4+\frac{16\sqrt{6}}{\sqrt{5}}-\frac{12\sqrt{3}}{\sqrt{2}}-\frac{8\sqrt{3}}{\sqrt{7}}\right). \qquad \square \end{aligned}$$

§6. Conclusion

In this study, we have defined the first and second inverse Nirmala indices of a molecular graph. Furthermore, the first and second inverse Nirmala indices for certain dendrimers are computed.

References

[1] V. R. Kulli,*College Graph Theory*, Vishwa International Publications, Gulbarga, India (2012).

[2] I. Gutman and O. E. Polansky, *Mathematical Concepts in Organic Chemishtry*, Springer, Berlin (1986).

[3] V. R. Kulli, *Multiplicative Connectivity indices of Nanostructures*, LAP LEMBERT Academic Publishing (2018).

[4] R. Todeschini and V. Consonni, *Molecular Descriptors for Chemoinformatics*, Wiley-VCH, Weinheim (2009).

[5] V. R. Kulli, Graph indices, *in Hand Book of Research on Advanced Application Graph Theory in Modern Society*, M. Pal. S. Samanta and A. Pal, (eds) IGI Global, USA (2019) 66-91.

[6] I. Gutman, Geometric approach to degree based topological indices: Sombor indices MATCH Common, *Math.Compute. Chem.*, 86 (2021) 11-16.

[7] K. C. Das, A. S. Cevik, I. N. Cangul and Y. Shang, on Sombor index, *Symmetry*, 13 (2021) 140.

[8] I. Gutman, Some basic properties of Sombor indices, *Open Journal of Discrete Applied Mathematics*, 4(1) (2021) 1-3.

[9] V. R. Kulli, Sombor indices of certain graph operators, *International Journal of Engineering Sciences and Research Technology*, 10(1) (2021) 127-134.

[10] V. R. Kulli, Multiplicative Sombor indices of certain nanotubes, *International Journal of Mathematical Archive*, 12 (2021).

[11] V. R. Kulli and I. Gutman, Computation of Sombor indices of certain networks, *SSRG International Journal of Applied Chemistry*, 8(1) (2021) 1-5.

[12] I. Milovanovic, E. Milovanovic and M. Matejic, On some mathematical properties of Sombor indices, *Bull. Int. Math. Virtual Inst.* 11(2) (2021) 341-353.

[13] I. Redzepovic, Chemical applicability of Sombor indices, *J. Serb. Chem. Soc* (2021) https://doi.org/10.2298/JSC201215006R.

[14] T. Reti, T. Doslic and A. Ali, On the Sombor index of graphs, *Contributions of Mathematics*, 3 (2021) 11-18.

[15] V. R. Kulli, Nirmala index, *International Journal of Mathematics trends and Technology*, 67(3) (2021) 8-12.

[16] V. R. Kulli, B. Chaluvaraju, V. Lokesha and S. A. Basha, Gourava indices of some dendrimers, *Research Review International Journal of Multidisciplinary*, 4(6) (2019) 212-215.

International J.Math. Combin. Vol.2(2021), 41-50

Results on Centralizers of Semiprime Gamma Semirings

Nondita Paul and Md Fazlul Hoque

(Department of Mathematics, Pabna University of Science and Technology, Pabna 6600, Bangladesh)

E-mail: nondita93@gmail.com, fazlulmath@pust.ac.bd

Abstract: Let M be a noncommutative 2-torsion free semiprime Γ-semiring satisfying a certain assumption with centre $Z_\alpha(M)$ and $T : M \to M$ be an additive mapping. We prove results: 1) If T is centralizing on a Jordan Γ-subring J of M, then T is commutating on J; 2) If T is centralizing right centralizer on M, then T is commutating; 3) If T is centralizing right centralizer on M, then T is centralizer and 4) If T is centralizing right centralizer on M, then T satisfies the relation

$$[x, y]_\alpha \beta T(x) = [T(x), y]_\alpha \beta x$$

for all $x, y \in M$ and $\alpha, \beta \in \Gamma$.

Key Words: Semiprime gamma ring, semiprime gamma semiring, centralizing, left and right centralizers.

AMS(2010): 16N60, 16W25, 16Y99.

§1. Introduction

The notion of gamma ring was first introduced in [1], which is currently notable as Γ_N-ring. Bernes [2] broadly generalized and extended the concept of Γ_N-ring to Γ-ring and shown that every Γ_N-ring is a Γ-ring. The Γ-ring is more general than the classical ring and it is concluded that Γ-ring need not to be a ring [1, 2]. Later, much theory relevant to the classical rings have been generalized and extended to the theory of Γ-rings, especially, Luh [3] and Kyuno [4] deeply studied on the structure of Γ-rings and explored various generalizations of analogous parts in ring theory.

Over the years, Bell and Martindale [5] and Zalar [6] developed some notable results on centralizing mappings of semiprime rings. Vukman [7-10] presented may remarkable findings via the concept of centralizers on prime and semiprime rings. Recently, the research on centralizers of prime and semiprime rings have been extended to prime and semiprime gamma rings and semiprime gamma semirings in the aspects of Jordan centralizers [12, 13], centralizers [11, 13C15], centralizers on Lie ideals [16, 17], centralizers with involutions [18, 19], Jordan derivations on Lie ideals [16] and generalized derivations on prime and semiprime gamma rings with centralizing and commuting [20, 21] as well.

[1]Received March 3, 2021, Accepted June 8, 2021.

H.S. Vandiver introduced the algebraic study of semiring in 1934 [22, 23] and Rao [24] extended such research to the Γ-semirings and established some basic theories on gamma rings as well as on gamma semiring. A number of important features on Γ-semirings are presented in [12, 25, 26]. However, the research on centralizing left/right centralizers on prime and semiprime gamma semiring is still unknown area. Thus the purpose of this article is to study on semiprime gamma semiring via centralizing right centralizers [11, 20]. The study is inspired by the work of [25, 26]. The results presented in this paper through out for right centralizers, which are also true for left centralizers because of left-right symmetry.

§2. Preliminaries

Let M and Γ be additive Abelian groups. If there exists a mapping $(x,\alpha,y) \to x\alpha y$ of $M \times \Gamma \times M \to M$, which satisfies the following conditions:

- (a) $x\alpha x \in M$;
- (b) $x\alpha(y+z) = x\alpha y + x\alpha z$ and $(x+y)\alpha z = x\alpha z + y\alpha z$;
- (c) $x(\alpha+\beta)y = x\alpha y + x\beta y$;
- (d) $(x\alpha y)\beta z = x\alpha(y\beta z)$

for all $x, y, z \in M$ and $\alpha, \beta \in \Gamma$, then M is called a Γ-ring. Every ring M is a Γ-ring with $M = \Gamma$.

Let M and Γ be two additive commutative semigroups. Then M is called a Γ-semiring if M is itself a Γ-ring. Obviously, every semiring M is a Γ-semiring with $M = \Gamma$. A non-empty subset A of a Γ-semiring M is said to be a sub Γ-semiring of M if $(A,+)$ is a subsemigroup of $(M,+)$ and $x\alpha y \in A$ for all $x, y \in A$ and $\alpha \in \Gamma$. A Γ-semiring M is said to have a zero element if there exists an element $0 \in M$ such that $0 + x = x = x + 0$ and $0\alpha x = 0 = x\alpha 0$ for all $x \in M$ and $\alpha \in \Gamma$. A Γ-semiring M is said to be prime if $x\alpha y = 0$ implies $x = 0$ or $y = 0$ for all $x, y \in S$ and $\alpha \in \Gamma$. A Γ-semiring S is said to be semiprime if $x\alpha x = 0$ implies $x = 0$ for all $x \in S$ and $\alpha \in \Gamma$. A Γ-semiring M is said to be n-torsion free if $nx = 0$ implies $x = 0$ for all $x \in M$. A Γ-semiring M is said to be commutative if $x\alpha y = y\alpha x$ for all $x, y \in M$ and $\alpha \in \Gamma$. Let M be a Γ-semiring. Then the set $Z_\alpha(M) = \{x \in M : x\alpha y = y\alpha x \quad \forall y \in M, \alpha \in \Gamma\}$ is called the centre of the Γ-semiring M. Let M be a Γ-ring. Then $[x,y]_\alpha = x\alpha y - y\alpha x$ is called the commutator of x and y with respect to α, where $x, y \in M$ and $\alpha \in \Gamma$.

We make the basic commutator identities following

$$[a\alpha b, c]_\beta = [a,c]_\beta \alpha b + a[\alpha,\beta]_c b + a\alpha[b,c]_\beta,$$
$$[a, b\alpha c]_\beta = [a,b]_\beta \alpha c + b[\alpha,\beta]_a c + b\alpha[a,c]_\beta$$

for all $a, b, c \in M$ and $\alpha, \beta \in \Gamma$. We consider the following assumption [11],

$$a\alpha b\beta c = a\beta b\alpha c \tag{2.1}$$

for all $a, b, c \in M$, and $\alpha, \beta \in \Gamma$, which we extensively used in this paper. According to the assumption(2.1), the above two identities reduce to

$$[a\alpha b, c]_\beta = [a, c]_\beta \alpha b + a\alpha[b, c]_\beta, \tag{2.2}$$

$$[a, b\alpha c]_\beta = [a, b]_\beta \alpha c + b\alpha[a, c]_\beta. \tag{2.3}$$

The identities (2.2) and (2.3) are also used thoroughly in this article.

An additive mapping $T : M \to M$ is called a left (right) centralizer if

$$T(x\alpha y) = T(x)\alpha y(T(x\alpha y) = x\alpha T(y))$$

holds for all $x, y \in M$ and $\alpha \in \Gamma$. An additive mapping $T : M \to M$ is centralizer if it is both a left and a right centralizer. For any fixed $a \in M$ and $\alpha \in \Gamma$, the mapping $T(x) = a\alpha x$ is a left centralizer and $T(x) = x\alpha a$ is a right centralizer. A mapping $T : M \to M$ is called centralizing if $[T(x), x]_\alpha \in Z_\alpha(M)$ for all $x \in M$, $\alpha \in \Gamma$. A mapping T of a Γ-semiring M into itself is said to be commuting if $[T(x), x]_\alpha = 0$. We recall if $T : M \to M$ is commuting, then $[T(x), y]_\alpha = [x, T(y)]_\alpha$ for all $x, y \in M$ and $\alpha \in \Gamma$. Obviously, every commuting mapping $T : M \to M$ is centralizing. If A be a subset of Γ-semiring M and $x\alpha y + y\alpha x \in A$ for all $x, y \in A$ and $\alpha \in \Gamma$, then A is called a Jordan subring of M.

§3. Main results

In this section, we obtain the following results with their proofs in sense of 2-torsion free semiprime Γ-semiring with the certain assumption (2.1) and using various commutation identities.

Theorem 3.1 *Suppose M is a 2- torsion free cancellative semiprime Γ-semiring satisfying the assumption (2.1) and J is a Jordan subring of M. If an additive mapping $T : M \to M$ is centralizing on J, then T is commuting on J.*

Proof By the definition of centralizing T on J, we have

$$[T(x), x]_\alpha \in Z_\alpha(M). \tag{3.1}$$

For the linearization, we put $x = x + y$ in (3.1), which yields

$$\begin{aligned} &[T(x), x]_\alpha + [T(x), y]_\alpha + [T(y), x]_\alpha + [T(y), y]_\alpha \in Z_\alpha(M), \\ &\Rightarrow [T(x), y]_\alpha + [T(y), x]_\alpha \in Z_\alpha(M) \end{aligned} \tag{3.2}$$

for all $x, y \in J$ and $\alpha \in \Gamma$. In particular, for $y = x\beta x$, we obtain

$$\begin{aligned} &[T(x), x\beta x]_\alpha + [T(x\beta x), x]_\alpha \in Z_\alpha(M) \quad \text{for all} \quad x, y \in J, \quad \alpha \in \Gamma, \\ &\Rightarrow [T(x), x]_\alpha \beta x + x\beta[T(x), x]_\alpha + [T(x\beta x), x]_\alpha \in Z_\alpha(M). \end{aligned}$$

Using the definition of the centre of Γ-semiring $Z_\alpha(M)$, we have

$$\begin{aligned}&[T(x),x]_\alpha\beta x+[T(x),x]_\alpha\beta x+[T(x\beta x),x]_\alpha\in Z_\alpha(M),\\ &\Rightarrow 2[T(x),x]_\alpha\beta x+[T(x\beta x),x]_\alpha\in Z_\alpha(M).\end{aligned}\tag{3.3}$$

Suppose $x\in J$ is a fixed element with $z=[T(x),x]_\alpha\in Z_\alpha(M)$ and $a=[T(x\beta x),x]_\alpha$. Then (3.3) can rewrite in the following form

$$[T(x),2z\beta x+a]_\alpha=0.\tag{3.4}$$

By the expansion of the commutation identities (3.4), we get

$$\begin{aligned}&[T(x),2z\beta x]_\alpha+[T(x),a]_\alpha=0,\\ &\Rightarrow 2z\beta[T(x),x]_\alpha+2[T(x),z]_\alpha\beta x+[T(x),a]_\alpha=0,\\ &\Rightarrow 2z\beta z+[T(x),a]_\alpha=0,\\ &\Rightarrow [T(x),a]_\alpha=-2z\beta z.\end{aligned}\tag{3.5}$$

On the other hand, we have

$$[T(x\beta x),x\beta x]_\alpha\in Z_\alpha(M)\tag{3.6}$$

for all $x\in J$ and $\alpha,\beta\in\Gamma$. This implies

$$[T(x\beta x),x]_\alpha\beta x+x\beta[T(x\beta x),x]_\alpha\in Z_\alpha(M).\tag{3.7}$$

Now using the relation (3.7), we can write $[T(x),a\beta x+x\beta a]_\alpha=0$ and apply (3.4), it takes the following explicit form

$$\begin{aligned}&[T(x),a]_\alpha\beta x+a\beta[T(x),x]_\alpha+[T(x),x]_\alpha\beta a+x\beta[T(x),a]_\alpha=0,\\ &\Rightarrow -2z\beta z\beta x+a\beta z+z\beta a+x\beta(-2z\beta z)=0,\\ &\Rightarrow -2z\beta z\beta x+z\beta a+z\beta a-2z\beta z\beta x=0,\quad \text{by using the definition of}\quad Z_\alpha(M),\\ &\Rightarrow 2z\beta a-4z\beta z\beta x=0\Rightarrow a=2z\beta x.\end{aligned}\tag{3.8}$$

Using (3.8) in (3.5), we have

$$\begin{aligned}&[T(x),2z\beta x]_\alpha=-2z\beta z,\\ &\Rightarrow 2\{[T(x),z]_\alpha\beta x+z\beta[T(x),x]_\alpha\}=-2z\beta z,\\ &\Rightarrow [T(x),z]_\alpha\beta x+z\beta[T(x),x]_\alpha=-z\beta z,\\ &\Rightarrow [T(x),z]_\alpha\beta x+z\beta[T(x),x]_\alpha=-z\beta z,\\ &\Rightarrow z\beta[T(x),x]_\alpha=-z\beta z,\\ &\Rightarrow z\beta z=-z\beta z\Rightarrow 2z\beta z=0.\end{aligned}\tag{3.9}$$

By the 2-torsion free semiprimeness of M, we conclude that $z\beta z = 0$ implies $z = 0$ for all $\beta \in \Gamma$. Therefore $[T(x), x]_\alpha = 0$ for all $x \in J$ and hence T is commutating on J. □

Theorem 3.2 *Suppose that M is a cancellative semiprime Γ-semiring satisfying the assumption* (2.1). *If $T : M \to M$ is a centralizing right centralizer, then T is commuting.*

Proof If we consider M is 2-torsion free cancellative semiprime Γ-semiring satisfying the assumption (2.1), then the theorem is nothing to prove for $J = M$ in account of Theorem 3.1. We now assume that M is not 2-torsion free Γ-semiring. In this case, we consider the following relation

$$2[x, T(x)]_\alpha = 0. \tag{3.10}$$

for all $x \in M$ and $\alpha \in \Gamma$. We now substitute $x + y$ for x in (3.10), which yields

$$\begin{aligned} & 2[x + y, T(x + y)]_\alpha = 0, \\ & \Rightarrow 2[x, T(y)]_\alpha + 2[y, T(x)]_\alpha = 0, \\ & \Rightarrow [x, T(y)]_\alpha = -[y, T(x)]_\alpha \end{aligned} \tag{3.11}$$

for all $x, y \in M$ and $\alpha \in \Gamma$. We now again linearise the assumption $[x, T(x)]_\alpha \in Z_\alpha(M)$ by the transformation $x = x + y$, which leads to

$$[x, T(y)]_\alpha + [y, T(x)]_\alpha \in Z_\alpha(M) \tag{3.12}$$

for all $x, y \in M$ and $\alpha \in \Gamma$. By using the definition of $Z_\alpha(M)$ in (3.12), we enable to express as

$$[([x, T(y)]_\alpha + [y, T(x)]_\alpha), x]_\beta = 0 \tag{3.13}$$

for all $x, y \in M$ and $\alpha, \beta \in \Gamma$. This implies

$$\begin{aligned} & ([x, T(y)]_\alpha + [y, T(x)]_\alpha)\beta x - x\beta([x, T(y)]_\alpha + [y, T(x)]_\alpha) = 0, \\ & \Rightarrow [x, T(y)]_\alpha \beta x + [y, T(x)]_\alpha \beta x - x\beta[x, T(y)]_\alpha - x\beta[y, T(x)]_\alpha = 0. \end{aligned} \tag{3.14}$$

Using (3.11) in (3.14), we obtain

$$[x, T(y)]_\alpha \beta x + [y, T(x)]_\alpha \beta x + x\beta[x, T(y)]_\alpha + x\beta[y, T(x)]_\alpha = 0. \tag{3.15}$$

Again from the assumption $[x, T(x)]_\alpha \in Z_\alpha(M)$ and the definition of $Z_\alpha(M)$, we found

$$\begin{aligned} [x, T(x)]_\alpha \beta y &= (x\alpha T(x) - T(x)\alpha x)\beta y \\ &= x\alpha T(x)\beta y - T(x)\alpha x\beta y \\ &= y\beta x\alpha T(x) - y\beta T(x)\alpha x \\ &= y\beta(x\alpha T(x) - T(x)\alpha x) = y\beta[x, T(x)]_\alpha \end{aligned} \tag{3.16}$$

for all $x, y \in M$ and $\alpha, \beta \in \Gamma$. Applying the result(3.16) in (3.11), we get

$$\begin{aligned}
&2[x, T(x)]_\alpha = 0, \\
&\Rightarrow [x, T(x)]_\alpha + [x, T(x)]_\alpha = 0, \\
&\Rightarrow y\beta[x, T(x)]_\alpha + y\beta[x, T(x)]_\alpha = 0, \quad \text{right multiplying by } y\beta, \\
&\Rightarrow [x, T(x)]_\alpha \beta y + y\beta[x, T(x)]_\alpha = 0, \quad \text{using (3.16)}, \qquad (3.17)
\end{aligned}$$

for all $x, y \in M$ and $\alpha, \beta \in \Gamma$. Adding the relations (3.15) and (3.17) and simplifying, we have

$$[(x\beta y + y\beta x), T(x)]_\alpha + [x\beta x, T(y)]_\alpha = 0. \qquad (3.18)$$

Now using $x\gamma y$ for y in the relation (3.18), we arrive at

$$[(x\beta x\gamma y + x\gamma y\beta x), T(x)]_\alpha + [x\beta x, T(x\gamma y)]_\alpha = 0 \qquad (3.19)$$

for all $x, y \in M$ and $\alpha, \beta, \gamma \in \Gamma$. By using assumption (2.1) in (3.19), we obtain

$$\begin{aligned}
&[(x\gamma x\beta y + x\gamma y\beta x), T(x)]_\alpha + [x\beta x, T(x\gamma y)]_\alpha = 0, \\
&\Rightarrow [x\gamma(x\beta y + y\beta x), T(x)]_\alpha + [x\beta x, T(x\gamma y)]_\alpha = 0, \\
&\Rightarrow [x, T(x)]_\alpha \gamma(x\beta y + y\beta x) + x\gamma[(x\beta y + y\beta x), T(x)]_\alpha + x\gamma[x\beta x, T(y)]_\alpha = 0. \qquad (3.20)
\end{aligned}$$

Using (3.18) in (3.20), it reduces to

$$\begin{aligned}
&[x, T(x)]_\alpha \gamma(x\beta y + y\beta x) - x\gamma[x\beta x, T(y)]_\alpha + x\gamma[x\beta x, T(y)]_\alpha = 0, \\
&\Rightarrow [x, T(x)]_\alpha \gamma(x\beta y + y\beta x) = 0, \\
&\Rightarrow [x, T(x)]_\alpha \gamma(x\beta y - y\beta x + 2y\beta x) = 0, \\
&\Rightarrow [x, T(x)]_\alpha \gamma(x\beta y - y\beta x) + 2[x, T(x)]_\alpha \gamma y\beta x = 0, \\
&\Rightarrow [x, T(x)]_\alpha \gamma(x\beta y - y\beta x) = 0, \quad \text{using (3.10)}, \\
&\Rightarrow [x, T(x)]_\alpha \gamma[x, y]_\beta = 0 \qquad (3.21)
\end{aligned}$$

for all $x, y \in M$ and $\alpha, \beta, \gamma \in \Gamma$. Replacing y by $T(x)$ and $\beta = \alpha$ in (3.21), we obtain

$$[x, T(x)]_\alpha \gamma[x, T(x)]_\alpha = 0 \qquad (3.22)$$

for all $x \in M$ and $\alpha, \gamma \in \Gamma$. For the semiprimeness of Γ-semiring, $[x, T(x)]_\alpha \gamma[x, T(x)]_\alpha = 0$ implies $[x, T(x)]_\alpha = 0$ for all $x \in M$ and $\alpha, \gamma \in \Gamma$. Therefore T is commuting and hence the theorem is proved. □

Theorem 3.3 *Suppose that M is a cancellative semiprime Γ-semiring satisfying the assumption (2.1). If $T : M \to M$ is a centralizing right centralizer on M, then T is centralizer.*

Proof Since T is a centralizing right centralizer on M, we have

$$T(x\alpha y) = x\alpha T(y) \qquad (3.23)$$

for all $x, y \in M$ and $\alpha \in \Gamma$. We aim to prove that $T(x\alpha y) = T(x)\alpha y$ for all $x, y \in M$ and $\alpha \in \Gamma$. According to the statement and Theorem 3.2, T is commuting on M. In this case, we can write $[x, T(x)]_\alpha = 0$. This implies

$$x\alpha T(x) = T(x)\alpha x \tag{3.24}$$

for all $x \in M$ and $\alpha \in \Gamma$. Now linearizing the relation (3.24) by setting $x = x + y$, yields

$$[x, T(y)]_\alpha + [y, T(x)]_\alpha = 0 \tag{3.25}$$

for all $x, y \in M$ and $\alpha \in \Gamma$. Applying $x\beta y$ for x and using the definition, we obtain

$$\begin{aligned}
&[x\beta y, T(y)]_\alpha + [y, T(x\beta y)]_\alpha = 0,\\
&\Rightarrow x\beta[y, T(y)]_\alpha + [x, T(y)]_\alpha\beta y + [y, T(x\beta y)]_\alpha = 0,\\
&\Rightarrow [x, T(y)]_\alpha\beta y + [y, x\beta T(y)]_\alpha = 0,\\
&\Rightarrow x\alpha T(y)\beta y - T(y)\alpha x\beta y + y\alpha x\beta T(y) - x\beta T(y)\alpha y = 0,\\
&\Rightarrow x\beta T(y)\alpha y - x\beta T(y)\alpha y + y\alpha x\beta T(y) - T(y)\alpha x\beta y = 0,\\
&\Rightarrow y\alpha x\beta T(y) - T(y)\alpha x\beta y = 0,\\
&\Rightarrow y\alpha x\beta T(y) = T(y)\alpha x\beta y
\end{aligned} \tag{3.26}$$

for all $x, y \in M$ and $\alpha, \beta \in \Gamma$. Let $T(y) = y$ in (3.26), then we have $y\alpha x\beta T(y) = y\alpha x\beta y$. This implies $y\beta x\alpha T(y) = y\beta x\alpha y$. By using the cancellation law, it shows that $x\alpha T(y) = x\alpha y$, which implies that $T(x\alpha y) = x\alpha y$ for all $x, y \in M$ and $\alpha \in \Gamma$. Thus for choosing $T(x) = x$, we write $T(x\alpha y) = T(x)\alpha y$. By using the assumption (2.1), this implies

$$x\alpha T(y) = T(x)\alpha y. \tag{3.27}$$

If we consider $z \in M$ and $\beta \in \Gamma$, then we can write $(T(x\alpha y) - x\alpha T(y))\beta z\beta(T(x\alpha y) - x\alpha T(y)) = 0$ for all $x, y \in M$ and $\alpha \in \Gamma$. By the definition of semiprime Γ-semiring M, it leads to $T(x\alpha y) - x\alpha T(y) = 0$. That is,

$$T(x\alpha y) = x\alpha T(y). \tag{3.28}$$

Comparing (3.27) and (3.28), we conclude that

$$T(x\alpha y) = T(x)\alpha y \tag{3.29}$$

for all $x, y \in M$ and $\alpha \in \Gamma$. Therefore, T is a centralizer on M and hence, the theorem is proved. □

The study of the above theorems, we can provide the following remarks.

Remark 3.1 Every centralizer on a cancellative semiprime Γ-semiring is commuting, because of $T(x\alpha x) = T(x)\alpha x = x\alpha T(x)$ for all $x \in M$ and $\alpha \in \Gamma$ and hence is a centralizing right centralizer.

Remark 3.2 An additive mapping T of a cancellative semiprime Γ-semiring M is a centralizer if and only if it is a centralizing right centralizer on M.

Corollary 3.1 *Suppose that T is a commuting right centralizer of a semiprime Γ-semiring M satisfying the assumption* (2.1)*, then T satisfies the relation $[x,y]_\alpha \beta T(x) = [T(x),y]_\alpha \beta x$ for all $x,y \in M$ and $\alpha, \beta \in \Gamma$.*

Proof By the statement, we have $T(x\alpha y) = x\alpha T(y)$ for all $x,y \in M$ and $\alpha \in \Gamma$. Since T is also commuting on M, it is easily seen that $[x,T(x)]_\alpha = 0$. Putting $x = x+y$ for linearization, we arrive at

$$[x,T(y)]_\alpha + [y,T(x)]_\alpha = 0 \tag{3.30}$$

for all $x,y \in M$ and $\alpha \in \Gamma$. Replacing y by $y\beta x$ in (3.30) and using the relation $[x,T(x)]_\alpha = 0$, we obtain

$$\begin{aligned}
&[x,T(y\beta x)]_\alpha + [y\beta x, T(x)]_\alpha = 0,\\
&\Rightarrow [x, y\beta T(x)]_\alpha + [y\beta x, T(x)]_\alpha = 0,\\
&\Rightarrow [x,y]_\alpha \beta T(x) + y\beta[x,T(x)]_\alpha + [y,T(x)]_\alpha \beta x + y\beta[x,T(x)]_\alpha = 0,\\
&\Rightarrow [x,y]_\alpha \beta T(x) + [y,T(x)]_\alpha \beta x = 0,\\
&\Rightarrow [x,y]_\alpha \beta T(x) - [T(x),y]_\alpha \beta x = 0,\\
&\Rightarrow [x,y]_\alpha \beta T(x) = [T(x),y]_\alpha \beta x
\end{aligned} \tag{3.31}$$

for all $x,y \in M$ and $\alpha, \beta \in \Gamma$. Hence, the theorem is proved. □

Corollary 3.2 *Suppose that M is a prime Γ-semiring and T is a commuting right centralizer on M. If $T(x) \in Z_\alpha(M)$ for all $x \in M$, then $T = 0$ or M is commutative.*

Proof Since $T(x) \in Z_\alpha(M)$, in this case we have $[T(x),y]_\alpha = 0$ for all $x,y \in M$ and $\alpha \in \Gamma$. We also have $[x,y]_\alpha \beta T(x) = [T(x),y]_\alpha \beta x$ for all $x,y \in M$ and $\alpha, \beta \in \Gamma$. Thus

$$[x,y]_\alpha \beta T(x) = 0 \tag{3.32}$$

for all $x,y \in M$ and $\alpha, \beta \in \Gamma$. Setting $y = y\gamma z$ in (3.32), we have

$$\begin{aligned}
&[x, y\gamma z]_\alpha \beta T(x) = 0,\\
&\Rightarrow \{[x,y]_\alpha \gamma z + y\gamma[x,z]_\alpha\}\beta T(x) = 0,\\
&\Rightarrow [x,y]_\alpha \gamma z \beta T(x) + y\gamma[x,z]_\alpha \beta T(x) = 0,\\
&\Rightarrow [x,y]_\alpha \gamma z\beta T(x) = 0, \quad \text{for all} \quad x,y,z \in M,\\
&\Rightarrow (x\alpha y - y\alpha x)\gamma z\beta T(x) = 0,\\
&\Rightarrow (x\alpha y\gamma z - y\alpha x\gamma z)\beta T(x) = 0.
\end{aligned}$$

For the prime Γ-semiringness of M, we have $(x\alpha y\gamma z - y\alpha x\gamma z) = 0$ or $\beta T(x) = 0$. Thus we have seen that $T = 0$ or M is commutative, and hence, the theorem is proved. □

References

[1] N. Nobusawa, On the generalization of the ring theory, *Osaka J. Math.*, 1 (1964), 81-89.

[2] W. E. Bernes, On the Γ-rings of Nobusawa, *Pacific J.Math.*, 18 (1966), 411-422.

[3] L. Luh, On the theory of simple Gamma rings, *Michigan Math. J.*, 16 (1969), 65-75.

[4] S. Kyuno, On prime Gamma ring, *Pacific J. Math.*, 75 (1978), 185-190.

[5] H. E. Bell, W. S. Martindale III, Centralizing mappings of semiprime rings, *Canad. Math. Bull.*, Vol.30 (1987), 92-101.

[6] B. Zalar, On centralizers of semiprime rings, *Commentationes Mathematicae Universitatis Carolinae*, 32 (1991), 609-614.

[7] J. Vukman, Commuting and centralizing mappings in prime rings, *Proc. math. Soc.*, 109 (1990), 47-52

[8] J. Vukman, Centralizers in prime and semiprime rings, *Comment. Math. Univ. Carolinae*, 38 (1997), 231-240.

[9] J. Vukman, An identity related to centralizers in semiprime rings, *Comment. Math. Univ. Carolinae*, 40 (3) (1999), 447-456.

[10] J. Vukman, Centralizers on semiprime rings, *Comment. Math. Univ. Carolinae*, 42 (2) (2001), 237-245.

[11] M. F. Hoque and A .C. Paul, On centralizers of semiprime gamma rings, *International Mathematical Forum*, Vol.6 (2011), No.13, 627-638.

[12] H. Hedayati and K. P. Shum, An introduction to Γ-semirings, *International Journal of Algebra*, Vol. 5, (2011), 709-726.

[13] K. K. Dey and A. C. Paul, On left centralizers of semiprime Γ-rings, *J. Sci. Res*, 4(2), 349-356 (2012).

[14] M. F. Hoque and A. C. Paul, Centralizers on semiprime gamma rings, *Italian Journal of Pure and Applied Mathematics*, 30 (2013), 289-302.

[15] M. F. Hoque and A.C. Paul, Centralizers on prime and semiprime gamma rings, *Italian Journal of Pure and Applied Mathematics*, 35 (2015), 575-586.

[16] M. M. Rahman and A.C.Paul, Jordan derivations on Lie ideals of prime gamma rings, *Mathematical Theory and Modelling*, Vol.3(3) (2013), 128-135.

[17] M. F. Hoque and A.C. Paul, Left centralizers on Lie ideals in prime and semiprime gamma rings, *Internaltional J. Math. Combin.*, Vol. 1 (2020), 10-19.

[18] M.F. Hoque, F. S. Alshammari and A.C. Paul, Left centralizers of semiprime gamma rings with involution, *Applied Mathematical Sciences*, Vol. 8, (2014), 4713-4722.

[19] M.F. Hoque and N. Rahman, The Jordan θ-centralizers of semiprime gamma semirings with involution, *Internaltional J. Math. Combin.*, Vol. 4 (2013), 15-30.

[20] M.F. Hoque and A. C. Paul, Prime gamma rings with centralizing and commuting generalized derivations, *Internaltional Journal of Algebra*, Vol. 7 (2013), 625-651.

[21] M.F. Hoque and A. C. Paul, Generalized derivations on semiprime gamma rings with involution, *Palestine Journal of Mathematics*, Vol. 3(2) (2014), 235-239.

[22] H. S. Vandiver, Note on a simple type of algebra in which cancellation law of addition does not hold, *Bull. Amer. Math. Soc.*, Vol.40(1934), 914-920.

[23] H. S. Vandiver, On some simple types of semirings, *Am. Math. Mon.*, 46(1939), 22-26.

[24] M. K. Rao, Γ-semirings-1, *Southeast Asian Bull. Math.*, 19 (1995) 49-54.

[25] D. Mary Florence, R. Murugesan and P. Namasivayam, Centralizers on semiprime semirings, *IOSR J. Math.*, Vol. 12 (3), 2016.

[26] D. Mary Florence, R. Murugesan and P. Namasivayam, On Right Centralizers of Semiprime Semirings, *Advances in Algebra*, Vol.11, N.1 (2018), 19-28.

International J.Math. Combin. Vol.2(2021), 51-67

Polynomial, Exponential and Approximate Algorithms for Metric Dimension Problem

Elsayed Badr[1], Atef Abd El-hay[2], Hagar Ahmed[1] and Mahmoud Moussa[4]

1. Scientific Computing Department, Faculty of Computers and Informatics, Benha University, Benha, Egypt
2. Department of Mathematics and Computer Science, Faculty of Science, Menoufia University, Menoufia, Egypt
3. Computer Science Department, Faculty of Computers and Informatics, Benha University, Benha, Egypt

E-mail: badrgraph@gmail.com, atef_1992@yahoo.com, mahmoud.mossa@fci.bu.edu.eg

Abstract: A robot can determine its location by a set of fixed landmarks (consider the robot path is like a graph). By a signal from the robot, it can determine how far it from each among a set of fixed landmarks. We can formulate this problem such that the robot can always determine its location as the following: how to compute the minimum landmarks and where these landmarks should be placed. The metric dimension problem of a given graph can answer about the above two questions. The metric basis of the graph represents the set of landmarks and the metric dimension of the graph is equal to the cardinality of the landmarks. The determining of the metric dimension of an arbitrary graph is an NP-complete problem. In this paper we determine the metric dimension of new classes of networks with polynomial algorithms. In particular, the metric dimension of the triangular snake graph, the ladder graph L_n, B_k, the k-home chain graph H_k and the k-kite chain graph K_k are determined. We propose an exponential algorithm for finding the metric dimension of a given graph. We also introduce the results of computer calculations that determined the metric dimension of various classes of networks by using an approximate algorithm namely integer linear programming. Finally, a comparative analysis between the proposed approximate and exponential algorithms shows that the LINGO solver outperforms the proposed algorithm for huge graphs.

Key Words: Metric dimension, resolving set, basis, integer programming, NP-hardness, robot navigation.

AMS(2010): 05C30.

§1. Introduction

A robot can determine its location by a set of fixed landmarks (consider the robot path is like a graph). It is known that a robot is different distances from a set of fixed landmarks. By a signal from the robot, it can determine how far it from each among a set of fixed landmarks. We can formulate this problem such that the robot can always determine its location as the following:

[1]Received March 10, 2021, Accepted June 10, 2021.

how to compute the minimum landmarks and where these landmarks should be placed. The metric dimension problem of a given graph can answer about the above two questions. The metric basis of the graph represents the set of landmarks and the metric dimension of the graph is equal to the cardinality of the landmarks. The concept of the metric dimension has proven to be useful in a variety of fields. Chartrand et al. [1] applied the resolving set of a metric dimension in chemistry to classify chemical compounds. Khuller et al. [2] applied resolving sets in robotic navigation, and Sebo et al. [3] applied them in combinatorial search and optimization problems.

A systematic definition of the metric dimension is proposed. Let G be a connected graph and $d(x, y)$ be the distance between vertices x and y. A subset of vertices $w = \{w_1, \cdots, w_k\}$ is called a resolving set for G if for every two distinct vertices $x, y \in V(G)$, there is a vertex $w_i \in w$ such that $d(x, w_i) \neq d(y, w_i)$. The metric dimension $md(G)$ of G is the minimum cardinality of a resolving set for G.

Figure 1 shows how the different signals determine the robot's location. Suppose the robot moves on the path graph (straight line) and there is a landmark vertex (v_4) that sends different signals (the distances are $3, 2, 1$, and 0 between v_1, v_2, v_3, and v_4 and the landmark vertex v_4, respectively) to the robot to determine its location.

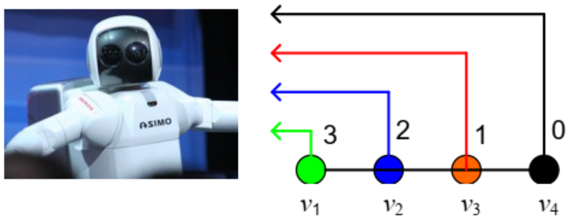

Figure 1. How the different signals determine the robot's location

Slater [4],[5] proposed the notion of a minimum resolving set. After that Slater proposed a different term (location set) for the resolving set for a connected graph G. He studied the location number of G as the cardinality of a minimum resolving set. Harary and Melter [6] used a different term (metric dimension) for the same problem. The metric dimension of some graphs such as trees, paths, and complete graphs were determined by Chartrand et al. [7]. They introduced the bounds of the metric dimensions for any connected graphs. They also formulated this problem as an integer linear programming problem. Gerey and Johnson [8] proved that the metric dimension problem is an NP-complete problem for an arbitrary graph. The metric dimension problem for grid graphs was studied by Melter and Tomescu [9]. The metric dimension of graphs obtained by the cartesian product of two or more graphs was studied by Caceres et al. [10]. Chartrand et al. [11] find each graph of order n that has metric dimension $1, n-2$ or $n-1$.

In this work we determine the metric dimension of new classes of networks with polynomial algorithms. In particular, the metric dimension of the triangular snake graph, the ladder graph L_n, B_k , the k-home chain graph H_k and the k-kite chain graph K_k are determined. We propose an exponential algorithm for finding the metric dimension of a given graph. We also introduce the results of computer calculations that determined the metric dimension of various classes of networks by using an approximate algorithm namely integer linear programming. Finally, a comparative analysis between the proposed approximate and exponential algorithms shows that the LINGO solver outperforms the proposed algorithm for huge graphs.

§2. Main Results: Polynomial Algorithms of Some Special Classes of Networks

Here, we prove that the metric dimension of the triangular snake graph $\Delta_k - snake$, the ladder graph L_n, the k-home chain graph H_k, the k-kite chain graph K_k and the k-envelop chain graph E_n equals 2. Samir Khuller et al [12] proved that for graph G with metric dimension 2 and metric basis $\{a, b\}$, the following are true:

(1) There is no more than one path (P) between a and b;

(2) The degree $(a) \leq 3$ and degree $(b) \leq 3$;

(3) The degree $(c) \leq 5$ such that $c \in P$, $c \neq a$ and $c \neq b$.

Theorem 2.1 *Let G be a triangular snake graph $(\Delta_k - snake)$ with k blocks and n vertices, then $md(G) = 2$.*

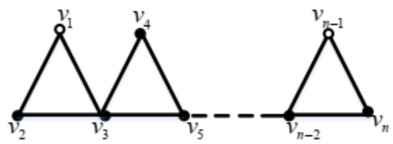

Figure 2. Triangular snake graph $(\Delta_k - snake)$.

Proof We label the triangular snake network $G = (\Delta_k - snake)$ as shown in Figure 2 such that k is the blocks number. It is clear that $\mid V(G) \mid$ is $n = 2k + 1$. Let $w = \{v_1, v_{2k}\}$ so that the proof has three cases, i.e., $k = 1$, $k > 1$ with the odd labeling of the vertices and $k > 1$ with the even labeling of the vertices.

Case 1. For $k = 1$, the proof is trivial because the graph $G = C_3$.

Case 2. For $k > 1$, the odd labeling of the vertices is the following:

Begin

for $(i = 1; i \leq n - 2; i = i + 2)$ **do**

$$d(v_i, w) = \left(\tfrac{i-1}{2}, \tfrac{n-i}{2}\right)$$

end

$d(v_n, w) = \left(\frac{(n-1)}{2}, 1\right)$

End

Case 3. For $k > 1$, the even labeling of the vertices is the following:

Begin

for$(i = 2; i \leq n - 3; i = i + 2)$ **do**

$$d(v_i, w) = \left(\tfrac{i}{2}, \tfrac{n-i+1}{2}\right)$$

end

$d(v_{n-1}, w) = \left(\frac{(n-1)}{2}, 0\right)$

End

This completes the proof. □

Obviously, there are no two vertices with the same labeling , we then obtain a resolving set w with $|\, w|$, so we have md $(\Delta_n - snake) = 2$. The proof of the algorithm of Theorem 1 involves a for-loop, so the algorithm complexity is $O(n)$, indicating that it is of polynomial time.

Theorem 2.2 *Let G be a ladder graph L_n, where $n \geq 4$, then $md(G) = 2$.*

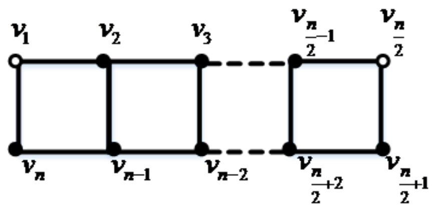

Figure 3. Ladder graph L_n.

Proof We label the triangular snake network $G = (\Delta_k - snake)$ as shown in Figure 2 such that k is the blocks number. It is clear that $|\, V(G)\, |$ is $n = 2k+1$. Let $w = \{v_1, v_{2k}\}$ so that the proof has three cases, i.e., $k = 1$, $k > 1$ with the odd labeling of the vertices and $k > 1$ with the even labeling of the vertices.

Case 1. For $k = 1$, the proof is trivial because the graph $G = C_3$.

Case 2. For $k > 1$, the odd labeling of the vertices is the following:

Begin

for$(i = 1; i \leq n-2; i = i+2)$ **do**

$d(v_i, w) = \left(\frac{i-1}{2}, \frac{n-i}{2}\right)$

end

$d(v_n, w) = \left(\frac{(n-1)}{2}, 1\right)$

End

Case 3. For $k > 1$, the even labeling of the vertices is the following:

Begin

for$(i = 2; i \leq n-3; i = i+2)$ **do**

$d(v_i, w) = \left(\frac{i}{2}, \frac{n-i+1}{2}\right)$

end

$d(v_{n-1}, w) = \left(\frac{(n-1)}{2}, 0\right)$

End

This completes the proof. □

We label a ladder graph $G = L_n$ as shown in Figure 3. It is clear that $|\, V(G)\, |$ is $n = 2k+2$ such that k is the blocks number of G. Let $w = \{v_1, v_{k+1}\}$

Begin

for $(i = 1; i \leq \frac{n}{2}; i++)$ **do**

$d(v_1, w) = \left(i-1, \frac{n}{2} - i\right)$

end

for $(i = n; i \leq \frac{n}{2} + 1; i-)$ **do**

$d(v_i, w) = \left(n - i + 1, i - \frac{n}{2}\right)$

end

End

Obviously, there are no two vertices with the same labelling, we then obtain a resolving set w with $\mid w|$, so we have $md(L_n) = 2$. The algorithm of the proof of Theorem 2 contains two for-loops, but they are not inner loops, so the algorithm complexity is $O(n)$, indicating that it is of polynomial time.

Theorem 2.3 *Let G be graph B_k , where $n \geq 4$, then $md(G) = 2$.*

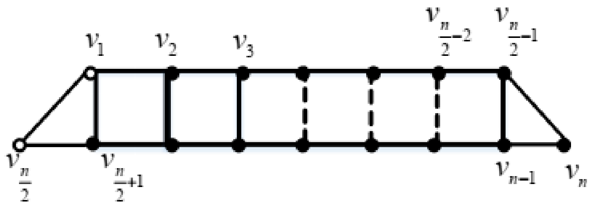

Figure 4. Graph B_k

Proof We label the triangular snake network $G = (\Delta_k - snake)$ as shown in Figure 2 such that k is the blocks number. It is clear that $\mid V(G) \mid$ is $n = 2k + 1$. Let $w = \{v_1, v_{2k}\}$ so that the proof has three cases, i.e., $k = 1$, $k > 1$ with the odd labeling of the vertices and $k > 1$ with the even labeling of the vertices.

Case 1. For $k = 1$, the proof is trivial because the graph $G = C_3$.

Case 2. For $k > 1$, the odd labeling of the vertices is the following:

Begin

for $(i = 1; i \leq n - 2; i = i + 2)$ **do**

$d(v_i, w) = \left(\frac{i-1}{2}, \frac{n-i}{2}\right)$

end

$d(v_n, w) = \left(\frac{(n-1)}{2}, 1\right)$

End

Case 3. For $k > 1$, the even labeling of the vertices is the following:

Begin

for $(i = 2; i \leq n - 3; i = i + 2)$ **do**

$d(v_i, w) = \left(\frac{i}{2}, \frac{n-i+1}{2}\right)$

end $d(v_{n-1}, w) = \left(\frac{(n-1)}{2}, 0\right)$

End

This completes the proof. □

We label a graph $G = B_k$ as shown in Figure 4 such that k is the blocks number. It is clear that $V(G)$ is $n = 2k + 4$. Let $w = \{v_1, v_{k+2}\}$. We want to prove that w is a resolving set by showing that $d(v_i, w) \neq d(v_j, w)$ for all $i \neq j$. Observe that:

Begin $j_1 = 0$; $j_2 = 1$

for $(i = 1; i \leq k+1; i++)$ **do**
$d(v_i, w) = (j_1, j_2)$
$j_1 = j_1 + 1; j_2 = j_2 + 1$
end
$d(v_{k+2}, w) = (1, 0)$ $j_1 = 1$; $j_2 = 1$
for $(i = k+1; i \leq n-1; i++)$ **do** $d(v_i, w) = (j_1, j_2)$
$j_1 = j_1 + 1; j_2 = j_2 + 1$
end
$d(v_n, w) = \left(\frac{n-2}{2}, \frac{n}{2}\right)$
End

Obviously, there are no two vertices with the same labelling, we then obtain a resolving set w with| w|, so we have $md(B_k) = 2$. The algorithm of the proof of Theorem 3 has two for-loops, but they are not inner loops, so the algorithm complexity is $O(n)$, indicating that it is of polynomial time.

Theorem 2.4 *Let G be a k-home chain graph H_k , where $k \geq 2$ then $md(G) = 2$.*

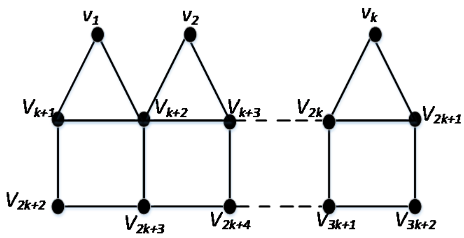

Figure 5. k-home chain graph H_k.

Proof We label the triangular snake network $G = (\Delta_k - snake)$ as shown in Figure 2 such that k is the blocks number. It is clear that $\mid V(G) \mid$ is $n = 2k+1$. Let $w = \{v_1, v_{2k}\}$ so that the proof has three cases, i.e., $k = 1$, $k > 1$ with the odd labeling of the vertices and $k > 1$ with the even labeling of the vertices.

Case 1. For $k = 1$, the proof is trivial because the graph $G = C_3$.

Case 2. For $k > 1$, the odd labeling of the vertices is the following:
Begin
for $(i = 1; i \leq n-2; i = i+2)$ **do**

$d(v_i, w) = \left(\frac{i-1}{2}, \frac{n-i}{2}\right)$
end
$d(v_n, w) = \left(\frac{(n-1)}{2}, 1\right)$
End

Case 3: for $k > 1$, the even labeling of the vertices is the following:
Begin
for $(i = 2; i \leq n-3; i = i+2)$ **do**

$d(v_i, w) = \left(\frac{i}{2}, \frac{n-i+1}{2}\right)$

end $\quad d(v_{n-1}, w) = \left(\frac{(n-1)}{2}, 0\right)$

End

This completes the proof. □

We label a graph $G = H_k$ as shown in Figure 5 such that k is the blocks number. It is clear that $\mid V(G) \mid$ is $n = 3k + 2$. Let $w = \{v_1, v_k\}$ .We want to prove that w is a resolving set by showing that $d(v_i, w) \neq d(v_j, w)$ for all $i \neq j$. Observe that:

Begin $d(v_1, W) = (0, k)$ $j = k - 1$

for $(i = 2; i \leq k - 1; i + +)$ **do**

$d(v_i, W) = (i, j), j = j - 1$

end

$d(v_k, W) = (k, 0)$, $d(v_{k+1}, W) = (1, k)$

for $(i = k + 2; i \leq 2k; i + +)$ **do**

$j_1 = 1, j_2 = k - 1$

$d(v_i, W) = (j_1, j_2)$

$j_1 = j_1 + 1; j_2 = j_2 \ - 1$

end

$d(v_{2k+1}, W) = (k, 1)$ $d(v_{2k+2}, W) = (2, k + 1)$

for $(i = 2k + 3; i \leq n - 1; i + +)$ **do**

$j_1 = 2, j_2 = k$

$d(v_i, W) = (j_1, j_2)$

$j_1 = j_1 + 1; j_2 = j_2 \ - 1$

end

$d(v_n, W) = (\frac{n+1}{3}, 2)$

End

Obviously, there are no two vertices with the same labelling; we then obtain a resolving set w with $\mid w|$, so we have $md(H_k) = 2$. The algorithm of the proof of Theorem 4 has three for-loops, but they are not inner loops, so the algorithm complexity is $O(n)$, indicating that it is of polynomial time algorithm.

Theorem 2.5 *Let G be a k-kite chain graph K_k where $k \geq 2$ with n vertices and k blocks, then* $md(G) = 2$.

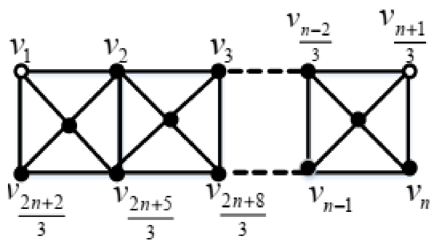

Figure 6. k-kite chain graph K_k.

Proof We label the triangular snake network $G = (\Delta_k - snake)$ as shown in Figure 2 such that k is the blocks number. It is clear that $\mid V(G) \mid$ is $n = 2k + 1$. Let $w = \{v_1, v_{2k}\}$ so that the proof has three cases, i.e., $k = 1$, $k > 1$ with the odd labeling of the vertices and $k > 1$ with the even labeling of the vertices.

Case 1. For $k = 1$, the proof is trivial because the graph $G = C_3$.

Case 2. For $k > 1$, the odd labeling of the vertices is the following:

Begin

for $(i = 1; i \leq n - 2; i = i + 2)$ **do**

$d(v_i, w) = \left(\frac{i-1}{2}, \frac{n-i}{2}\right)$

end

$d(v_n, w) = \left(\frac{(n-1)}{2}, 1\right)$ **End**

Case 3: for $k > 1$, the even labeling of the vertices is the following:

Begin

for $(i = 2; i \leq n - 3; i = i + 2)$ **do**

$d(v_i, w) = \left(\frac{i}{2}, \frac{n-i+1}{2}\right)$

end

$d(v_{n-1}, w) = \left(\frac{(n-1)}{2}, 0\right)$ **End**

This completes the proof. □

We label the k-kite chain graph $G = K_k$ as shown in Figure 6 such that k is the blocks number of K_k. It is clear that $\mid V(G) \mid$ is $n = 3k + 2$. Let $w = \{v_1, v_{k+1}\}$. We want to prove that w is a resolving set by showing that $d(v_i, w) \neq d(v_j, w)$ for all $i \neq j$. Observe that:

Begin

for $(i = 1; i \leq k + 1; i + +)$ **do**

$d(v_i, W) = (i - 1, k - i + 1)$

end

$j_1 = 1; j_2 = k$

for $(i = k + 2; i \leq 2k + 1; i + +)$ **do**

$d(v_i, W) = (j_1, j_2)$;$j_1 = j_1 + 1$; $j_2 = j_2 - 1$

end

$j_3 = 1; j_4 = k + 1$

for $(i = 2k + 2; i \leq 3k + 1; i + +)$ **do**

$d(v_i, W) = (j_3, j_4)$; $j_3 = j_3 + 1; j_4 = j_4 - 1$

end

End

Obviously, there are no two vertices with the same labelling, and so we obtain a resolving set w with$\mid w \mid$. Thus,$md(K_k) = 2$. The algorithm of the proof of Theorem 5 has three for-loops, but they are not inner loops, so the algorithm complexity is $O(n)$, indicating that it is of polynomial time.

§3. An Exponential Algorithm for a Given Network

In the previous section, we proposed polynomial time algorithms for special cases (triangular snake graph $\Delta_k - snake$, the ladder graph L_n, B_k, the k-home chain graph H_k and the k-kite chain graph K_k). Here, we introduce an algorithm that gives the metric dimension of an arbitrary graph G. Unfortunately, the time complexity of this algorithm is exponential time $O(2^n)$. Recall that Gerey and Johnson [8] showed that determining the metric dimension of an arbitrary graph is an NP-complete problem.

Algorithm 1. Finding the metric dimension of a given graph

Input : An adjacency matrix $A[n][n]$ of an n-vertex simple connected graph G.

Output: The metric dimension of G.

Begin Apply Floyed -Warshall's method to compute the distance matrix $D[n][n]$ of G.

Initialization:

$S_{1*n} = 0; E_{n*n} = 0$; $counter = cardinality = 0$ and $metric\_dimesion = inf$

Generating all subsets

while ($counter < 2^n - 1$)
  for $(i = n; i \geq 1; i-)$ **do**
    if $S[i] = 0$ **then**
      $S[i] = 1$
      $max = i + 1$
        for $(j = max; j \leq n; j++)$ **do**
          $S[j] = 0$
          end
      $counter = counter + 1$
      $cardinality$ = non-zero elements of $S[i]$
      break;
    end
  end
  Check all subsets of $P(V_G)$ *whether resolving set or not.*
  for $(i = n; i \geq 1; i-)$ **do**
    for $(j = n ; j \geq 1; j-)$ **do**
      $E[i][, j] = 0$
    end
  end
  for $(i = n; i \geq 1; i-)$ **do**
    for $(j = n; j \geq 1; j-)$ **do**

if $S[j] = 1$ **then**
$E[i][, j] = D[i][, j]$
end
end
end
for $(i = n; i \geq 1; i-)$ **do**
for $(j = i + 1; j \geq 1; j-)$ **do**
if $E[i][:] = E[j][:]$ **then**
break
end
end
if ($E[i][:] = E[j][:]$) **then**
break
end
end
if ($E[i][:]$ or $E[j][:]$) and (metric_dimension > cardinality) **then**
metric_dimension = cardinality;
end
end while
End Begin

Example 3.1 We show the intermediate stages of above Algorithm for the cycle graph. It is clear that the graph $G = C_3$ has 3 vertices and 3 edges. The graph G has adjacency matrix A and distance matrix D such that $A = D = \begin{bmatrix} 0 & 1 & 1 \\ 1 & 0 & 1 \\ 1 & 1 & 0 \end{bmatrix}$. Algorithm 1 can calculate 2^n subsets as follows:

$$S_0 = \begin{bmatrix} 0 & 0 & 0 \end{bmatrix} S_1 = \begin{bmatrix} 0 & 0 & 1 \end{bmatrix} S_2 = \begin{bmatrix} 0 & 1 & 0 \end{bmatrix} S_3 = \begin{bmatrix} 0 & 1 & 1 \end{bmatrix}$$

$$S_4 = \begin{bmatrix} 1 & 0 & 0 \end{bmatrix} S_5 = \begin{bmatrix} 1 & 0 & 1 \end{bmatrix} S_6 = \begin{bmatrix} 1 & 1 & 0 \end{bmatrix} S_7 = \begin{bmatrix} 1 & 1 & 1 \end{bmatrix}$$

Now, checks each of the above subsets $S_i : i = 0, \cdots, 2^n - 1$ to determine whether a resolving set as follows: the matrix E_i is calculated for each subset S_i such that:

$$E_0 = \begin{bmatrix} 0 & 0 & 0 \\ 0 & 0 & 0 \\ 0 & 0 & 0 \end{bmatrix} E_1 = \begin{bmatrix} 0 & 0 & 1 \\ 0 & 0 & 1 \\ 0 & 0 & 0 \end{bmatrix} E_2 = \begin{bmatrix} 0 & 1 & 0 \\ 0 & 0 & 0 \\ 0 & 1 & 0 \end{bmatrix} E_3 = \begin{bmatrix} 0 & 1 & 1 \\ 0 & 0 & 1 \\ 0 & 1 & 0 \end{bmatrix}$$

$$E_4 = \begin{bmatrix} 0 & 0 & 0 \\ 1 & 0 & 0 \\ 1 & 0 & 0 \end{bmatrix} E_5 = \begin{bmatrix} 0 & 0 & 1 \\ 1 & 0 & 1 \\ 1 & 0 & 0 \end{bmatrix} E_6 = \begin{bmatrix} 0 & 1 & 0 \\ 1 & 0 & 0 \\ 1 & 1 & 0 \end{bmatrix} E_7 = \begin{bmatrix} 0 & 1 & 1 \\ 1 & 0 & 1 \\ 1 & 1 & 0 \end{bmatrix}$$

If there exist two rows are equal in the matrix E_i then the subset S_i is non-resolving set otherwise it is resolving set; the algorithm determines that S_3, S_5, S_6 and S_7 are resolving sets and the others are non-resolving sets. Finally Algorithm 1 determines the metric dimension that is equal to the number of elements of the smallest resolving set for G so $md(G) =\mid S_3 \mid=\mid S_5 \mid=\mid S_6 \mid= 2$.

Complexity of Algorithm 1. Obviously, Algorithm 1 is an exponential algorithm. It consists of one while-loop that has four for-loops each with an inner loop. So the total complexity of Algorithm 1 is

$$\approx \left[O(n^2) + O(n^2) + O(n^2) + O(n^2)\right] O(2^n) \approx \left[4O(n^2)\right] O\left(2^n\right) \approx O\left(2^n\right).$$

§4. Formulation of the Problem as Integer Linear Programming Model

In the previous section, we proposed an exponential algorithm that determines the metric dimension for a given graph but this algorithm cannot determine the metric dimension of very large graphs in a reasonable time. In this section we introduce a powerful technique "integer linear programming technique" that determines the metric dimension for a very large graph. This technique finds the metric dimension in a reasonable time. We now describe this problem of determining the metric dimension and a basis for a graph in terms of an integer linear programming problem [13-16]. Chartrand et al [11] formulated the problem of finding the metric dimension as follows: Let G be a connected graph of order n with $V(G) = \{v_1, v_2, \cdots, v_n\}$ and let $D = [d_{ij}]$ be the distance matrix of G, that is, $d_{ij} = d(v_i, v_j)$ for $1 \leq i; j \leq n$. For $x_i \in \{0, 1\}$; $1 \leq i \leq n$, define the function z by: $z(x_1, x_2, \cdots, x_n) = \sum_1^n x_i$ such that the number of constraints equals to $\frac{n!}{2!(n-2)!}$then, the integer linear programming will be as follows:

Minimum $z = x_1 + x_2 + \cdots + x_n$

Subject to:

$for\ (i = 1;\ i = n;\ i++)\ do$

$for\ (j = 1;\ j = n;\ j++)\ do$

$\mid d_{i1} - d_{j1} \mid x_1 + \mid d_{i2} - d_{j2} \mid x_2 + \mid d_{i3} - d_{j3} \mid x_3 > 0$

end

end

where $x_i \in \{0, 1\}$.

Example 4.1 From the above formulation, we have the following mathematical model for the cycle graph C_3 with three vertices. $min\ z = x_1 + x_2 + x_3$ subject to $0x_1 + x_2 + x_3 > 0$, $x_1 + 0x_2 + x_3 > 0$, $x_1 + x_2 + 0x_3 > 0$ and $x_1, x_2, x_3 \in \{0, 1\}$. When we solve the above mathematical model, we obtain the objective function $z = 2$ so the metric dimension for C_3 is 2.

§5. Numerical Experiments

A connected graph which consists of k- blocks (triangles) and the block-cut-point graph is a path is called k-triangular snake (or Δ_k-snake) [12]. A connected graph in which the k blocks are isomor1phic to the cycle C_n and the block-cutpoint graph is a path is denoted by kC_n-snake [13]. The ladder graph L_n is the Cartesian product of P_1 and P_n is the path graph on n nodes. We describe our numerical experiments and present the computational results, which demonstrate the efficiency of the proposed algorithm on a set of test problems (path, cycle, ladder and Δ_k-snake). Table 1 describes the computing environment. MATLAB solver was used to solve the mathematical model.

Table 1. Description of the computing environment

CPU	Intel (R) Core (TM) i3-3217U CPU@ 1.80 GHz
RAM Size	4 GB RAM
MATLAB version	R2018a (9.4.0.813654)

Table 2 and Figure 6 show that the LINGO solver outperforms the proposed exponential Algorithm 1, with respect to CPU time, for determining the metric dimension for the cycle and path graphs. The LINGO solver can solve the problem for graphs with large sizes in a reasonable time. The proposed exponential Algorithm 1 can find the metric dimension for a given graph but in a non-reasonable time. However, the LINGO solver is not guaranteed to obtain the exact metric dimension for general arbitrary graph so it is an approximate algorithm.

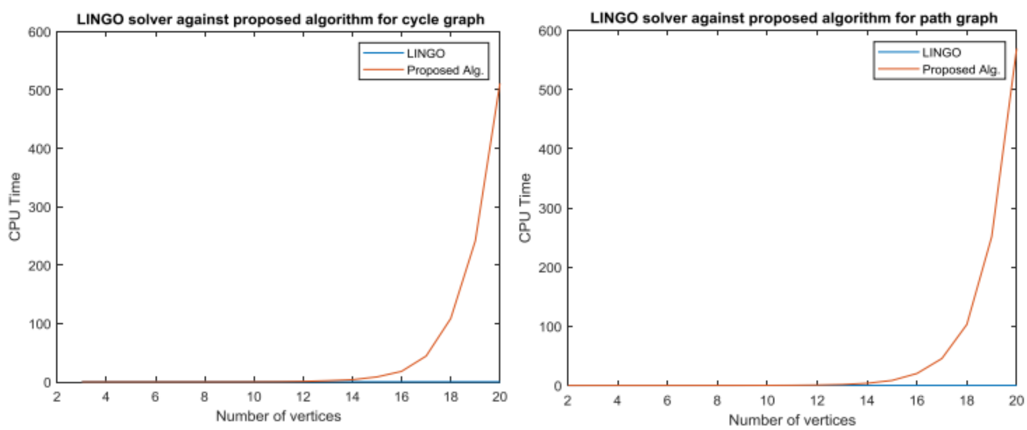

Figure 7. A comparison between the proposed algorithm and LINGO solver for finding the metric dimension for cycle and path graphs

Table 2. A comparison between the proposed algorithm and LINGO solver for finding the metric dimension for cycle and path graphs

	Cycle				Path			
	d	md	LINGO CPU	Algorithm 1 CPU	d	md	LINGO CPU	Algorithm1 CPU
1	–	–		–	0	1	0.00102	0.00173
2	–	–		–	1	1	0.00103	0.00436
3	1	2	0.03165	0.0060	2	1	0.02167	0.00573
4	2	2	0.03816	0.00602	3	1	0.02818	0.00584
5	2	2	0.04210	0.00621	4	1	0.03212	0.00781
6	3	2	0.04324	0.00817	5	1	0.03326	0.00861
7	3	2	0.04405	0.01283	6	1	0.03408	0.01692
8	4	2	0.04956	0.02309	7	1	0.03959	0.02898
9	4	2	0.04966	0.04872	8	1	0.04844	0.05044
10	5	2	0.04977	0.11682	9	1	0.04975	0.12025
11	5	2	0.04979	0.27877	10	1	0.04979	0.27940
12	6	2	0.04985	0.76805	11	1	0.04985	0.66518
13	6	2	0.04999	2.01020	12	1	0.04996	1.55260
14	7	2	0.05397	3.69079	13	1	0.05386	3.64734
15	7	2	0.05429	8.48939	14	1	0.05438	8.45053
16	8	2	0.05756	18.02579	15	1	0.05764	20.24835
17	8	2	0.05981	44.24297	16	1	0.05993	45.47590
18	9	2	0.06087	108.54759	17	1	0.06096	102.98411
19	9	2	0.06445	241.59339	18	1	0.06455	251.55695
20	10	2	0.06762	511.26855	19	1	0.06776	569.33483

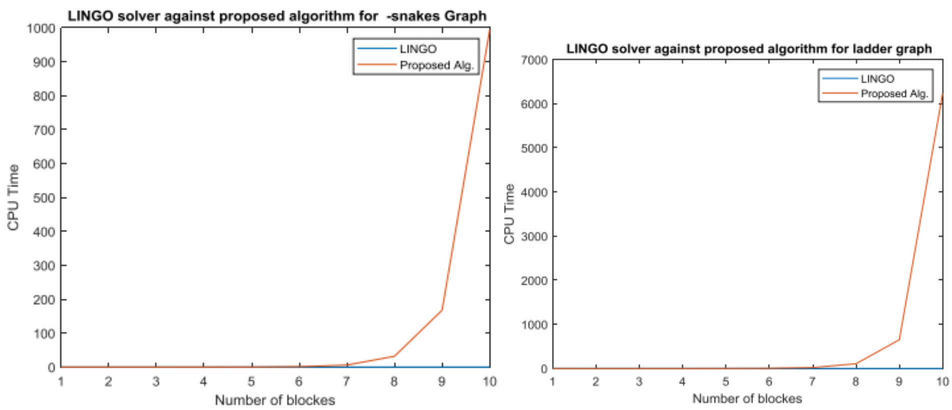

Figure 8. A comparison between the proposed algorithm and LINGO solver for finding the metric dimension for Δ_k-snakes and ladder graphs

It is clear that the curve for the LINGO solver is not visible in Figure 7, Figure 8 and Figure 9 because it runs essentially along on the x-axis. Table 3 and Figure 8 show that the LINGO solver outperforms the proposed algorithm, with respect to CPU time, for finding the metric dimension for the Δ_k-snake and ladder graphs.

Table 3. A comparison between the proposed algorithm and LINGO solver for finding the metric dimension for Δ_k-snakes and ladder graphs

Δ_k-snakes graph						Ladder graph					
k	n	d	md	LINGO CPU	Algorithm1 CPU	k	n	d	md	LINGO CPU	Algorithm1 CPU
1	3	1	2	0.05337	0.00674	1	4	2	2	00.2791	0.00930
2	5	2	2	0.05624	0.00718	2	6	3	2	0.03037	0.01330
3	7	3	2	0.05803	0.01141	3	8	4	2	0.03301	0.02808
4	9	4	2	0.05951	0.03922	4	10	5	2	0.03336	0.11058
5	11	5	2	0.06009	0.20711	5	12	6	2	0.03389	0.62880
6	13	6	2	0.06476	1.19454	6	14	7	2	0.03431	3.71727
7	15	7	2	0.06445	6.00546	7	16	8	2	0.03594	19.96398
8	17	8	2	0.06501	31.78448	8	18	9	2	0.04105	107.23148
9	19	9	2	0.06679	167.52252	9	20	10	2	0.04293	651.14236
10	21	10	2	0.07332	994.01483	10	22	11	2	0.05581	6233.951601

Table 4 and Figure 9 show that the comparison between the proposed exponential Algorithm 1 and the LINGO solver for determining the metric dimension for complete graphs with a metric dimension larger than 2. The LINGO solver outperforms the proposed exponential Algorithm 1 in terms of the CPU time. There is no guarantee of the superiority of the LINGO solver in determining the exact metric dimension for a general arbitrary graph. The proposed exponential Algorithm 1 has this guarantee for a given graph.

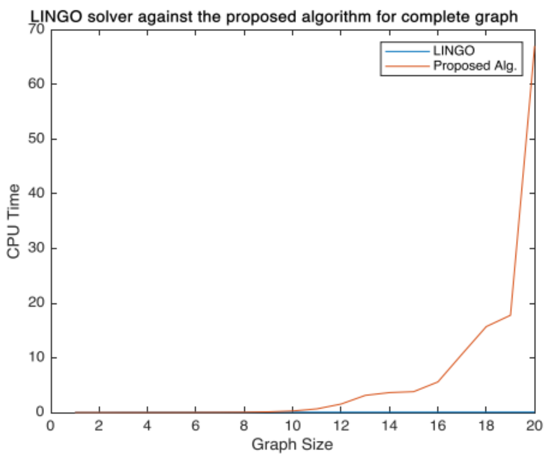

Figure 9: A comparison between the proposed algorithm and LINGO solver for finding the metric dimension for Δ_k-snakes and ladder graphs

Table 4. Comparison between the proposed algorithm and LINGO solver for finding the metric dimension for complete graphs.

	complete			
n	d	md	LINGO CPU	Algorithm1 CPU
1	0	1	0.00101	0.001000
2	1	1	0.00102	0.004620
3	1	2	0.02165	0.004850
4	1	3	0.02815	0.006700
5	1	4	0.03210	0.009000
6	1	5	0.03320	0.016920
7	1	6	0.03401	0.029990
8	1	7	0.03952	0.050440
9	1	8	0.04820	0.120250
10	1	9	0.04943	0.279400
11	1	10	0.04968	0.665180
12	1	11	0.04992	1.552600
13	1	12	0.04998	3.140139
14	1	13	0.05385	3.647340
15	1	14	0.05447	3.819237
16	1	15	0.05782	5.596174
17	1	16	0.05905	10.697527
18	1	17	0.06079	15.722732
19	1	18	0.06444	17.793874
20	1	19	0.06782	67.070074

§6. **Conclusion**

We determined the metric dimension of new classes of networks with polynomial algorithms. In particular, we proved that the metric dimension of the triangular snake graph. $\Delta_k - snake$, the ladder graph L_n, B_k, the k-home chain graph H_k and the k-kite chain graph K_k equals 2. We proposed an exponential algorithm for finding the metric dimension of a given graph. We also introduced the results of computer calculations that determined the metric dimension of various classes of networks by using an approximate algorithm, namely, integer linear programming. Finally, a comparative analysis between the approximate algorithm (the LINGO solver) and the proposed exponential algorithm showed that the LINGO solver outperforms the proposed algorithm for very large graphs. In future work, we will apply variant integer linear programming models [23-24] on the variant networks [25-26].

References

[1] Chartrand G., Erwin D., Johns G. L and Zhang P., Boundary vertices in graphs, *Discrete Math.*, 2003, 263(1-3): 2534.

[2] Khuller S., Raghavachari B., Rosenfeld A., Landmarks in graphs, *Appl. Math.*, 1996.

[3] Sebo and Tannier, On metric generators of graphs, *Math. Oper. Res.*, 2004.

[4] Slater P.J., Leaves of trees, *Congr. Numer.*, 1975, 14 , 549-559.

[5] Slater P.J., Dominating and reference sets in graphs, *J. Math. Phys. Sci.*, 1988, 22, 445-455.

[6] Harary F., Melter R.A., On the metric dimension of a graph, *Ars. Combin.*, 1976, 2, 191-195.

[7] Chartrand G., Eroh L., Johnson M.A., Oellermann O.R., Resolvability in graphs and the metric dimension of a graph, *Discrete Appl. Math.*, 2000, 105, 99-113.

[8] Garey M. R., Johnson D. S., *Computers and Intractibility: A Guide to the Theory of NP Completeness*, W. H. Freeman and Company, (1979).

[9] Melter R. A., Tomescu I., Metric bases in digital geometry, *Comput. Vis. Graph*, Image Process, 1984, 25, 113–121.

[10] Caceres J., Hernando C., Mora M., Puertas M. L., Pelayo I. M., Seara C., Wood, D. R., On the metric dimension of some families of graphs, *Electron. Notes Discrete Math.*, 2005, 22, 129–133.

[11] Chartrand G., Eroh L., Johnson M. A., Oellermann O. R., Resolvability in graphs and the metric dimension of a graph, *Discrete App. Math.*, 2000, 105, 99–113.

[12] Samir Khuller, Balaji Raghavachari, Azriel Rosenfeld, Landmarks in graphs, *Discrete Applied Mathematics*, 1996, 70, 217-229.

[13] Bazaraa M.S., Jarvis J.J., Sherali H.D., *Linear Programming and Network Flows*, third ed., John Wiley, NY, 2004.

[14] Badr E. S., Paparrizos K., Samaras N., Sifaleras A., On the basis inverse of the exterior point simplex algorithm, *Proc. of the 17th National Conference of Hellenic Operational Research Society* (HELORS), 16-18 June, Rio, Greece, pp. 677-687, 2006.

[15] Badr E.S., Paparrizos K., Baloukas Thanasis, Varkas G., Some computational results on the efficiency of an exterior point algorithm, in *Proc. Of the 18th National Conference of Hellenic Operational Research Society* (HELORS), 15-17 June, Rio, Greece, pp. 1103-1115, 2006.

[16] Badr E. M., Moussa M. I., An upper bound of radio k-coloring problem and its integer linear programming model, *Wireless Networks*, 2019, Online.

[17] Hertz A., An IP-based swapping algorithm for the metric dimension and minimal doubly resolving set problems in hypercubes, *Optimization Letters*, 2017, 1-13.

[18] Diaz J., Pottonen O., Serna M., Leeuwen E. J., Complexity of metric dimension on planar graphs, *Journal of Computer and System Sciences*, 2017, 83.1,132–158.

[19] J. Díaz, O. Pottonen and E.J. Leeuwen (2011), Planar metric dimension is NP-complete, *ArXiv*, abs/1107.2256.

[20] Liu J.B., NADEEM M. F., SIDDIQUI H. M. A., NAZIR W., Computing metric dimension of certain families of Toeplitz graphs, *IEEE Access*, 2019, 4, 1-8.

[21] Imran M., Siddiqui M. K., Naeem R., On the metric dimension of generalized Petersen multigraphs, *IEEE Access*, 2018, Vol. 6, 74328-74338.

[22] Badr E. M., AlGendy H. S., A hybrid water cycle - particle swarm optimization for solving the fuzzy underground water confined steady flow, *Indonesian Journal of Electrical Engineering and Computer Science*, 2020 Vol. 19, No. 1, 492–504.

[23] E. M. Badr and Sultan Almotiari (2019), On a dual direct cosine simplex type algorithm and its computational behavior, *Mathematical Problems in Engineering*, Volume 2020, Article ID 7361092, 8 pages. https://doi.org/10.1155/2020/7361092.

[24] E. Badr, S. Almotairi, A. Elrokh, A. Abdel-Hay and B. Almutairi, An integer linear programming model for solving radio mean labeling problem, *IEEE Access*, Vol. 8, 162343-162349, 2020, doi: 10.1109/ACCESS.2020.3021896.

[25] E. M. Badr, M. I. Moussa & K. Kathiresan (2011), Crown graphs and subdivision of ladders are odd graceful, *International Journal of Computer Mathematics*, 88:17, 3570- 3576.

[26] M.I.Moussa and E. M. Badr (2016), Ladder and subdivision of ladder graphs with pendant edges are odd graceful, *Journal on Application of Graph Theory in Wirless Ad hoc Networks and Sensor Networks* (GRAPHS-HOC) Vol.8, No.1, March 2016.

International J.Math. Combin. Vol.2(2021), 68-79

Maximal k-Degenerate Graphs with Diameter 2

Allan Bickle

(Department of Mathematics, Penn State University, Altoona Campus, Altoona, PA 16601, USA)

E-mail: aub742@psu.edu

Abstract: A graph is k-degenerate if its vertices can be successively deleted so that when deleted, they have degree at most k. A k-tree is a graph that can be formed by starting with K_{k+1} and iterating the operation of making a new vertex adjacent to all the vertices of a k-clique of the existing graph. A structural characterization of maximal 2-degenerate graphs with diameter 2, containing 45 distinct infinite classes of graphs, is proven. A forbidden subgraph characterization of k-trees with diameter 2 is proven.

Key Words: Degeneracy, diameter, k-tree, k-path.

AMS(2010): 05C25.

§1. Introduction

In this paper, we work toward a characterization of the maximal k-degenerate graphs with diameter 2.

Definition 1.1 *Let k be a positive integer. A graph is k-degenerate if its vertices can be successively deleted so that when deleted, they have degree at most k. A graph is maximal k-degenerate if no edges can be added without violating this condition.*

A k-tree is a graph that can be formed by starting with K_{k+1} and iterating the operation of making a new vertex adjacent to all the vertices of a k-clique of the existing graph.

A k-leaf is a degree k vertex of a maximal k-degenerate graph.

Lick and White introduced k-degenerate graphs in 1970 [13], and their properties have been studied by many authors [2, 7, 8, 9, 10, 11, 12, 14, 16, 19]. For $n \geq k+1$, a maximal k-degenerate graph has at least one k-leaf, and a k-tree has at least 2.

The three maximal 2-degenerate graphs of order 5 are shown below [3]. The two on the left are 2-trees.

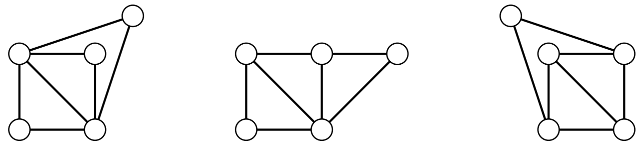

$K_2 + \overline{K}_3$ $\qquad$ $P_4 + K_1$ $\qquad$ W_5^-

[1]Received February 6, 2021, Accepted June 10, 2021.

Undefined notation and terminology will generally follow [3]. In particular, the join of graphs G and H is denoted $G+H$, and the distance between vertices u and v is $d(u,v)$. The eccentricity $e_G(v)$ of a vertex v is the maximum distance between v and any other vertex of G. If G is a graph, the square G^2 is formed by adding all edges between pairs of vertices with distance 2 in G.

We solve two special cases of the problem of characterizing the maximal k-degenerate graphs with diameter 2. One restricts the problem to maximal 2-degenerate graphs, the other restricts it to k-trees (which are all maximal k-degenerate). The first provides a structural characterization, and the latter provides a forbidden subgraph characterization.

This work is inspired by a previous paper [6]. I coauthored with Zhongyuan Che on the Wiener index of maximal k-degenerate graphs. We showed that the Wiener index is minimized when these graphs have diameter 2. We also characterized 2-trees with diameter at most 2.

Proposition 1.2([6]) *The following are equivalent for a 2-tree G:*

(1) *G has diameter at most 2;*

(2) *G does not contain P_6^2;*

(3) *G is $T+K_1$ for any tree T, or any graph formed by adding any number of vertices adjacent to pairs of vertices of K_3.*

§2. Maximal 2-Degenerate Graphs with Diameter 2

In this section, we provide a structural characterization of maximal 2-degenerate graphs with diameter 2.

Definition 2.1 *A dominating vertex of a graph is a vertex adjacent to all other vertices. A fan is the graph $P_{n-1}+K_1$.*

Lemma 2.2 *If G is a maximal 2-degenerate graph with order $n \geq 3$ containing a dominating vertex, then G is a 2-tree that can be represented as $T+K_1$ for some tree T. If G has exactly two 2-leaves, then it is a fan.*

Proof We use induction on n. When $n=3$, $G=K_3$ and the result holds. Let G be a maximal 2-degenerate graph with order n containing dominating vertex u, and assume the result holds for all graphs with order $n-1$. Then G has a 2-leaf v, which is adjacent to u. Now $G-v$ is maximal 2-degenerate with order $n-1$ [13], so it is a 2-tree that can be represented as $T+K_1$. Then the other neighbor of v is a neighbor of u, so G is a 2-tree that can be represented as $T+K_1$.

If G has exactly two 2-leaves, then deleting its dominating vertex produces a tree with exactly two leaves, a path. Thus G is a fan. □

Definition 2.3 *When constructing a maximal 2-degenerate graph, we duplicate a 2-leaf by adding another 2-leaf with the same neighborhood. The inside graph H of a maximal 2-degenerate graph G is formed by deleting all the 2-leaves. The stem set of G is the set of* *neighbors of 2-leaves.*

Note that in a maximal 2-degenerate graph with diameter 2, any 2-leaf can be duplicated arbitrarily many times. The new 2-leaf is distance two from its duplicate, and hence at most two from every other vertex. Thus the result is a maximal 2-degenerate graph with diameter 2.

Lemma 2.4 *In any maximal 2-degenerate graph with diameter 2 and order $n > 3$, either*

(A) all 2-leaves have a single common neighbor, or

B) the stem set is $S = \{u, v, w\}$, and there are 2-leaves with neighborhoods $\{u, v\}$, $\{u, w\}$, and $\{v, w\}$.

Proof Any maximal 2-degenerate graph with diameter 2 has at least one 2-leaf. No 2-leaves can have disjoint neighborhoods, since then they would be at least distance 3 apart. If all 2-leaves have the same neighborhood, the result follows. If two 2-leaves have distinct neighborhoods, we may call them $\{a, b\}$ and $\{a, c\}$. Any other 2-leaf must have neighborhood $\{b, c\}$ or $\{a, x\}$ for some x. □

Theorem 2.5 *Let G be a maximal 2-degenerate graph with diameter 2. Then G is a 2-tree that can be represented as $T + K_1$ for some tree T, or the inside graph of G is one of the 44 possibilities shown below. (Vertices labeled x may be duplicated arbitrarily many times.) There must be at least one 2-leaf of G neighboring any pair of black vertices or pair of black and gray vertices, and there may be at least one 2-leaf of G neighboring any pair of black and lightgray vertices.*

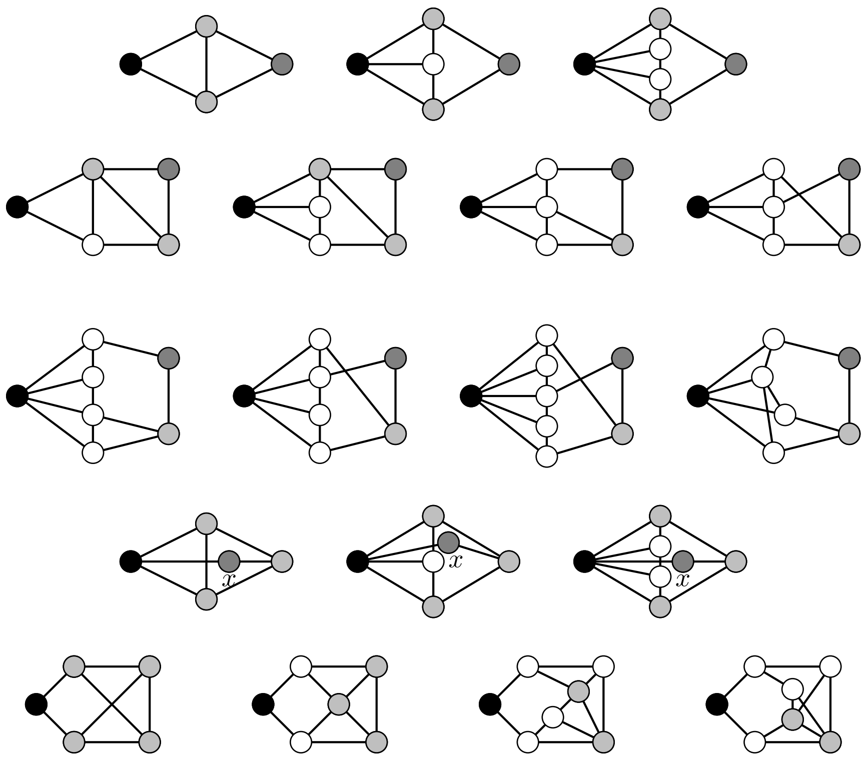

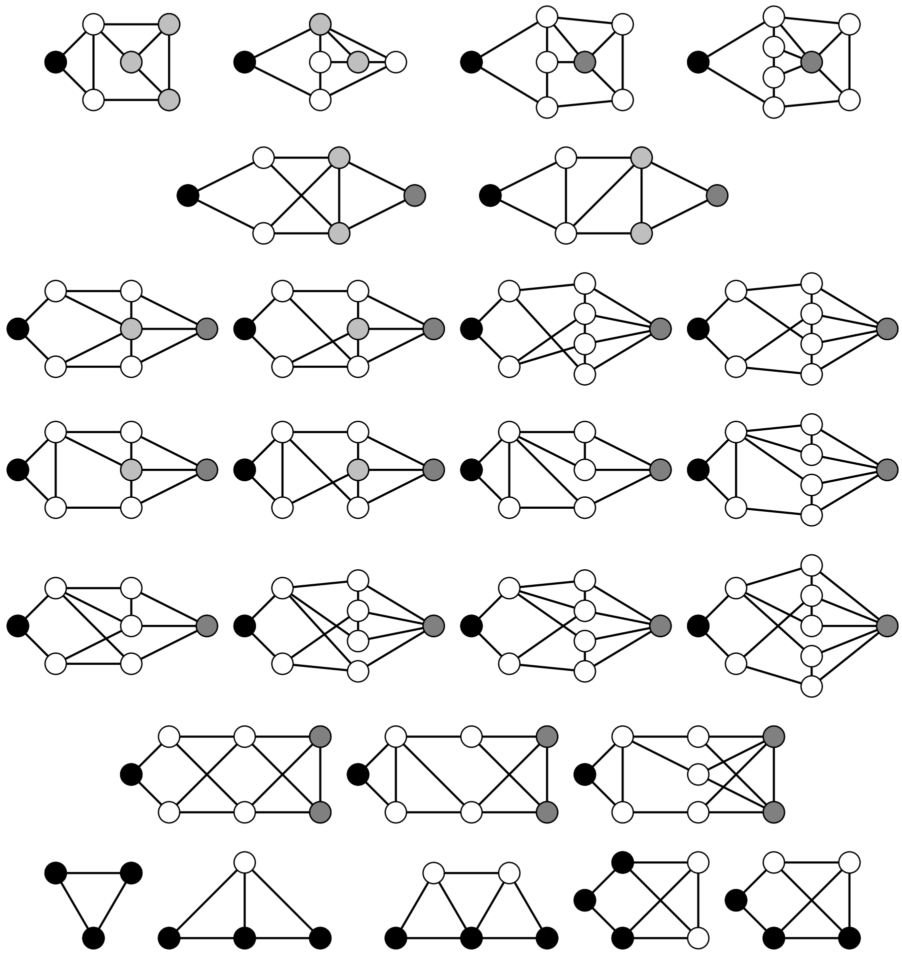

The proof of this theorem has many cases. We use Case A.2.1 to mean case A, Subcase 2, Subsubcase 1, and similarly for the other cases. Figures are referenced in parentheses, with labels beginning with their main case (A or B). We say an inside graph is valid if it is the inside graph of a maximal 2-degenerate graph with diameter 2.

Proof Let G be a maximal 2-degenerate graph with diameter 2 with inside graph H. By Lemma 2.4, there are two possibilities for the positions of the 2-leaves.

Case A. All 2-leaves of G have a single common neighbor u.

Case A.1 If u is a dominating vertex of H, it does the same for G, so by Lemma 2.2, G is a 2-tree that can be represented as $T + K_1$ for some tree T.

Case A.2 If u has eccentricity 2 in H, let v_1, ... v_j be distance 1 from u, $w_1, \cdots, w_k$ be distance 2 from u. Now no 2-leaf of H has neighborhood $\{u, v_i\}$ since a 2-leaf of G that neighbors it and u is more than 2 from w_1.

Case A.2.1 If w_1 is a 2-leaf of H, there is a 2-leaf of G that neighbors it and u. Then w_1 neighbors all other w_i, and since w_1 neighbors some v_i, $k \leq 2$. If $k = 1$, then u is a dominating vertex of $H - w_1$. By Lemma 2.2, $H - w_1$ is a 2-tree. Now its 2-leaves are not 2-leaves of H, aside from possibly u. Then w_1 is adjacent to all (two) of them, and $H - w_1$ is a fan with at most five vertices (A1, A2, A3).

Since all 2-leaves of G have a single common neighbor u, it is colored black (uniquely, in Case A). Any 2-leaf of H must be black or gray, and any vertex distance 3 from u will be gray. If $\{u, u'\}$ is a dominating set of H, then u' will be lightgray if not already colored. Since these statuses are trivial to check, verification will be left to the reader for the other figures.

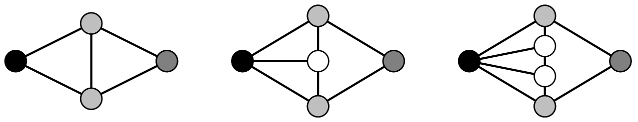

$A1$ $A2$ $A3$

If $k = 2$, there is no 2-leaf of H with neighborhood $\{u, w_2\}$, since a 2-leaf of G neighboring it is not within 2 of w_1. Then w_2 is a 2-leaf of $H - w_1$. As before, $H - w_1 - w_2$ is a 2-tree, and w_1 and w_2 have two or three neighbors in it, including all its 2-leaves. Now $T = H - w_1 - w_2 - u$ is a tree with all vertices either neighbors of w_2 or within 2 of w_1.

If T a path, its length is at most 5. If $T = P_2$, there is one possibility (A4). If $T = P_3$, w_1 may neighbor a leaf and w_2 may or may not neighbor the nonleaf, or w_1 may neighbor the nonleaf (A5, A6, A7). If $T = P_4$, w_1 may neighbor a leaf or nonleaf (A8, A9). If $T = P_5$, w_1 must neighbor the middle vertex, and w_2 neighbors the leaves (A10). If T has three leaves, w_2 neighbors two, and w_1 neighbors the third, so $T = K_{1,3}$ (A11).

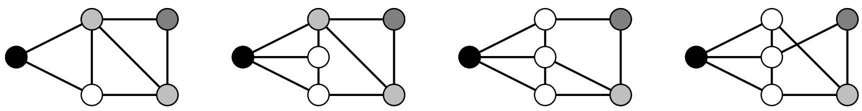

$A4$ $A5$ $A6$ $A7$

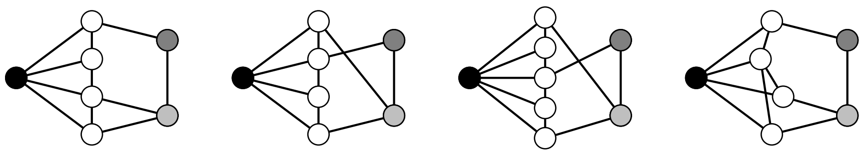

$A8$ $A9$ $A10$ $A11$

Case A.2.2 Suppose there is a 2-leaf v_1 of H neighboring u and w_1. Then there is a 2-leaf of G neighboring u and v_1. Then there is no w_2, but v_1 may be duplicated arbitrarily many times. Let K be the inside graph of H (delete v_1 and all its duplicates). Then w_1 is a 2-leaf of K. Then u is a dominating vertex of $K - w_1$, so by Lemma 2.2, $K - w_1$ is a fan. This fan must have order 3, 4, or 5 (A12, A13, A14).

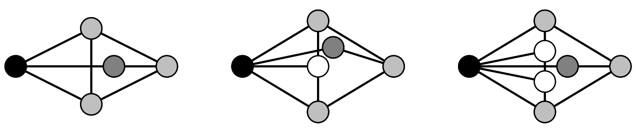

$A12$ $A13$ $A14$

Case A.2.3 If u is a 2-leaf of H and no w_i is, $j = 2$. If both v_1 and v_2 are 2-leaves of

$H-u$, then $H-u-v_1-v_2$, has order at most 4, so it is K_2 (A15), K_3 (A16), or K_4-e. In the latter case, there are two ways to attach v_1 and v_2 to K_4-e (A17, A18).

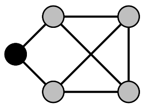
*A*15

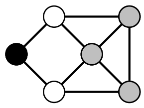
*A*16

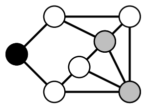
*A*17

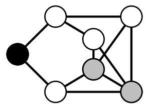
*A*18

Assume v_1 is a 2-leaf of $H-u$ and v_2 is not. If $v_1 \leftrightarrow v_2$, say $w_1 \leftrightarrow v_1$. Then v_2 is adjacent to all other w's. If $v_2 \leftrightarrow w_1$, v_2 is adjacent to all vertices, so by Lemma 2.2, H is a 2-tree, and some w_i is a 2-leaf, contrary to assumption. If $v_2 \not\leftrightarrow w_1$, then w_1 is a 2-leaf of $H-u-v_1$. By Lemma 2.2, $H-u-v_1-w_1$ is a fan. Now some 2-leaf of G has neighborhood $\{u, w_i\}$, so all ws must be adjacent, and $k=3$ (A19).

Assume $v_1 \not\leftrightarrow v_2$. Since v_1 is a 2-leaf of $H-u$, its neighbors are (say) w_1 and w_2. Now v_2 is adjacent to all other w's, and $k>2$. Now some 2-leaf of G has either v_2 or w_i as a neighbor, so one of these vertices neighbors all w's (excluding itself). Then $H-u-v_1$ has a dominating vertex, so by Lemma 2.2, it is a fan with 2-leaves w_1 and w_2. If v_2 is the dominating vertex, the fan has order at most 5, due to v_1. Order 5 duplicates A14, but order 4 yields a new case (A20). If (say) w_3 is the dominating vertex, the fan has order 5 or 6 (A21, A22).

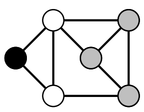
*A*19

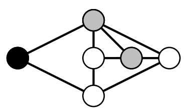
*A*20

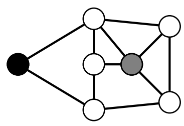
*A*21

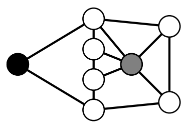
*A*22

Case A.3 If $e_H(u) > 2$ and vertex y is at least 3 from u, then $\{u, y\}$ is the neighborhood of a 2-leaf a of G. If $d_H(u,y) \geq 4$, there is a vertex z with $d_H(u,z) = 2$ and $d_H(a,z) > 2$, so this is impossible. Thus $e_H(u) = 3$. Let v_1, ... v_j be distance 1 from u, w_1, ... w_k be distance 2 from u, and x_1, ... x_l be distance 3 from u. Note $j, k \geq 2$ since H has no cut-vertex [13].

Now all vertices in the stem set other than u must be adjacent to each w_i and x_i (else a 2-leaf has eccentricity more than 2). No v_i is in the stem set, since it cannot be adjacent to an x_i. Since K_4 is not 2-degenerate, there are at most 3 stems excluding u, and $l \leq 2$. No w_i is a 2-leaf of H, since if there were, it would be adjacent to a v_i, and all w_i and x_i. Now x_1 is a 2-leaf only if there is no x_2, so H has at most two 2-leaves.

Case A.3.1 Assume u and x_1 are 2-leaves of H. Then $j=k=2$, and there is no x_2. Thus H has order 6, and $H-u-x_1 = K_4-e$. There are three ways it can be arranged, but the case where $w_1 \not\leftrightarrow w_2$ combines into the case where $v_1 \not\leftrightarrow v_2$. In the third case, $H = P_6^2$ (A23, A24).

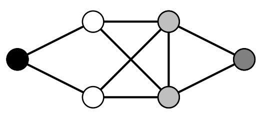
*A*23

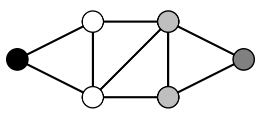
*A*24

Case A.3.2 Assume u is the only 2-leaf of H, and $l = 1$ (there is no x_2). Then at least one of v_1 and v_2 are 2-leaves of $H - u$. If both are 2-leaves, then $3 \leq k \leq 4$ since each w_i is adjacent to some v_i. If $k = 3$, then $H - u - v_1 - v_2 = K_4 - e$ by Lemma 2.2. Then v_1 and v_2 have one common neighbor, and there are two choices (A25, A26). If $k = 4$, then $H - u - v_1 - v_2$ is $P_4 + K_1$ or $K_{1,3} + K_1$ by Lemma 2.2. If it is $P_4 + K_1$, there are three choices for the adjacencies between the v's and w's, two of which produce valid inside graphs (A27, A28). If it is $K_{1,3} + K_1$, some v and w have distance more than 2.

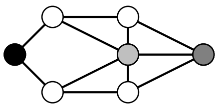
A25

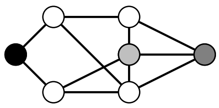
A26

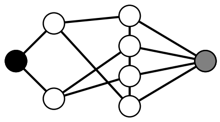
A27

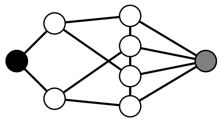
A28

Assume only v_1 is a 2-leaf of $H - u$. If its neighbors are v_2 and (say) w_1, at least one of which are 2-leaves of $H - u - v_1$. If v_2 is a 2-leaf of $H - u - v_1$, $k = 3$, and its neighbors are either adjacent or not (A29, A30). If v_2 is a not 2-leaf of $H - u - v_1$, w_1 is, with neighbors x_1 and v_2 or (say) w_2. If $w_1 \leftrightarrow v_2$, x_1 and v_2 are adjacent to all remaining w's. Thus w_2 is the only 2-leaf of this graph, which is W_5^- (A31). If $w_1 \leftrightarrow w_2$, x_1 and v_2 are adjacent to all w's of $H - u - v_1 - w_1$. Thus w_2 is the only 2-leaf of this graph, which is W_5^- (A32).

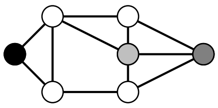
A29

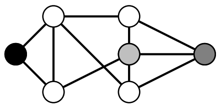
A30

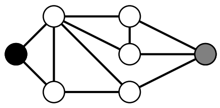
A31

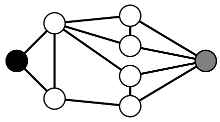
A32

Suppose v_1 is the only 2-leaf of $H - u$ with neighbors (say) w_1 and w_2, and w_1 is a 2-leaf of $H - u - v_1$. If w_1 has neighbors x_1 and v_2, then $H - u - v_1 - w_1$ has order at least 4. Now w_2 is adjacent to all other w's (so v_1 is distance 2 from them) and v_2 is adjacent to all w's, except perhaps w_2. Since x_1 is adjacent to all w's, $H - u - v_1 - w_1$ contains $K_{3,k-2}$, so $k \leq 4$. There are two possibilities (A33, A34). If w_1 has neighbors w_3 and x_1, then w_3 neighbors v_2 and x_1. As before, $H - u - v_1 - w_1 - w_3$ contains $K_{3,k-3}$, so $k \leq 5$. There are two possibilities (A35, A36).

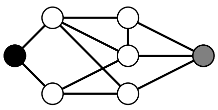
A33

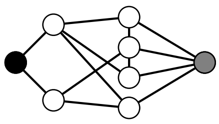
A34

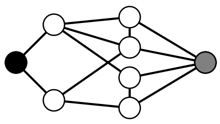
A35

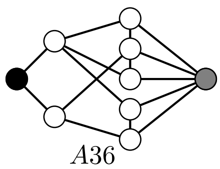
A36

Case A.3.3 Assume u is the only 2-leaf of H, and $l = 2$. Then $2 \leq k \leq 4$. Now one or both of v_1 and v_2 are 2-leaves of $H - u$. If $k = 2$, there are two cases, both leading to valid graphs (A37, A38). If $k = 3$, there is one way to make both v_1 and v_2 2-leaves of $H - u$. However, some v and w will have distance more than 2, so this is not to a valid graph. If only v_1 is a 2-leaf this leads to a valid graph (A39). If $k = 4$, there is one way to connect each w to a v, but this does not lead to a valid graph.

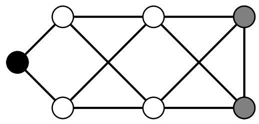

*A*37

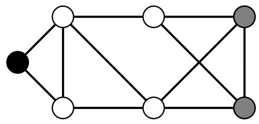

*A*38

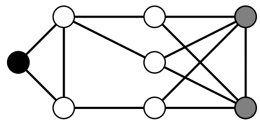

*A*39

Case A.3.4 Assume u is not a 2-leaf. Then x_1 is the only 2-leaf of H, so there is no x_2. Then essentially the same argument as in Case A.3.2 repeats, with u and x_1 switching roles, and the same graphs are found.

Case B. The stem set is $S = \{u, v, w\}$, and there are 2-leaves with neighborhoods $\{u, v\}$, $\{u, w\}$, and $\{v, w\}$. Thus u, v, and w will be colored black.

Each 2-leaf of the inside graph H is in S, so H has at most three 2-leaves.

Case B.1 If H has three 2-leaves, it may be K_3 (B1). If not, it has order at least 4, so none of the 2-leaves of H are neighbors. Then each 2-leaf of G has distance more than 2 from a 2-leaf of H, which is impossible.

Case B.2 If H has two 2-leaves, the third vertex in S must be in both of their neighborhoods. Thus H has order at most 5. Thus H is $K_4 - e$ or $P_4 + K_1$ (B2, B3).

Case B.3 If H has one 2-leaf v, then u must be one of its neighbors. If u is a 2-leaf of $H - v$, H has order 5, so it is W_5^-. There are two distinct choices for which vertex is w (B4, B5). If u is not a 2-leaf of $H - v$, v has another neighbor, x, that is. Then u is adjacent to every vertex of $H - v - x$. If u is adjacent to x, then by Lemma 2.2, H is a 2-tree, so it has at least two 2-leaves, a contradiction. If u is not adjacent to x, then by Lemma 2.2, $H - v - x$ is a 2-tree.

Now x is adjacent to all 2-leaves of $H - v - x$, so $H - v - x$ is a fan. Now w must be one of the 2-leaves of $H - v - x$, but it cannot neighbor all vertices of the fan unless the fan is K_3 and $H = W_5^-$, a previous case.

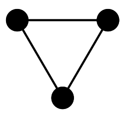

*B*1

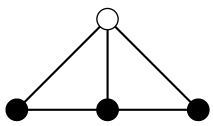

*B*2

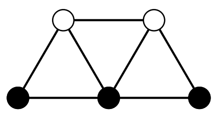

*B*3

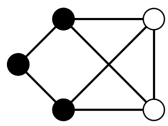

*B*4

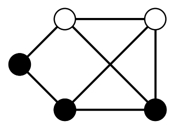

*B*5

This completes the proof. □

A structural characterization of maximal 2-degenerate graphs with diameter 2 allows us to evaluate or bound parameters on this class, which would otherwise be difficult. Sharp bounds have been proved for the maximum degree of maximal planar graphs with diameter 2 [18, 20]. We state sharp bounds on the maximum degree Δ of maximal 2-degenerate graph with diameter 2. A maximal 2-degenerate graph with $\Delta = n - 1$ must have diameter at most 2. A maximal 2-degenerate graph with $\Delta = n - 2$ need not have diameter at most 2 (for example, add one vertex to a fan with at least 5 vertices). Proposition 1.2 implies 2-trees with diameter 2 have $\Delta \geq \frac{2}{3}n$, and this bound is sharp.

Corollary 2.6 *A maximal 2-degenerate graph G with order n and diameter at most 2 has*

$$\Delta(G) \geq \begin{cases} n-1 & 1 \leq n \leq 4 \\ 3 & n = 5 \\ 4 & 6 \leq n \leq 8 \\ n-5 & 9 \leq n \leq 11 \\ n-6 & 12 \leq n \leq 16 \\ \left\lceil \frac{2}{3}(n-1) \right\rceil & n \geq 16 \end{cases},$$

and this bound is sharp for all n.

Proof For $1 \leq n \leq 4$, there is only one maximal 2-degenerate graph, which has a dominating vertex. For $n = 5$, there are three such graphs, one (W_5^-) of which has no dominating vertex. The fact that maximal 2-degenerate graphs have size $m = 2n-3$ and minimum degree 2 implies $\Delta \geq 4$ for $n \geq 6$. For $6 \leq n \leq 8$, this is attained by adding 2-leaves to A4 and A23.

Let G be a graph found under Case A, and H its inside graph. Then H has a stem that is adjacent to all 2-leaves of G with at most 5 vertices not adjacent to it, and only A39 attains this. Adding the 2-leaves of G to A39 as evenly as possible produces vertices with degree $n-6$ and $n-4-\left\lfloor \frac{n-8}{2} \right\rfloor$. Thus $\Delta \geq n-6$ for A39 when $n \geq 12$. Otherwise, $\Delta \geq n-5$ for graphs in Case A, and this is attained by graphs constructed from A37 when $n \geq 9$.

Let G be a graph found under Case B, and H its inside graph with stem set $\{u, v, w\}$. Consider summing the degrees of u, v, and w. There are $n-3$ other vertices, each of which is adjacent to at least two of u, v, and w. The graph induced by u, v, and w has at least two edges. Thus $2n-2 = 2(n-3)+4 \leq d(u)+d(v)+d(w) \leq 3\Delta$, so $\Delta \geq \left\lceil \frac{2}{3}(n-1) \right\rceil$. This is attained by graphs constructed from B3. For $n \geq 16$, $\left\lceil \frac{2}{3}(n-1) \right\rceil \leq n-6$, so the bound is as stated. □

We have seen that some maximal 2-degenerate graphs with diameter 3 are contained in a maximal 2-degenerate graph with diameter 2 (graphs A23-A39 above). The smallest maximal 2-degenerate graphs not contained in a maximal 2-degenerate graph with diameter 2 have order 7. They are all those with order 7 and diameter 3, excluding those listed in Theorem 2.5 (A25, A26, A29-A31, A33, A37, A38).

Proposition 2.7 *Let G be a maximal 2-degenerate graph. Then G is contained in a maximal 2-degenerate graph with diameter at most 3.*

Proof If G has diameter at most 3, we are done. If not, consider a vertex v with maximum eccentricity. Let S be the set of all vertices with distance more than 2 from v. Add 2-leaves adjacent to v and each vertex in S, and call the set vertices added S'. Now the distance between v and any other vertex is at most 2. Vertices in S' are all distance 2 from each other. A vertex in S' and a vertex in G have distance at most 3, since there is now a path through v. Thus no new pairs with distance more than 3 are created. This process can be repeated with other vertices until a graph is constructed that contains G and has diameter at most 3. □

§3. Diameter 2 k-Trees

In this section, we prove a forbidden subgraph characterization of k-trees with diameter 2.

Definition 3.1 *A k-path graph G is an alternating sequence of distinct k- and $k+1$-cliques $e_0, t_1, e_1, t_2, \cdots, t_p, e_p$, starting and ending with a k-clique and such that t_i contains exactly two k-cliques e_{i-1} and e_i.*

Note that k-paths are also known a linear k-trees [1]. They are closely related to pathwidth [17]; in particular, they are the maximal graphs with proper pathwidth k. I have have further examined k-paths in two forthcoming papers [4, 5]. There is a simple characterization of k-paths.

Theorem 3.2([15]) *Let G be a k-tree with $n > k+1$ vertices. Then G is a k-path graph if and only if G has exactly two k-leaves.*

A k-path with a dominating vertex has nice structure.

Lemma 3.3 *A k-path has diameter at most 2 if and only if it has a dominating vertex. When $k \geq 2$, a k-path with a dominating vertex can be represented as $P + K_1$, where P is a $k-1$-path.*

Proof Every k-path with order $n \leq k+2$ has diameter at most 2 and a dominating vertex. Consider constructing the k-path from $K_k + \overline{K}_2$, which has k-leaves u and v_1, and $N(u) = S_1 = N(v_1)$. Iteratively add vertex v_i with neighborhood S_i, so that S_i replaces one vertex of S_{i-1} with v_{i-1}. As long as S_1 and S_i contain a common vertex, the graph has diameter 2 and a dominating vertex. Once S_1 and S_i do not contain a common vertex, the graph has diameter more than 2 and no dominating vertex.

For the second claim, we use induction on order n. When $n = k$, $G = K_k$ and the result holds. Let G be a k-path with order $n > k$ containing a dominating vertex u, and assume the result holds for all graphs with order $n-1$. Then G has a k-leaf v, which is adjacent to u. Now $G - v$ is a k-path with a dominating vertex, so it can be represented as $P' + K_1$, where P' is a $k-1$-path. Then the other neighbors of v induce a clique in P', so G can be represented as $P + K_1$. □

Note for $k \geq 2$, a k-tree with diameter 2 need not have a dominating vertex.

Adding a k-leaf to a k-tree cannot change any existing distances. Thus when constructing a k-tree, the diameter can increase, but it cannot decrease, as it can in a maximal k-degenerate graph.

Definition 3.4 *A k-tree is minimal with respect to diameter 3 if deleting any k-leaf results in a k-tree with diameter 2.*

We can characterize these graphs. A tree is minimal with respect to diameter 3 if and only if it is P_4. We have seen in Proposition 1.2 that a 2-tree is minimal with respect to diameter 3 if and only if it is P_6^2. In general, P_{2k+2}^k is the smallest k-tree with diameter 3, but for $k \geq 3$ it is not the only one.

Algorithm 3.5 Let P be a $k-2$-path, $k \geq 3$, of order $n-4$ with k-leaves w and x. Join dominating vertices y and z to P, forming $P+K_2$. Add u with neighborhood $N_P(w) \cup \{w, y\}$, and v with neighborhood $N_P(x) \cup \{x, z\}$. Let $\mathbb{G}_k$ be the class of all graphs formed this way.

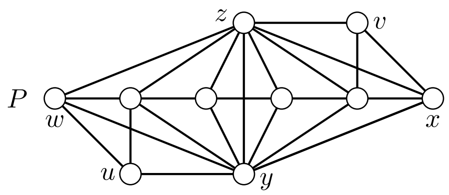

Theorem 3.6 *A graph G is a k-tree minimal with respect to diameter 3 if and only if $G \in \mathbb{G}_k$.*

Proof ($\Leftarrow$) Let G be a graph in $\mathbb{G}_k$ constructed using the algorithm. Then G is a k-tree, $d(u,v) = 3$, and u and v are the only pair with distance more than 2.

($\Rightarrow$) Let G be as stated. A k-tree with diameter 3 must contain a pair of vertices distance 3 apart. Thus in a minimal k-tree with diameter 3, the vertices at distance 3 must be k-leaves, and no other vertices are k-leaves. Thus G is a k-path with leaves (say) u and v. Since G is minimal, $G-u$ has diameter 2. By Lemma 3.3, it has a dominating vertex y, so $G-u-y$ is a $k-1$-path. Similarly, $G-v$ has a dominating vertex z. Thus $G-\{u,v,y,z\}$ is a $k-2$-path. Then u and v must each neighbor one of y and z, and one of the k-leaves of the $k-2$-path. Thus G can be constructed using the algorithm, so $G \in \mathbb{G}_k$. □

Equivalently, a k-tree has diameter at most 2 if and only if it does not contain any graph in $\mathbb{G}_k$. When $k = 3$ and $n \geq 8$, the algorithm produces a unique 3-tree of order n minimal with respect to diameter 3 (shown below for $n = 8$).

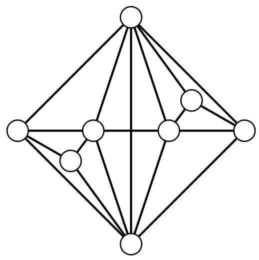

References

[1] A. Abiad, B. Brimkov, A. Erey, L. Leshock, X. Martinez-Rivera, S. O, S. Song, J. Williford, On the Wiener index, distance cospectrality and transmission regular graphs, *Discrete Appl. Math.*, 230 (2017), 1-10.

[2] A. Bickle, Structural results on maximal k-degenerate graphs, *Discuss. Math. Graph Theory*, 32 4 (2012), 659-676.

[3] A. Bickle, *Fundamentals of Graph Theory*, AMS (2020).

[4] A. Bickle, k-Paths of k-trees, Accepted by *Congr. Num.*.

[5] A. Bickle, How to count k-paths, 2020+. *To Appear.*

[6] A. Bickle, Z. Che, Wiener indices of maximal k-degenerate graphs, *Graphs and Combinatorics*, 37 2 (2021), 581-589.

[7] M. Borowiecki, J. Ivanco, P. Mihok, G. Semanisin, Sequences realizable by maximal k-degenerate graphs, *J. Graph Theory*, 19 (1995), 117-124.

[8] S. Caminiti, E. Fusco, On the number of labeled k-arch graphs, *J. Integer Seq.*, 10 7 (2007).

[9] Z. Filakova, P. Mihok, G. Semanisin, A note on maximal k-degenerate graphs, *Math Slovaca*, 47 (1997), 489-498.

[10] G. Franceschini, F. Luccio, L. Pagli, Dense trees: a new look at degenerate graphs, *J. Discrete Algorithms*, 4 3 (2006), 455-474.

[11] Z. Goufei, A note on graphs of class 1, *Discrete Math.*, 263 (2003), 339-345.

[12] R. Klein, J. Schonheim, Decomposition of K_n into degenerate graphs, In *Combinatorics and Graph Theory*, Hefei 6-27, April 1992. World Scientific. Singapore, New Jersey, London, Hong Kong, 141-155.

[13] D. R. Lick, A. T. White, k-degenerate graphs, *Canad. J. Math.*, 22 (1970), 1082-1096.

[14] J. Mitchem, Maximal k-degenerate graphs, *Util. Math.*, 11 (1977), 101-106.

[15] L. Markenzon, C. M. Justel, N. Paciornik, Subclasses of k-trees: Characterization and recognition, *Discrete Appl. Math.* 154 5 (2006), 818-825.

[16] H. P. Patil, A note on the edge-arboricity of maximal k-degenerate graphs, *Bull. Malaysian Math Soc.*, 7 2 (1984), 57-59.

[17] A. Proskurowski, J. Telle, Classes of graphs with restricted interval models, *Discrete Math. Theoret. Comput. Sci.*, 3 (1999), 167–176.

[18] K. Seyffarth, Maximal planar graphs of diameter two, *J. Graph Theory*, 13 5 (1989), 619-648.

[19] J. M. S. Simes-Pereira, A survey of k-degenerate graphs, *Graph Theory Newsletter*, 5 (1976), 1-7.

[20] Y. Yang, J. Linb, Y. Dai, Largest planar graphs and largest maximal planar graphs of diameter two, *J. Comput. Appl. Math.*, 144 (2002) 349–358.

International J.Math. Combin. Vol.2(2021), 80-88

Total Eccentric Index and NK-Index for Generalized Complementary Prisms

S. Arockiaraj

(Department of Mathematics, Mepco Schlenk Engineering College, Sivakasi- 626 005, Tamilnadu, India)

Vijaya Kumari

(Department of Mathematics, Vijaya College, Mulky- 574 154, Karnataka, India)

E-mail: psarockiaraj@gmail.com, vijayasullal@gmail.com

Abstract: The total eccentricity of a graph G is defined as $\zeta(G) = \sum\limits_{v\in V(G)} ecc(v)$ and the Narumi-Katayama index of a graph G is defined as $NK(G) = \prod\limits_{v\in V(G)} deg(v)$. In this paper, we have obtained the total eccentricity and the bounds for Narumi-Katayama index for the generalized complimentary prisms of graphs.

Key Words: Complementary prism, generalized complementary prism, eccentricity.

AMS(2010): 05C12.

§1. Introduction

Throughout this paper, all graphs we considered are simple and connected. For a vertex $v \in V(G)$, $deg(v)$ denotes the degree of v. For vertices $u, v \in V(G)$, the distance $d(u, v)$ is defined as the length of the shortest path between u and v in G. The eccentricity $\zeta(v)$ of a vertex v is the maximum among the distances from v to all the remaining vertices. The total eccentricity of the graph G, denoted by $\zeta(G)$ is defined as the sum of eccentricities of all the vertices of the graph G [3]. That is,

$$\zeta(G) = \sum_{v\in V(G)} ecc(v).$$

In 1984, Narumi-Katayama [7] proposed a definition of a simple topological index which is defined as

$$NK(G) = \prod_{v\in V(G)} deg(v).$$

On this graph invariant, several works [5,6,8-10] are reported and the name "Narumi-Katayama index" is used.

In [8], I. Gutman et al. considered the problem of extremal Narumi-Katayama index and offered a few results filling the gap. For graphs without isolated vertices, I. Gutman et

[1]Received February 9, 2021, Accepted June 12, 2021.

[2]Vijaya Kumari, a Research Scholar of Karpagam University, Coimbatore, Tamilnadu, India

al. [8] presented the minimal, second-minimal and third-minimal (maximal, second-maximal and third-maximal, resp.) NK-values for extremal graphs. Moreover, the maximal (second-maximal) Narumi-Katayama index of n-vertex tree (unicyclic graph) is determined [8] and the maximal Narumi-Katayama index of n-vertex bicyclic graphs is given. For connected n-vertex graphs, the minimal and second minimal Narumi-Katayama index are showed [8]. Consequently, the second-minimal Narumi-Katayama index among n-vertex trees and the minimal Narumi-Katayama index among n-vertex unicyclic graphs are presented [8].

KM. Kathiresan and S. Arockiaraj introduced some generalization of complementary prisms and studied the Wiener index of those generalized complementary prisms [9].

Let G and H be any two graphs on p_1 and p_2 vertices, respectively and let R and S be subsets of $V(G) = \{u_1, u_2, \cdots, u_{p_1}\}$ and $V(H) = \{v_1, v_2, \cdots, v_{p_2}\}$ respectively. The complementary product $G(R)\square H(S)$ has the vertex set $\{(u_i, v_j) : 1 \leq i \leq p_1, 1 \leq j \leq p_2\}$ and (u_i, v_j) and (u_h, v_k) are adjacent in $G(R)\square H(S)$ satisfying

(i) if $i = h, u_i \in R$ and $v_j v_k \in E(H)$, or if $i = h, u_i \notin R$ and $v_j v_k \notin E(H)$ or

(ii) if $j = k, v_j \in S$ and $u_i u_h \in E(G)$, or if $j = k, v_j \notin S$ and $u_i u_h \notin E(G)$.

In other words, $G(R)\square H(S)$ is the graph formed by replacing each vertex $u_i \in R$ of G by a copy of H, each vertex $u_i \notin R$ of G by a copy of $\overline{H}$, each vertex $v_j \in S$ of H by a copy of G and each vertex $v_j \notin S$ of H by a copy of $\overline{G}$. If $R = V(G)$ (respectively, $S = V(H)$), the complementary product can be written as $G\square H(S)$ (respectively, $G(R)\square H$). The complementary prism $G\overline{G}$ obtained from G is $G\square K_2(S)$ with $|S| = 1$. That is, $G\overline{G}$ has a copy of G and a copy of $\overline{G}$ with a matching between the corresponding vertices.

In $G\overline{G}$, we have an edge $v\overline{v}$ for each vertex v in G. The authors consider this edge as K_2 or $K_{1,1}$ or P_2. By taking m copies of G and n copies of $\overline{G}$, they generalize the complementary prism as a graph $G\square H(S)$, where $H = K_{m+n}$ (or $K_{m,n}$) and S is a subset of $V(H)$ having m vertices and $H = C_{2m}$ (or P_{2m}) whose vertex set is $\{v_1, v_2, \cdots, v_{2m}\}$ and $S = \{v_1, v_3, \cdots, v_{2m-1}\}$.

In [1,2], the eccentric connective index and first and second Zagreb indices have been bound for the generalized complementary prisms.

Motivated by these works, the total eccentricity and the bounds for Narumi-Katayama index for the generalized complementary prisms of graphs have been found in this paper.

§2. Main Results

Proposition 2.1 *Let G be any graph with k number of full degree vertices and k' number of isolated vertices. Then for any $m, n > 1$,*

$$\zeta(G_{m+n}) = 3p(m + n) - mk - nk'.$$

Proof For any vertex $v \in V(G_{m+n})$,

$$ecc(v) = \begin{cases} 2, & \text{if } ecc_G(v) = 1 \\ 3, & \text{otherwise} \end{cases}$$

Hence,

$$\begin{aligned} \zeta(G_{m+n}) &= \sum_{v \in V(G_{m+n})} ecc(v) \\ &= \sum_{i=1}^{m} \sum_{v \in i^{th} \ copy \ of \ G} ecc(v) + \sum_{i=1}^{n} \sum_{v \in i^{th} \ copy \ of \ \overline{G}} ecc(v) \\ &= 3mp - mk + 3np - nk' \\ &= 3p(m+n) - mk - nk'. \end{aligned}$$ □

Proposition 2.2 *For any* $m, n > 1, \zeta(G_{m,n}) = 3mn.$

Proof For any vertex $v \in V(G_{m,n})$, its eccentricity is 3. Hence

$$\zeta(G_{m,n}) = \sum_{v \in V(G_{m,n})} ecc(v) = 3mn.$$ □

Proposition 2.3 *For any* $m \geq 2, \zeta(G^c_{m,m}) = 2mp(m+1).$

Proof In $G^c_{m,m}, ecc(v) = m+1$, for all $v \in V(G^c_{m,m})$. Hence,

$$\zeta(G^c_{m,m}) = \sum_{v \in V(G^c_{m,m})} ecc(v) = 2mp(m+1).$$ □

Proposition 2.4 *For any* $m > 1$, $\zeta(G^P_{m,m}) = mp(3m+1).$

Proof Let $v_{i,j}, \overline{v_{i,j}}, 1 \leq j \leq p$ be the vertices of the i^{th} copy of G and $\overline{G}$ respectively in $G^P_{m,m}$ for $1 \leq i \leq m$. Notice that for $1 \leq i \leq \lceil \frac{m}{2} \rceil$ and $1 \leq j \leq p$, $ecc(v_{i,j}) = 2m + 2 - 2i$; for $1 \leq i \leq \lfloor \frac{m}{2} \rfloor$ and $1 \leq j \leq p$, $ecc(\overline{v_{i,j}}) = 2m + 1 - 2i$; for $\lceil \frac{m}{2} \rceil + 1 \leq i \leq m$ and $1 \leq j \leq p$, $ecc(v_{i,j}) = ecc(\overline{v}_{m+1-i,j})$; for $\lfloor \frac{m}{2} \rfloor + 1 \leq i \leq m$ and $1 \leq j \leq p$, $ecc(\overline{v_{i,j}}) = ecc(v_{m+1-i,j})$.

From these,

$$\begin{aligned} \zeta(G^P_{m,m}) &= \sum_{v \in V(G^P_{m,m})} ecc(v) \\ &= 2p[(m+1) + (m+2) + \cdots + 2m] \\ &= 2p[m^2 + 1 + 2 + \cdots + m] \\ &= 2p\left[m^2 + \frac{m(m+1)}{2}\right] = mp[3m+1]. \end{aligned}$$ □

Proposition 2.5 *If* $G, \overline{G} \in F_{22}$, *then* $\zeta(G\overline{G}) = 4p.$

Proof If G and $\overline{G}$ are members of F_{22}, then any two vertices with in G or with in $\overline{G}$ are with in distance 2. If u and v are at distance 2 in G, then $\overline{u}\,\overline{v}, u\overline{u} \in E(G\overline{G})$ and hence u and $\overline{v}$ are at a distance 2 in $G\overline{G}$. Hence $ecc(v) = 2$ for all $v \in V(G\overline{G})$. Therefore,

$$\zeta(G\overline{G}) = \sum_{v \in V(G\overline{G})} ecc(v) = 4p. \qquad \square$$

Proposition 2.6 *If* $G \in F_{11}$, *then* $\zeta(G\overline{G}) = 5p$.

Proof If $G \in F_{11}$, then G is a complete graph and $\overline{G}$ is a totally disconnected graph. So $G\overline{G}$ is simply $K_p \circ K_1$.

In $G\overline{G}$, the vertices on the copy of G are of eccentricity 2 and vertices on the copy of $\overline{G}$ are of eccentricity 3. Hence $\zeta(G\overline{G}) = 5p$. $\square$

Proposition 2.7 *If* $G \in F_{12}$, *then* $\zeta(G\overline{G}) = 5p$.

Proof Let u be the full degree vertex in G. If v is any vertex other than u in G, then $d(u,v) = 1$ and $d(u,\overline{v}) = 2$. So $ecc(u) = 2$ in $G\overline{G}$. As $\overline{u}$ is an isolated vertex in $\overline{G}$, by the edges $\overline{u}u$, uv and $v\overline{v}$, any vertex $\overline{v}$ in the copy of $\overline{G}$ will be reached at a distance 3 from $\overline{u}$ and any vertex v in the copy of G will be reached at a distance 2. So $ecc(\overline{v}) = 3$ in $G\overline{G}$ for all $\overline{v}$ in the copy of $\overline{G}$.

Let v be a vertex of eccentricity 2 in G. Whenever x is a vertex of distance 2 from v in G, the edges $x\overline{x}$ and $\overline{x}\,\overline{v}$ give that $d(v,\overline{x}) = 2$. Whenever x is an adjacent vertex to v, the edges vx and $x\overline{x}$ give again that $d(v,\overline{x}) = 2$. Hence $ecc(v) = 2$ in $G\overline{G}$. So for any vertex $v \in V(G\overline{G})$,

$$ecc(v) = \begin{cases} 2, & \text{if } v \text{ is in the copy of } G \\ 3, & \text{if } v \text{ is in the copy of } \overline{G}. \end{cases}$$

Hence,

$$\zeta(G\overline{G}) = \sum_{v \in V(G\overline{G})} ecc(v) = 2p + 3p = 5p. \qquad \square$$

Proposition 2.8 *If* $G \in F_{23}$, *then* $\zeta(G\overline{G}) = 5p$.

Proof If v is a vertex of eccentricity 2 (or 3) in G, then v is also of eccentricity 2 (or 3) in $G\overline{G}$. But in $\overline{G}$, the vertex $\overline{v}$ corresponding to v in G is of eccentricity 3 (or 2) and hence $\overline{v}$ is also of eccentricity 3 (or 2) in $G\overline{G}$. That is,

$$ecc(v) = \begin{cases} 2, & \text{if } ecc_G(v) = 2 \text{ or } ecc_{\overline{G}}(v) = 3 \\ 3, & \text{if } ecc_G(v) = 3 \text{ or } ecc_{\overline{G}}(v) = 3. \end{cases}$$

So exactly p number of vertices are of eccentricity 2 in $G\overline{G}$ and the remaining p vertices are of eccentricity 3 in $G\overline{G}$. Hence $\zeta(G\overline{G}) = 5p$. $\square$

Proposition 2.9 *If* $G \in F_{24}$ *with* k *number of vertices of eccentricity 2, then* $\zeta(G\overline{G}) = 6p - k$.

Proof When $G \in F_{24}$, $\overline{G} \in F_{22}$ and hence $ecc(\overline{v}) = 2$ in $G\overline{G}$ whenever u and v are at distance more than 2 in G, by the edges $u\ \overline{u}, \overline{u}\ \overline{v}, \overline{v}v$ in $G\overline{G}$, $d(u,v) = 3$ in $G\overline{G}$. Also if u is a vertex of eccentricity 2 in G, then it is also u is a vertex of eccentricity 2 in $G\overline{G}$. Thus exactly k number of vertices are of eccentricity 2 in $G\overline{G}$ and the remaining vertices are of eccentricity 3 in $G\overline{G}$. Hence $\zeta(G\overline{G}) = 2k + 3(2p - k) = 6p - k$. □

Proposition 2.10 *If $G \in F_3$, then $\zeta(G\overline{G}) = 5p$.*

Proof If $G \in F_3$, then $\overline{G} \in F_{22}$ and hence $ecc(\overline{v}) = 2$ in $G\overline{G}$ whenever $\overline{v}$ is in the copy of $\overline{G}$. Also since $ecc_G(v) \geq 3, ecc(v) = 3$ in $G\overline{G}$. Hence $\zeta(G\overline{G}) = 5p$. □

Proposition 2.11 *For any positive integers m and n,*

$$NK(G_{m+n}) \geq [2(m+n-1)]^{(m+n)p}[NK(G)]^{\frac{m}{2}}[NK(\overline{G})]^{\frac{n}{2}}.$$

Proof In the graph G_{m+n},

$$deg(u) = \begin{cases} deg_G(u) + m + n - 1, & \text{when } u \text{ is in a copy of } G \\ deg_{\overline{G}}(u) + m + n - 1, & \text{when } u \text{ is in a copy of } \overline{G}. \end{cases}$$

We know that $A.M. \geq G.M.$ and $a + b \geq 2\sqrt{ab}$. Therefore

$$\begin{aligned}
NK(G_{m+n}) &= \prod_{u \in V(G_{m+n})} deg(u) \\
&= \prod_{u \in \ copies\ of\ G} deg(u). \prod_{\overline{u} \in \ copies\ of\ \overline{G}} deg(\overline{u}) \\
&= \prod_{i=1}^{m} \left(\prod_{u \in\ i^{th}\ copy\ of\ G} deg(u) \right) . \prod_{i=1}^{n} \left(\prod_{\overline{u} \in\ i^{th}\ copy\ of\ \overline{G}} deg(\overline{u}) \right) \\
&= \left[\prod_{u \in V(G)} (deg(u) + m + n - 1) \right]^{m} \left[\prod_{\overline{u} \in V(\overline{G})} (m + n - 1 + deg_{\overline{G}}(\overline{u})) \right]^{n} \\
&\geq \left[\prod_{u \in V(G)} 2\sqrt{deg_G(u)(m+n-1)} \right]^{m} \left[\prod_{\overline{u} \in V(\overline{G})} 2\sqrt{(m+n-1)deg_{\overline{G}}(\overline{u})} \right]^{n} \\
&= \left(2\sqrt{m+n-1}\right)^{mp} \left(\prod_{u \in V(G)} deg_G(u) \right)^{\frac{m}{2}} \left(2\sqrt{m+n-1}\right)^{np} \left(\prod_{\overline{u} \in V(\overline{G})} deg_{\overline{G}}(\overline{u}) \right)^{\frac{n}{2}} \\
&= \left[2\sqrt{m+n-1}\right]^{(m+n)p} [NK(G)]^{\frac{m}{2}} [NK(\overline{G})]^{\frac{n}{2}}.
\end{aligned}$$
□

Proposition 2.12 *For any positive integers m and n,*

$$NK(G_{m,n}) \geq 2^{(m+n)p} \left(n^{\frac{m}{2}} m^{\frac{n}{2}}\right)^{p} (NK(G))^{\frac{m}{2}} \left(NK(\overline{G})\right)^{\frac{n}{2}}.$$

Proof In the graph $G_{m,n}$,

$$deg(u) = \begin{cases} deg_G(u) + n, & \text{when } u \text{ is in a copy of } G \\ deg_{\overline{G}}(u) + m, & \text{when } u \text{ is in a copy of } \overline{G}. \end{cases}$$

Therefore,

$$\begin{aligned} NK(G_{m,n}) &= \prod_{u \in V(G_{m,n})} deg(u) \\ &= \prod_{u \in \text{ copies of } G} deg(u). \prod_{\overline{u} \in \text{ copies of } \overline{G}} deg(\overline{u}) \\ &= \left[\prod_{i=1}^{m} \prod_{u \in \ i^{th} \text{ copy of } G} deg(u)\right] . \left[\prod_{i=1}^{n} \prod_{\overline{u} \in \ i^{th} \text{ copy of } \overline{G}} deg(\overline{u})\right] \\ &= \left[\prod_{u \in V(G)} (deg_G(u) + n)\right]^m . \left[\prod_{\overline{u} \in V(\overline{G})} (deg_{\overline{G}}(\overline{u}) + m)\right]^n \\ &\geq \left[\prod_{u \in V(G)} (2\sqrt{deg_G(u) n})\right]^m . \left[\prod_{\overline{u} \in V(\overline{G})} (2\sqrt{deg_{\overline{G}}(\overline{u}) m})\right]^n \\ &= \left(2\sqrt{n}\right)^{mp} \left[\prod_{u \in V(G)} deg_G(u)\right]^{\frac{m}{2}} \left(2\sqrt{m}\right)^{np} \left[\prod_{\overline{u} \in V(\overline{G})} deg(\overline{u})\right]^{\frac{n}{2}} \\ &= 2^{(m+n)p} \left(n^{\frac{m}{2}} m^{\frac{n}{2}}\right)^p NK(G)^{\frac{m}{2}} NK(\overline{G})^{\frac{n}{2}}. \end{aligned}$$

□

Proposition 2.13 *For any positive integers $m \geq 2$,*

$$NK(G^c_{m,m}) \geq 8^{mp}[NK(G)NK(\overline{G})]^{\frac{m}{2}}.$$

Proof In the graph $G^c_{m,m}$,

$$deg(u) = \begin{cases} deg_G(u) + 2, & \text{when } u \text{ is in a copy of } G \\ deg_{\overline{G}}(u) + 2, & \text{when } u \text{ is in a copy of } \overline{G} \end{cases}$$

Therefore,

$$\begin{aligned} NK(G^c_{m,m}) &= \prod_{u \in V(G^c_{m,m})} deg(u) = \prod_{u \in \text{ copies of } G} deg(u). \prod_{\overline{u} \in \text{ copies of } \overline{G}} deg(\overline{u}) \\ &= \prod_{i=1}^{m} \left[\prod_{u \in \ i^{th} \text{ copy of } G} deg(u)\right] . \prod_{i=1}^{m} \left[\prod_{\overline{u} \in 1^{th} \text{ copy of } \overline{G}} deg(\overline{u})\right] \end{aligned}$$

$$= \left[\prod_{u\in V(G)} (deg_G(u)+2)\right]^m . \left[\prod_{\overline{u}\in V(\overline{G})} (deg_{\overline{G}}(\overline{u})+2)\right]^m$$

$$\geq \left[\prod_{u\in V(G)} (2\sqrt{2deg_G(u)})\right]^m . \left[\prod_{\overline{u}\in V(\overline{G})} (2\sqrt{2deg_{\overline{G}}(\overline{u})})\right]^m$$

$$= \left(2\sqrt{2}\right)^{mp} \left[\prod_{u\in V(G)} deg_G(u)\right]^{\frac{m}{2}} \left(2\sqrt{2}\right)^{mp} \left[\prod_{\overline{u}\in V(\overline{G})} deg_{\overline{G}}(\overline{u})\right]^{\frac{m}{2}}$$

$$= 8^{mp}[NK(G)NK(\overline{G})]^{\frac{m}{2}}.$$

This completes the proof. □

Proposition 2.14 *For any positive integers $m \geq 2$,*

$$NK(G^P_{m,m}) \geq 2^{\frac{5m}{2}}[NK(G)NK(\overline{G})]^{\frac{m}{2}}.$$

Proof In the graph $G^P_{m,m}$,

$$deg(u) = \begin{cases} deg_G(u)+1, & \text{when } u \text{ is in the first copy of } G \\ deg_G(u)+2, & \text{when } u \text{ is in the remaining copies of } G \\ deg_{\overline{G}}(u)+1, & \text{when } u \text{ is in the last copy of } \overline{G} \\ deg_{\overline{G}}(u)+2, & \text{when } u \text{ is in the remaining copies of } \overline{G} \end{cases}$$

Therefore,

$$NK(G^P_{m,m}) = \prod_{u\in V(G^P_{m,m})} deg(u)$$

$$= \prod_{u\in \text{ copies of } G} deg(u). \prod_{\overline{u}\in \text{ copies of } \overline{G}} deg(\overline{u})$$

$$= \left(\prod_{i=1}^{m} \prod_{u\in\ i^{th} \text{ copy of } G} deg(u)\right) . \left(\prod_{i=1}^{m} \prod_{\overline{u}\in\ i^{th} \text{ copy of } \overline{G}} deg(\overline{u})\right)$$

$$= \left(\prod_{u\in \text{ first copy of } G} deg(u)\right) \left(\prod_{i=1}^{m} \prod_{u\in\ i^{th} \text{ copy of} G} deg(u)\right)$$

$$\left(\prod_{i=1}^{m-1} \prod_{\overline{u}\in i^{th} \text{ copy of} \overline{G}} deg(\overline{u})\right) \left(\prod_{\overline{u}\in\ m^{th} \text{ copy of } \overline{G}} deg(\overline{u})\right)$$

$$= \left(\prod_{u \in \ first\ copy\ of G} (deg_G(u)+1) \right) \left(\prod_{i=2}^{m} \prod_{u \in V(G)} (deg_G(u)+2) \right)$$
$$\left(\prod_{i=1}^{m-1} \prod_{\overline{u} \in V(\overline{G})} (deg_{\overline{G}}(\overline{u})+2) \right) \cdot \left(\prod_{\overline{u} \in \ m^{th}\ copy\ of \overline{G}} (deg_{\overline{G}}(\overline{u})+1) \right)$$
$$\geq \left(\prod_{u \in V(G)} 2\sqrt{deg_G(u)} \right) \left(\prod_{u \in V(G)} 2\sqrt{2deg_G(u)} \right)^{m-1}$$
$$\left(\prod_{\overline{u} \in V(\overline{G})} 2\sqrt{2deg_{\overline{G}}(\overline{u})} \right)^{m-1} \left(\prod_{\overline{u} \in V(\overline{G})} 2\sqrt{deg_{\overline{G}}(\overline{u})} \right)$$
$$= 2^{3m-1} \prod_{u \in V(G)} (deg_G(u))^{\frac{1}{2}} \prod_{u \in V(G)} (deg_G(u))^{\frac{m-1}{2}}$$
$$\prod_{\overline{u} \in V(\overline{G})} (deg_{\overline{G}}(\overline{u}))^{\frac{m-1}{2}} \prod_{\overline{u} \in V(\overline{G})} (deg_{\overline{G}}(\overline{u}))^{\frac{1}{2}}$$
$$= 2^{3m-1} \left[\prod_{u \in V(G)} deg(u) \right]^{\frac{m}{2}} \left[\prod_{\overline{u} \in V(\overline{G})} deg(\overline{u}) \right]^{\frac{m}{2}}$$
$$= 2^{3m-1} \left[NK(G) NK(\overline{G}) \right]^{\frac{m}{2}}. \qquad \square$$

References

[1] S. Arockiaraj and Vijayakumari, Eccentric connectivity index of generalized complementary prisms, *Int. J. of Appl. Math.*, 4(2) (2013).

[2] S. Arockiaraj and Vijayakumar, The first and second Zagreb indices of generalized complementary prisms, *International Journal of Mathematics and its Applications*, 3(2) (2015), 55–63.

[3] P. Dankelmann, W. Goddard and C.S. Swart, The average eccentricity of a graph and its subgraphs, *Util. Math.*, 65 (2004), 41–51.

[4] B. Eskender and E. Vumar, Eccentric connectivity index and eccentric distance sum of some graph operations, *Transactions on Combinatorics*, 2(1) (2013), 103–111.

[5] D.J. Klein and V.R. Rosenfeld, The degree-product index of Narumi and Katayama, *MATCH Communications in Mathematical and in Computer Chemistry*, 64 (2010), 607–618.

[6] D.J. Klein and V.R. Rosenfeld, *The Narumi-Katayama degree-product index and the degree-product polynomial* in : I. Gutman, B. Furtula (Eds.), *Novel Molecular Structure Descriptors-Theory and Applications* II, Univ. Kragujevac, Kragujevac, 2010.

[7] H. Narumi and M. Katayama, Simple topological index, A newly devised index characterizing the topological nature of structural isomers of saturated hydrocarbons, *Memoirs of the Faculty of Engineering*, Hokkaido University, 16 (1984), 209–214.

[8] I. Gutman and M. Ghorbani, Some properties of the Narumi-Katayama index, *Applied*

Mathematics Letters, 25 (2012), 1435–1438.

[9] KM. Kathiresan and S. Arockiaraj, On the Wiener index of generalised complementary prism, *Bull. Inst. Combin. Appl.*, 59 (2010), 31–45.

[10] R. Todeschini and V. Consonni, *Molecular descriptors for Chemoinformatics*, Wiley-VCH, Weinheim, 2009.

[11] Z. Tomovic and I. Gutman, Narumi-Katayama index of phenylenes, *Journal of the Serbian Chemical Society*, 66 (2001), 243–247.

Famous Words

We know nothing of what will happen in future , but by the analogy of past experience.

By Abraham Lincoln, an American president

Author Information

Submission: Papers only in electronic form are considered for possible publication. Papers prepared in formats, viz., .tex, .dvi, .pdf, or.ps may be submitted electronically to one member of the Editorial Board for consideration in the **International Journal of Mathematical Combinatorics** (*ISSN 1937-1055*). An effort is made to publish a paper duly recommended by a referee within a period of $3 - 4$ months. Articles received are immediately put the referees/members of the Editorial Board for their opinion who generally pass on the same in six week's time or less. In case of clear recommendation for publication, the paper is accommodated in an issue to appear next. Each submitted paper is not returned, hence we advise the authors to keep a copy of their submitted papers for further processing.

Abstract: Authors are requested to provide an abstract of not more than 250 words, latest Mathematics Subject Classification of the American Mathematical Society, Keywords and phrases. Statements of Lemmas, Propositions and Theorems should be set in italics and references should be arranged in alphabetical order by the surname of the first author in the following style:

Books

[4]Linfan Mao, *Combinatorial Geometry with Applications to Field Theory*, InfoQuest Press, 2009.
[12]W.S.Massey, *Algebraic topology: an introduction*, Springer-Verlag, New York 1977.

Research papers

[6]Linfan Mao, Mathematics on non-mathematics - A combinatorial contribution, *International J.Math. Combin.*, Vol.3(2014), 1-34.
[9]Kavita Srivastava, On singular H-closed extensions, *Proc. Amer. Math. Soc.* (to appear).

Figures: Figures should be drawn by TEXCAD in text directly, or as EPS file. In addition, all figures and tables should be numbered and the appropriate space reserved in the text, with the insertion point clearly indicated.

Copyright: It is assumed that the submitted manuscript has not been published and will not be simultaneously submitted or published elsewhere. By submitting a manuscript, the authors agree that the copyright for their articles is transferred to the publisher, if and when, the paper is accepted for publication. The publisher cannot take the responsibility of any loss of manuscript. Therefore, authors are requested to maintain a copy at their end.

Proofs: One set of galley proofs of a paper will be sent to the author submitting the paper, unless requested otherwise, without the original manuscript, for corrections after the paper is accepted for publication on the basis of the recommendation of referees. Corrections should be restricted to typesetting errors. Authors are advised to check their proofs very carefully before return.

June 2021

Contents

An International Journal on Mathematical Combinatorics

ISSN 1937-1055